Quantum-Classical Correspondence in Response Theory

by

Maksym Kryvohuz

B.S., Moscow Inst. of Phys. and Tech., Moscow (2001)
M.S., Moscow Inst. of Phys. and Tech., Moscow (2003)

Submitted to the Department of Chemistry
in partial fulfillment of the requirements for the degree of

Doctor of Philosophy

at the

MASSACHUSETTS INSTITUTE OF TECHNOLOGY

June 2008

Author..... .....
Department of Chemistry
March 14, 2008

Certified by ....
Jianshu Cao
Professor of Chemistry
Thesis Supervisor

Accepted by..... .....
Robert W. Field
Chairman, Department Committee on Graduate Students

This doctoral thesis has been examined by a Committee of the Department of Chemistry as follows:

Professor Troy Van Voorhis....
Chairman, Thesis Committee
Assistant Professor of Chemistry

Professor Jianshu Cao....
Thesis Supervisor
Professor of Chemistry

Professor Robert W. Field.....
Haslam and Dewey Professor of Chemistry

Quantum-Classical Correspondence in Response Theory

by

Maksym Kryvohuz

Submitted to the Department of Chemistry
on March 14, 2008, in partial fulfillment of the
requirements for the degree of
Doctor of Philosophy

Abstract

In this thesis, theoretical analysis of correspondence between classical and quantum dynamics is studied in the context of response theory. Thesis discusses the mathematical origin of time-divergence of classical response functions and explains the failure of classical dynamic perturbation theory. The method of phase space quantization and the method of semiclassical corrections are introduced to converge semiclassical expansion of quantum response function. The analysis of classical limit of quantum response functions in the Weyl-Wigner representation reveals the source of time-divergence of classical response functions and shows the non-commutativity of the limits of long time and small Planck constant. The classical response function is obtained as the leading term of the $\hbar$-expansion of the Weyl-Wigner phase space representation and increases without bound at long times as a result of ignoring divergent higher order contributions. Systematical inclusion of higher order contributions improves the accuracy of the $\hbar$ expansion at finite times. The time interval for the quantum-classical correspondence is estimated for quasi-periodic dynamics and is shown to be inversely proportional to anharmonicity. The effects of dissipation on the correspondence between classical and quantum response functions are studied. The quantum-classical correspondence is shown to improve if coupling to the environment is introduced. In the last part of thesis the effect of quantum chaos on photon echo-signal of two-electronic state molecular systems is studied. The temporal photon echo signal is shown to reveal key information about the nuclear dynamics in the excited electronic state surface. The suppression of echo signals is demonstrated as a signature of level statistics that corresponds to the classically chaotic nuclear motion in the excited electronic state.

Thesis Supervisor: Jianshu Cao
Title: Professor of Chemistry

Acknowledgements

Upon the completion of my PhD study in the Department of Chemistry, I want to acknowledge a number of people who made significant contributions on my way towards a PhD degree. First of all, I would like to express my sincere thanks to my advisor, Prof. Jianshu Cao, for his valuable guidance, motivation, and generous support. It has been a great experience to work with him.

I am truly grateful to Prof. Robert Silbey and Prof. Robert Field for their support during my stay at MIT and help in my further academic career. Prof. Troy van Voorhis is greatly acknowledged for valuable comments while chairing the thesis committee.

I also want to express my sincere gratitude to my former teachers, and in particular to my physics teacher, Viktor Goncharenko, who introduced me to science and conveyed to me his excitement about it. His encouragement, never-ending optimism and friendly support all these years has led me to MIT and finally to a PhD degree.

Finally, I am expressing my gratitude to Madlyen Suprun for her support these years, her love, motivation and patience, to my parents, Zoya Kryvohuz and Nikolai Kryvohuz, for all the moments, days and years they have invested in me, for their love and support, and to my sister, Lyudmila Nakonechnaya, for her constant support and love. This thesis is dedicated to my family.

Contents

List of Figures

List of Tables

Chapter 1

Introduction

1.1 Motivation

A complete knowledge of the optical polarization is sufficient for the interpretation of any spectroscopic measurement and is the central object in the theory of optical spectroscopy [1]. The standard theoretical approach for the computation of optical polarization employs perturbation theory and represents polarization in terms of the power series of applied electric field. The n-th order polarization is completely described by the n-th order response function which carries complete microscopic information necessary for the calculation of optical measurements [2, 1].

Quantum mechanical perturbation theory provides an expression for the response function in terms of nested commutators of radiation-matter interaction operators [1]. The exact evaluation of this expression is a challenge even for small number of degrees of freedom N, and the complexity of calculations growths exponentially with N. The latter motivates the investigation of semiclassical approach to the calculation of response functions [3, 4, 5, 6]. The classical limit of the quantum response function is usually obtained by replacing commutation relations with Poisson brackets and neglecting terms of higher order in the Plank constant [7]. However, this leads to vital differences between the results from quantum and classical calculations. The simple classical limit of the response function diverges with time because of the instability of classical nonlinear dynamics [8, 9].

For a given energy of the system, both linear and nonlinear classical response functions diverge. It was pointed out by van Kampen that even a weak perturbation leads to the failure of classical nonequilibrium perturbation theory at sufficiently long times [10]. Despite this argument, the application of linear response theory does not lead to practical difficulties since phase space averaging over the initial density matrix with Boltzmann distribution cancels the divergence at long times [8]. However, the divergence of nonlinear response functions for microcanonical ensembles cannot be cancelled [11]. Thus the question of the validity of the application of the classical response theory arises.

On the other hand, we know that classical mechanics still well describes our quantum mechanical world in many cases. This suggests to investigate the limits of the validity of classical approach and to indicate the region where the quantum mechanical effects start to dominate. Because of the central role that response functions play in spectroscopic measurements it is thus of importance to study the quantum-classical correspondence in the context of response theory and to draw the borders between classical and quantum-mechanical dynamics.

The elucidation of the classical-quantum correspondence of response functions has conceptual and practical implications. (1) Spectroscopic measurements are often interpreted in terms of classical dynamics. For example, an effective Hamiltonian has been used to describe the bending spectrum of acetene at high excitation energy from high-resolution spectroscopy [12, 13]. Through classical or semi-classical approximations, the measured spectrum can then be mapped to normal-mode or local mode motions solved from the effective Hamiltonian. Heisenberg's correspondence relation and its generalization to non-linear response functions provide the theoretical basis for such mapping. (2) The dynamics of polyatomic molecules has stimulated topics such as intramolecular vibrational relaxation, isomerization, and energy localization [14, 15, 16, 17, 18, 19, 20, 21]. A fundamental question is the manifestation of classical chaos in quantum dynamics and possible spectroscopic signals [2, 22, 23, 24]. (3) Of particular interest is the solute-solvent system, where the solvent has to be treated classically and solute quantum mechanically [25, 26, 27, 28, 29]. (4) Another important direction is the possibility of

developing classical pictures of quantum concepts, such as phase coherence and relaxation. Thesè pictures will advance theoretical understanding of quantum coherence control [30, 31, 32, 33, 34, 35] and vibrational line-sphapes [36, 37, 38, 39, 40, 41, 42].

1.2 Overview

In the present thesis quantum-classical correspondence is studied in the context of response theory. In Chapter 2 the issues of the classical response theory are outlined. The divergence of nonlinear response functions is shown to persist for microcanonical systems with any type of equilibrium phase space distribution density.

In Chapter 3 the issue with the simple classical limit of the response function is indicated. To resolve the problem of divergence of classical response functions in microcanonical ensembles the concept of phase space quantization is proposed. It is shown that by imposing an uncertainty volume on the order of Planck constant around the classical microcanonical surface in phase space and by averaging over this volume the classical response functions are made to converge to their quantum mechanical analogs. The Heisenberg correspondence principle between the quantum matrix element and the classical Fourier component is restored in this approach. The implementation of the proposed phase space quantization approach is illustrated for the two-dimensional Henon-Heiles system of coupled oscillators.

In Chapter 4 the mathematical origin for the divergence of the classical response functions is found. The issue of divergence is shown to arise from the non-commutative behavior of long time $\lim_{t\to\infty}$ and the small Planck constant $\lim_{\hbar\to 0}$. The original quantum expression of response functions requires setting the limit $t \to \infty$ before taking the limit of $\hbar \to 0$. The latter is violated in classical mechanics, where the limit $\hbar \to 0$ is always taken first, thus resulting in problems at long times in response theory. The time interval of the validity of classical response theory is derived for the systems with quasiperiodic dynamics. The semiclassical corrections to the classical response function are obtained in the form of power series of the Planck constant and is shown to converge the classical

linear response function of microcanonical Morse oscillator to its quantum mechanical analog.

The semiclassical representation proposed in Chapter 4 is tested on the system of a particle in square-well potential and is shown to recover quantum recurrences of momentum-momentum correlation function, which are absent in classical form of the correlation function.

In Chapter 5 the effects of dissipation on the cross-over time of the quantum-classical correspondence in response theory is discussed. It is shown that dissipative effects increase the time of the quantum-classical agreement, thus making the system of interest more classical.

In Chapter 6 the quantum signature of chaos is discussed in the context of nonlinear spectroscopy. The classical non-linear response functions was proposed by Mukamel to carry the signature of chaotic dynamics [3] because stability matrices at long times show exponential divergence for chaotic dynamics and linear divergence for regular dynamics. The quantum-mechanical signature of chaos is discussed in Chapter 6 and non-linear spectroscopic experiment is proposed to illustrate quantum effects of the underlying classical dynamics. The suppression of photon-echo signal in the proposed experiment may serve as an indicator of quantum chaos.

Chapter 2

Classical divergence of non-linear response functions

2.1 Introduction

Response theory predicts the response of a physical system to an external disturbance perturbatively and forms the theoretical basis of describing many experimental measurements. It was first pointed out by van Kampen that even a weak perturbation leads to the failure of classical nonequilibrium perturbation theory at sufficiently long times.[10] Despite this argument, the application of linear response theory does not lead to practical difficulties because phase space averaging over the initial density matrix with Boltzmann distribution cancels the divergence at long times. Yet, thermal distribution may not remove the divergence of nonlinear response functions. In this chapter we study the divergence of classical response functions of quasi-periodic systems. The analytical treatment of the behavior of the classical response function has not been studied except for a few exactly solvable anharmonic systems such as quartic [8] and Morse [6, 5] oscillators, showing that in some cases classical response functions diverge at long times. However, the divergent behavior in the general case of systems with regular dynamics has not been systematically investigated. The proof of the divergence has important implications for the conceptual development of quantum-classical correspondence in response theory

and can be established by employing the methods of Fourier expansion and asymptotic decomposition.

The response function is well-defined quantum mechanically in eigenstate space and is expressed by a set of nested commutators

$$\begin{aligned} & R_q^{(n)} \quad (t_n, ..., t_1) \\ & = \quad \left(\frac{\imath}{\hbar}\right)^n \langle [[...[\widehat{\alpha}(\tau_n), \widehat{\alpha}(\tau_{n-1})], ..., \widehat{\alpha}(\tau_1)], \widehat{\alpha}(0)] \rangle, \end{aligned} \tag{2.1}$$

where $\tau_n = \sum_{i=1}^{n} t_i$ and $\widehat{\alpha}(\widehat{\mathbf{x}}(t), \widehat{\mathbf{p}}(t))$ is the system polarizability or dipole momentum operator. The classical limit of the quantum response function (4.2) is usually obtained in the limit of $\hbar \to 0$ by replacing quantum commutators with Poisson brackets and neglecting higher order terms in the Plank constant,

$$\begin{aligned} & R_c^{(n)}(t_n, ..., t_1) \\ & = (-1)^n \langle \{\{...\{\alpha(\tau_n), \alpha(\tau_{n-1})\}, ..., \alpha(\tau_1)\}, \alpha(0)\} \rangle, \end{aligned} \tag{2.2}$$

where $\{...\}$ are Poisson brackets. Yet, thus defined, classical response theory has several difficulties. The expression (4.3) contains stability matrices which grow in time linearly for integrable systems [8] and exponentially for chaotic systems [43]. It was thus noted that the stability matrix may be a sensitive probe of classical chaos [3]. The growth results in the divergent behavior of classical response functions for a given initial condition in phase space.

Yet, while individual trajectories may be sensitive to the perturbation of initial conditions leading to the divergence of the classical response functions, the phase space averaging over the initial density matrix in some cases eliminates these difficulties and makes, for instance, linear response finite at all times [3]. Averaging over the Boltzmann distribution successfully cancels the divergence and does not lead to practical difficulties in applying linear response theory. In fact, the ensemble averaged molecular dynamics simulation technique has been applied extensively in condensed phase vibrational spectroscopy. Mukamel and Leegwater considered the question whether the thermal averaging over initial conditions can cancel the divergence of the nonlinear response function in the

same way as it does for the linear response function [8]. They found that for a quartic oscillator the third-order response function $R^{(3)}(t_3 = const, 0, t_1)$ indeed converges after thermal averaging. However, Noid, Ezra and Loring have shown that $R^{(3)}(t, 0, t)$ diverges even after thermal averaging for the canonical ensemble of noninteracting Morse oscillators [5]. Before this divergent behavior of the classical nonlinear response functions was pointed out, the MD simulations of liquids supported the idea of convergence by Boltzmann averaging [44, 45]. A many-body system in thermodynamic limit such as liquid can be described with dissipative dynamics. Dissipation suppresses the interference among the classical trajectories making the nonlinear response function finite at all times. Nevertheless, for a non-dissipative quasiperiodic dynamics, the thermal averaging over the initial density matrix does not necessarily remove divergence of the classical nonlinear response functions [11]. In this chapter we generalize the above results to all non-dissipative systems with quasi-periodic dynamics and show that there always exists a direction in $(t_n, ..., t_1)$ space along which the nonlinear response function $R_c^{(n)}(t_n, ..., t_1)$ diverges and no smooth distribution function of phase space initial conditions can remove this divergence.

2.2 Classical Response Functions of Systems with Regular Dynamics

Regular dynamics allow simple analytical description and have a convenient representation in action-angle variables [7, 46, 47, 48]. Making use of the quasi-periodicity, we expand a dynamic function $\alpha(t)$ in Fourier series [7] $\alpha(t) = \sum_{\mathbf{n}} \alpha_{\mathbf{n}} e^{i\mathbf{n}\boldsymbol{\varphi}}$, where $\boldsymbol{\varphi} = \boldsymbol{\omega} t + \boldsymbol{\varphi_0}$ are angle variables and $\boldsymbol{\omega}(\mathbf{J}), \alpha_{\mathbf{n}}(\mathbf{J})$ are functions of actions $\mathbf{J}$ only. For the purpose of simplicity, we consider one-dimensional systems. The discussion can be easily extended to a system with an arbitrary number of degrees of freedom, replacing scalars with vectors. Substituting a one-dimensional form of Fourier series into the expression (4.3) for the classical response function and using the identity $Tr[\{A, B\}C] = Tr[A\{B, C\}]$, we get

the following results for the three lowest order response functions

$$
\begin{aligned}
&R_c^{(1)}(t) = -Tr\left(\alpha(t)\{\alpha(0),\rho\}\right) \\
&= -\sum_{n,k}\int dJ\alpha_n e^{\imath n\omega t}\int d\varphi_0 F_k(J,\varphi_0)e^{\imath(n+k)\varphi_0}
\end{aligned}
\tag{2.3}
$$

$$
\begin{aligned}
&R_c^{(2)}(t_2,t_1) = Tr\left(\{\alpha(t_2+t_1),\alpha(t_1)\}\{\alpha(0),\rho\}\right) \\
&= \sum_{n,m,k}\int dJ e^{\imath(n+m)\omega t_1+\imath n\omega t_2} \\
&\times\left\{\imath\left(\alpha_n n\frac{\partial\alpha_m}{\partial J}-\alpha_m m\frac{\partial\alpha_n}{\partial J}\right)+t_2 mn\alpha_n\alpha_m\frac{\partial\omega}{\partial J}\right\} \\
&\times\int d\varphi_0 F_k(J,\varphi_0)e^{\imath(n+m+k)\varphi_0}
\end{aligned}
\tag{2.4}
$$

$$
\begin{aligned}
&R_c^{(3)}(t_3,0,t_1) \\
&= -Tr(\{\alpha(t_3+t_1),\alpha(t_1)\}\{\alpha(t_1),\{\alpha(0),\rho\}\}) \\
&= -\sum_{n,m,k,l}\int dJ e^{\imath(n+m+l)\omega t_1+\imath n\omega t_3} \\
&\times\left\{\imath\left(\alpha_n n\frac{\partial\alpha_m}{\partial J}-\alpha_m m\frac{\partial\alpha_n}{\partial J}\right)+t_3 mn\alpha_n\alpha_m\frac{\partial\omega}{\partial J}\right\} \\
&\times\int d\varphi_0 e^{\imath(n+m+l+k)\varphi_0} \\
&\times\left\{\imath\alpha_l l\frac{\partial F_k}{\partial J}-\left(\frac{\partial\alpha_l}{\partial J}+\imath t_1 l\alpha_l\frac{\partial\omega}{\partial J}\right)\left(\frac{\partial F_k}{\partial\varphi_0}+\imath k F_k\right)\right\},
\end{aligned}
\tag{2.5}
$$

where $F_k(J,\varphi_0) = \imath\alpha_k k\frac{\partial\rho}{\partial J}-\frac{\partial\alpha_k}{\partial J}\frac{\partial\rho}{\partial\varphi_0}$. Classical expressions for non-linear response functions (2.4)-(2.5) contain terms with time-dependent pre-exponential factors that can diverge at long times. Below we prove that non-linear response functions indeed diverge at $t_n\to\infty$ and no phase-space distribution density can remove the divergence. Obviously, the presence of these terms in the above expressions is a consequence of the anharmonicity $\frac{\partial\omega}{\partial J}\neq 0$ whereas harmonic systems $\frac{\partial\omega}{\partial J}\equiv 0$ do not encounter any difficulties in application of classical response theory [5] (it should be mentioned that for a completely harmonic system, non-linear response function treated here are identically zero if the dipole moment depends linearly on position). In the rest of the present chapter we assume that the system is anharmonic and does not have stationary points $\frac{\partial\omega}{\partial J}=0$.

We start with the linear response function (2.3). After the integration over φ_0 is carried out, the expression for $R_c^{(1)}(t)$ takes the form

$$R_c^{(1)}(t) = -\sum_{n,k} \int f_{nk}(J) e^{\imath n\omega t} dJ \tag{2.6}$$

The integrals in Eq.(2.6) have a form of the Fourier integral $G(t) = \int_a^b f(x) e^{\imath t S(x)} dx$, which has well-known asymptotic decompositions at large values of parameter t. For physical applications, the interval $[a, b]$ can always be chosen to be finite and the distribution density $\rho(J, \varphi)$, potential surface $U(r(J, \varphi))$, and anharmonic frequency $\omega(J)$ are usually smooth functions (two times continuously differentiable functions at least). Thus, the following asymptotic decomposition at large values of parameter t is valid .

$$G(t) = \frac{f(b)}{\imath t S'(b)} e^{\imath t S(b)} - \frac{f(a)}{\imath t S'(a)} e^{\imath t S(a)} + O(t^{-2}) \tag{2.7}$$

which for the linear response function (2.6) results in

$$R_c^{(1)}(t) = \frac{1}{t} \sum_{nk} \left(C_{nk}^{(1)} e^{\imath n\omega_1 t} + C_{nk}^{(2)} e^{\imath n\omega_2 t} \right) + O(t^{-2}) \tag{2.8}$$

where $C_{nk}^{(1)}, C_{nk}^{(2)}, \omega_1$ and ω_2 are constants. From Eq.(2.8) one can see that the linear response function decays to zero as $O(1/t)$ or faster for *any* smooth phase-space distribution density ρ. The latter justifies the convergence of the linear response function for thermal distributions $\rho = \frac{1}{Z} e^{-\beta H}$ [8]. The direct application of Eq.(2.7) to the Morse potential with thermal distribution results in the asymptotic behavior shown in Fig.2.1. The exact numerical calculation agrees with the asymptotic expression (2.8) at long times.

Next, we examine the behavior of the classical second-order response function (2.4). Integrating out φ_0 the expression (2.4) can be written in the following form

$$\begin{aligned} R_c^{(2)}(t_2, t_1) &= \sum_{n,m,k} \int f_{nmk}(J) e^{\imath (n+m)\omega t_1 + \imath n\omega t_2} dJ \\ &+ t_2 \sum_{n\neq 0, m\neq 0, k} \int g_{nmk}(J) e^{\imath (n+m)\omega t_1 + \imath n\omega t_2} dJ \end{aligned} \tag{2.9}$$

The first term in Eq.(2.9) will converge at large t_1 and t_2 similar to the linear response function discussed previously. The problem is the second term. Different from the linear

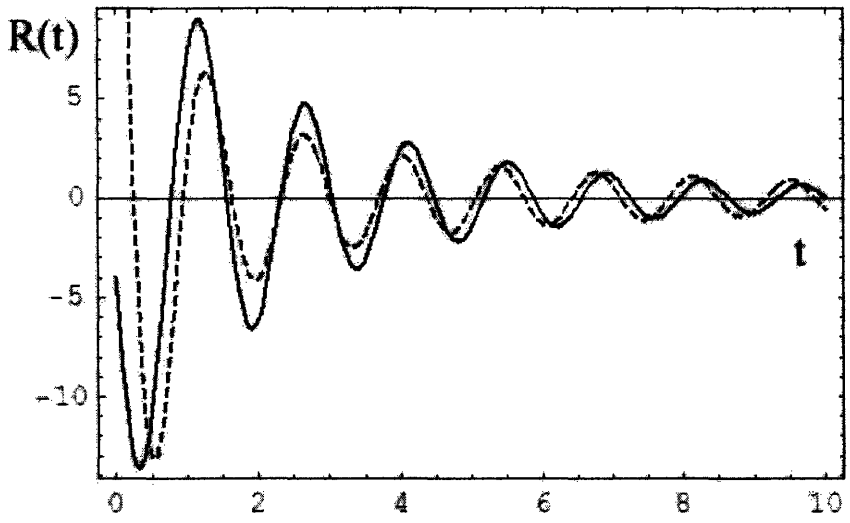

Figure 2.1: The linear response function for the $1D$ Morse oscillator. The solid line represents the exact calculation with the classical formula (2.3), the dashed line corresponds to the first asymptotic term $O(1/t)$ from Eq.(2.8).

response function, the expression for the second order response function has directions in (t_1, t_2) plane, along which the power of the exponent in (2.9) is zero or time-independent. These directions are defined by

$$(n+m)t_1 + nt_2 = C, \tag{2.10}$$

and obviously depend on the type of polarization function $\alpha(t)$ in the way that a particular polarization function has particular spectral components α_k and thus a particular set of values of n and m. We now consider one of these directions by fixing n and m at values n^* and m^*, and assume that $n^* \neq 0$, then $t_2 = -\left(\frac{n^*+m^*}{n^*}\right) t_1 + \frac{C}{n^*}$. Along this direction the second order response function (2.9) becomes

$$\begin{aligned} R_c^{(2)}(t_2(t_1), t_1) &= \sum_{n,m,k} \int dJ (f_{nmk}(J) + \frac{C}{n^*} g_{nmk}(J)) \\ &\times \; e^{\imath \frac{1}{n^*}(mn^* - nm^*)\omega t_1 + \imath \frac{n}{n^*}\omega C} \\ &- \left(\frac{n^*+m^*}{n^*}\right) t_1 \sum_{n,m\,k} \int dJ g_{nmk}(J) \\ &\times \; e^{\imath \frac{1}{n^*}(mn^* - nm^*)\omega t_1 + \imath \frac{n}{n^*}\omega C}, \end{aligned} \tag{2.11}$$

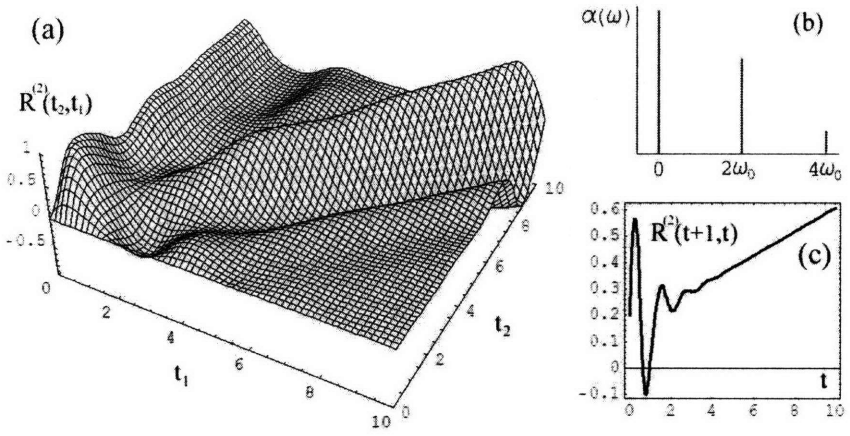

Figure 2.2: The second-order classical response function for the $1D$ Morse oscillator with the fourth-order polarization $\alpha = (b + b^+)^4$ is shown in (a). The spectrum of $\alpha(t)$ is presented in the top right corner (b), where ω_0 is the fundamental frequency. The behavior of the classical second-order response function along the direction $t_2 = t_1 + 1$ is shown in the inset (c).

where C is a constant from the expression (2.10). In summation over n and m in Eq.(2.11), all the integrals with $(mn^* - nm^*) \neq 0$ in the exponent will decay as $O(1/t_1)$ or faster, as discussed for the linear response function, and thus the first part of the expression (2.11) will decay at $t_1 \to \infty$, while the second part will remain bounded $O(1)$. Yet, the integrals with $(mn^* - nm^*) = 0$ result in the linear divergence $O(t_1)$ of the second term in the expression (2.11). There will be at least one such term ($n = n^*$, $m = m^*$) in the summation over n and m while all such terms must satisfy the condition $m/n = m^*/n^*$. Taking the above arguments into account, the expression (2.11) at large t_1 behaves as

$$R_c^{(2)}(t_2(t_1), t_1) \sim t_1 \int dJ \sum_{\frac{m}{n}=\frac{m^*}{n^*}} \tilde{g}_{nm}(J) e^{i\frac{n}{n^*}\omega C}. \tag{2.12}$$

The case when the summation in Eq.(2.12) can be exactly zero is when $\tilde{g}_{-n,-m} = -\tilde{g}_{n,m}$ and $C = 0$. Yet if $C \neq 0$, the right side of the expression (2.12) does not disappear. Then there exist infinitely many lines $(n + m)t_1 + nt_2 = C$ in (t_1, t_2)-plane, along which the second-order classical response function diverges in a non-oscillatory manner as $O(t_1)$ and there is *no* smooth phase space distribution function that can remove this divergence.

One should also note that $R_c^{(2)}(t_2 = const, t_1)$ and $R_c^{(2)}(t_2, t_1 = const)$ are bounded, as follows directly from Eq.(2.9) using decomposition (2.7).

The numerical examples of the classical second order response function are shown in Fig.2.2 for the Morse and in Fig.2.3 quartic oscillator. The obvious difference of the divergent behavior in both figures comes from the fact that polarizations $\alpha(t)$ have different spectral components as shown in Figs 2.2(b) and 2.3(b). Thus, the direction of the most intensive divergence is $t_1 - t_2 = C_1$ in Fig.2.2(b) for the Morse oscillator with polarization $\alpha = (b + b^+)^4$ [6] and $2t_1 - t_2 = C_2$ in Fig.2.3(b) for the quartic oscillator with polarization $\alpha = x$.

The same line of reasoning can be applied to analyze the behavior of the classical third-order response function $R^{(3)}(t_3, 0, t_1)$. Rewriting Eq. (2.5) in the form

$$\begin{aligned}
&R_c^{(3)}(t_3, 0, t_1) \\
&= \sum_{n,m,k,l} \int b_{nmkl}(J) e^{\imath(n+m+l)\omega t_1 + \imath n\omega t_3} dJ \\
&+ t_1 \sum_{n,m,k,l} \int f_{nmkl}(J) e^{\imath(n+m+l)\omega t_1 + \imath n\omega t_3} dJ \\
&+ t_3 \sum_{n,m,k,l} \int g_{nmkl}(J) e^{\imath(n+m+l)\omega t_1 + \imath n\omega t_3} dJ \\
&+ t_1 t_3 \sum_{n,m,k,l} \int h_{nmkl}(J) e^{\imath(n+m+l)\omega t_1 + \imath n\omega t_3} dJ,
\end{aligned} \tag{2.13}$$

the directions $(n+m+l)t_1 + nt_3 = C, C \neq 0$ result in non-oscillatory quadratic divergence $O(t_1^2)$ of $R^{(3)}(t_3(t_1), 0, t_1)$ for *any* smooth phase-space distribution density. Again, using the decomposition (2.7) one can see that $R_c^{(3)}(t_3, 0, t_1 = const)$ and $R_c^{(3)}(t_3 = const, 0, t_1)$ are bounded functions of time. The latter agrees with the results reported in Refs.[8, 5] for the quartic and Morse potentials.

The numerical results for $R^{(3)}(t_3, 0, t_1)$ are presented in Fig.2.4 for the system of thermally distributed quartic oscillators. The numerical calculations observe the linear divergence along the diagonal $t_1 = t_3 = t$ due to the smallness of the quadratic terms $O(t_1^2)$ along the directions $(n+m+l)t_1 + nt_3 = 0$ within the length of the numerical calculation. The same divergence was observed in [5] for the thermally distributed Morse oscillators.

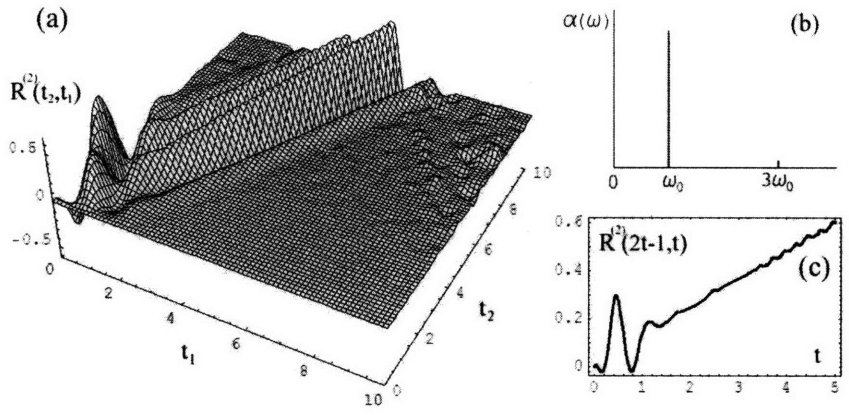

Figure 2.3: The second-order classical response function for the $1D$ quartic oscillator with polarization $\alpha = x$ is shown in (a). The typical spectrum of $\alpha(t)$ is presented in the top right corner (b), where ω_0 is the fundamental frequency. The behavior of the classical second-order response function along the direction $t_2 = 2t_1 - 1$ is shown in the inset (c).

The low temperature approximation $\beta D >> 1$ used in [5] means that the motion of the system takes place in nearly harmonic region, resulting in almost a single spectral component $|\alpha_1|$ of $\alpha(t) = x(t)$ (like that on Fig.2.3(b). Thus the term, quadratic in time, is exactly zero as it follows from Eq.(2.5)

$$\begin{aligned} R_c^{(3)}(t,0,t) &\simeq t\int\left(\sum_{n=\pm1} n^4|\alpha_n|^4\right)\frac{\partial\omega}{\partial J}\frac{\partial^2\rho}{\partial J^2}dJ \\ &- t^2\int\left(\sum_{n=\pm1} n^5|\alpha_n|^4\right)\imath\left(\frac{\partial\omega}{\partial J}\right)^2\frac{\partial\rho}{\partial J}dJ. \end{aligned} \tag{2.14}$$

It is possible now to generalize the discussion to the n-th order response function. Substituting Fourier decompositions of $\alpha(t)$ into the expression for the classical response function $R_c^{(n)}(t_n,...,t_1)$, one obtains the terms containing exponents $e^{\imath\omega(k_1t_1+...+k_nt_n)}$ with the time-dependent prefactors $t_1^\alpha t_2^\beta ... t_n^\delta, \alpha+\beta+...+\delta \leq n-1$. These terms diverge in time as $O(t_1^\alpha t_2^\beta ... t_n^\delta)$ on the plane $k_1^*t_1+...+k_n^*t_n = const$ in $(t_1,...,t_n)$ space. In particular, the direction $t_n = C_n, t_{n-1} = C_{n-1}, ..., t_3 = C_3, k_2^*t_2 + k_1^*t_1 = C$ allows the same range of discussions as for $R^{(2)}(t_2(t_1),t_1)$ and $R^{(3)}(t,0,t)$ stated above, showing that no phase space distribution function can remove the divergence of $R^{(n)}(C_n,...,C_3,(C-k_1^*t_1)/k_2^*,t_1)$ along this direction.

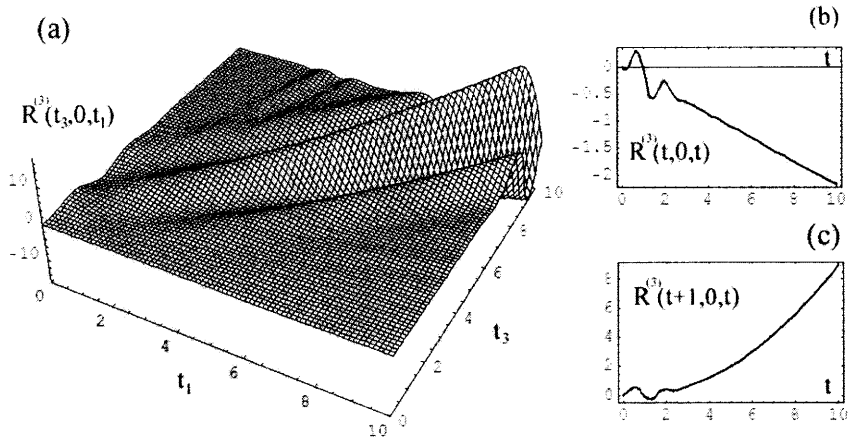

Figure 2.4: The third-order classical response function $R^{(3)}(t_3, 0, t_1)$ for the $1D$ quartic oscillator with polarization $\alpha = x$ is shown in (a). The linear divergent behavior of $R^{(3)}(t, 0, t)$ is shown in the inset (b) with the quadratic divergence of $R^{(3)}(t_3, 0, t_1)$ along the direction $t_3 = t_1 + 1$ presented in the inset (c).

2.3 Conclusions

In the present chapter we have studied the divergent behavior of the classical response function for a system with regular dynamics and demonstrated that no smooth phase space distribution function of the initial conditions can remove the divergence of the classical nonlinear response function for quasi-periodic systems. Our analysis generalizes the analytical and numerical results obtained earlier for Morse and cubic oscillators [6, 5, 8]. It shows the conceptual difficulty of taking the classical limit of the quantum response theory because the quantum nonlinear response function is finite and the classical nonlinear response function diverges for systems with regular dynamics. One possible reason was pointed out by van Kampen,[10] who argued the validity of the application of classical time-dependent perturbation theory. Another reason resides in the fact that, while both infinite quantum mechanical and classical perturbation series represent the same physical quantity, which is polarization $P(t)$, individual expansion terms are not necessarily equivalent. In contrast to the quasi-periodic motion, the chaotic and dissipative dynamics [49, 45, 44, 50, 43] appear to observe the convergence of the classical response functions. The correspondence of the classical limit with the quantum and experimental quantities

remains a challenge and is a subject for future study.

Chapter 3

Non-divergent Classical Response Functions from Uncertainty Principle: Quasi-periodic Systems

3.1 Introduction

The difficulty of quantum mechanical calculations of the nonlinear response functions for large anharmonic systems provides a strong motivation for investigating the semiclassical approach for evaluating these observables [3, 4, 5, 6]. The classical limit of the quantum response function is usually obtained by replacing commutation relations with Poisson brackets and neglecting terms in higher order of the Plank constant [7]. However, this leads to vital difference between the results from quantum and classical approaches such as long-time divergence as discussed in previous chapter. The problem of classical divergence is a conceptual question of quantum-classical correspondence, which is the subject of discussion in the present chapter.

An analytical approach to the calculation of the classical response function was reported in Ref. [6], where the algebraic structure of the one-dimensional Morse oscillator was explored. It was shown that the replacement of the microcanonical distribution function with the uniform distribution function of the width $\hbar$ and $2\hbar$ results in exact quantum

mechanical expression for the linear response function with linear polarization operator $\alpha = (b + b^+)$ and quadratic polarization operator $\alpha = (b + b^+)^2$, respectively, and almost exact expression for the second-order nonlinear response function with polarization operator $\alpha = (b+b^+)^2$. Yet, a general form of polarization operator may result in divergence of the classical second and higher order response functions. In the present chapter we generalize the approach proposed in Ref. [6] and show that using the uncertainty principle (or phase space quantization) we conveniently obtain the classical result that has well-defined quantum correspondence, both conceptually and numerically. We consider the quantum response function for a given eigenstate and its classical microcanonical limit. Starting with the classical expression for the response function we replace the microcanonical phase-space distribution density with the uniform distribution density within the phase-space volume $O(\hbar^n)$ around the classical trajectory. It may seem that this replacement should not lead to any considerable changes since in classical limit $\hbar \to 0$ the latter distribution density becomes the microcanonical δ-function. Yet, the behavior of the classical response function changes drastically once the replacement is made. Finally we obtain the non-divergent classical expression which corresponds to the quantum mechanical one through the Heisenberg's correspondence principle, where each time-dependent quantum matrix element $\langle u|\alpha(t)|v\rangle$ is replaced with the $(u-v)$th classical Fourier component of $\alpha(t)$, evaluated along the classical trajectory with mean action $(J_u + J_v)/2$ [51, 52]. This correspondence principle was also used in spectral analysis technique proposed in Ref. [53] and showed a good agreement between the quantum and semiclassical linear spectral intensities and frequencies. The semiclassical approach developed in present chapter has a convenient representation in action-angle variables. Thus we assume that the system under consideration with N degrees of freedom has N independent first integrals, i.e. the bounded motion in phase space is equivalent to motion on N-torus [54]. This assumption restricts the variety of systems and includes only those with quasiperiodic motion, that is separable systems or non-separable systems with a weak coupling [7].

The discussion in the present chapter is organized as follows: In Sec.3.2 the expression for the linear response function of N-dimensional systems is obtained. We show in general

that the uncertainty width $O(\hbar)$ is necessary to match classical and quantum results. In Section 3.3 the classical expression for the nonlinear response function is considered. Starting with the lowest order nonlinear response function we show that n-dimensional uncertainty $O(\hbar^n)$ around the microcanonical energy surface in multidimensional phase space is necessary to obtain a non-divergent classical formula for the nth-order nonlinear response function. Classical and quantum expressions for the nonlinear response function turn out to have the same form. The result is generalized for the system with N degrees of freedom. The numerical calculations for the 2nd-order nonlinear response function of a two-dimensional system (coupled oscillators) are presented in Section 3.4, followed by general comments and conclusions in Sec. 3.5.

3.2 Linear Response

The expression for the response function can be obtained by using time-dependent perturbation theory [2, 1], giving

$$R_Q^{(n)}(t_n, ..., t_1) = \left(\frac{\imath}{\hbar}\right)^n \langle [[...[\widehat{\alpha}(\tau_n), \widehat{\alpha}(\tau_{n-1})], ..., \widehat{\alpha}(\tau_1)], \widehat{\alpha}(0)] \rangle, \tag{3.1}$$

where the operator $\alpha(t)$ stands for the time-dependent polarizability in Raman spectroscopy or the time-dependent dipole momentum in IR spectroscopy. The classical mechanical expression for the response function [3] may be obtained in the limit $\hbar \to 0$

$$R_C^{(n)}(t_n, ..., t_1) = (-1)^n \langle \{\{...\{\alpha(\tau_n), \alpha(\tau_{n-1})\}, ..., \alpha(\tau_1)\}, \alpha(0)\} \rangle, \tag{3.2}$$

where $\{...\}$ are Poisson brackets. In this section we concentrate on the linear response function $R_Q^{(1)}(t) = (\imath/\hbar)\langle [\alpha(t), \alpha(0)] \rangle$ and its classical correspondence $R_C^{(1)}(t) = -\langle \{\alpha(t), \alpha(0)\} \rangle$. Using identity Tr[{A,B}C] = Tr[A{B,C}] we write

$$R_C^{(1)}(t) = -\mathrm{Tr}(\{\alpha(t), \alpha(0)\}\rho) = -\mathrm{Tr}(\alpha(t)\{\alpha(0), \rho\}). \tag{3.3}$$

As mentioned in the introduction, we assume that the motion of the system is quasiperiodic, and therefore we consider classical response functions in action-angle variables, which can be found employing the technique of the EBK quantization [55, 56, 57]. Making use

of the quasiperiodicity of motion in the limit of infinitely long time interval, $T \to \infty$, we can express any dynamical variable f(t) as a convergent Fourier expansion [7, 51]:

$$f(t) = \sum_{n_1 n_2 \ldots n_N} f_{n_1 n_2 \ldots n_N} e^{i(n_1\omega_1 + n_2\omega_2 + \ldots + n_N\omega_N)t} \tag{3.4}$$

or in terms of angle variables $\vec{\varphi} = \vec{\omega}t + \vec{\varphi}_0$ as:

$$f(t) = \sum_{n_1 n_2 \ldots n_N} \widetilde{f}_{n_1 n_2 \ldots n_N} e^{i(n_1\varphi_1 + n_2\varphi_2 + \ldots + n_N\varphi_N)t}, \tag{3.5}$$

where $\{\omega_i\}$ are N fundamental frequencies and $\{\varphi_{0i}\}$ are N arbitrary constants. It is assumed that all frequencies ω_i are incommensurate. The fundamental frequencies are easy to obtain considering the Fourier transform of the generalized coordinates – the highest peak in the Fourier spectrum of such a coordinate corresponds to one fundamental frequency [55, 56, 57]. Action J_j can then be expressed in terms of fundamental frequencies and Fourier coefficients of Cartesian coordinates Q_j as [55, 56, 57]

$$\begin{aligned} J_j &= \sum_{n_1 n_2 \ldots n_N} n_j(n_1\omega_1 + n_2\omega_2 + \ldots + n_N\omega_N) \\ &\times \left[|Q_{1 n_1 n_2 \ldots n_N}|^2 + |Q_{2 n_1 n_2 \ldots n_N}|^2 + \ldots + |Q_{N n_1 n_2 \ldots n_N}|^2\right] \end{aligned} \tag{3.6}$$

The difficulty of practical application of the numerical EBK quantization grows with increasing the number of degrees of freedom N. Yet, theoretically decomposition (3.5) may be applied to the system with arbitrary N, which allows analytical description of a many-body quasiperiodic systems. With this, we continue to consider classical response function in action-angle variables.

3.2.1 One-dimensional System

First, we consider a one-dimensional system with coordinates $\{J, \varphi\}$. The Poisson bracket in Eq. (3.3) is then

$$\{\alpha(0), \rho\} = \frac{\partial\alpha(0)}{\partial\varphi_0}\frac{\partial\rho}{\partial J} - \frac{\partial\alpha(0)}{\partial J}\frac{\partial\rho}{\partial\varphi_0} \tag{3.7}$$

where ρ is the normalized distribution function. Considering distributions $\rho = \rho(J)$ uniform in φ, we will have only the first term in Eq. (3.7) and the classical expression for

the linear response function in Eq. (3.3) is then

$$R_C^{(1)} = -\oint d\varphi_0 dJ \alpha(t) \frac{\partial \alpha(0)}{\partial \varphi_0} \frac{\partial \rho(J)}{\partial J} \tag{3.8}$$

According to Eq. (3.5) we can express polarization $\alpha(t)$, a dynamical variable, as a Fourier series

$$\alpha(t) = \sum_n \alpha_n e^{in\varphi} \tag{3.9}$$

where $\varphi = \omega t + \varphi_0$ and $\omega = d\varphi/dt = \partial E/\partial J$ is a fundamental frequency. On substituting Eq. (3.9) into Eq. (3.8) and integrating out φ_0 we have

$$R_C^{(1)}(t) = 2\pi i \sum_n \int n|\alpha_n|^2 e^{in\omega t} \frac{\partial \rho(J)}{\partial J} dJ \tag{3.10}$$

Considering microcanonical distribution $\rho = (1/2\pi)\delta(J - J_0)$, the integral in Eq. (3.10) gives well-known linear time divergence [10] of the classical response function

$$R_C^{(1)}(t) = \sum_n e^{in\omega t} \left(tn^2 |\alpha_n|^2 \frac{\partial \omega}{\partial J} - in \frac{\partial |\alpha_n|^2}{\partial J} \right) \Bigg|_{J=J_0}. \tag{3.11}$$

If, instead, we introduce an uncertainty Δ around the trajectory $J = J_0$,

$$\rho(J) = \begin{cases} \frac{1}{2\pi} \frac{1}{\Delta}, \text{ if } J_0 - \frac{\Delta}{2} < J < J_0 + \frac{\Delta}{2}, \\ 0, \text{ otherwise }, \end{cases} \tag{3.12}$$

then Eq. (3.10) becomes

$$R_C^{(1)}(t) = \sum_n \frac{in}{\Delta} |\alpha_n|^2 e^{in\omega t} \Big|_{J=J_0-\Delta/2} - \sum_n \frac{in}{\Delta} |\alpha_n|^2 e^{in\omega t} \Big|_{J=J_0+\Delta/2}. \tag{3.13}$$

We now compare this result with quantum-mechanical formula for the linear response function

$$R_Q^{(1)}(t) = \sum_u \frac{i}{\hbar} |\langle g|\alpha|u\rangle|^2 e^{-i(E_u - E_g)t/\hbar} - \sum_u \frac{i}{\hbar} |\langle g|\alpha|u\rangle|^2 e^{-i(E_g - E_u)t/\hbar}, \tag{3.14}$$

and notice that they will have similar expressions if $\Delta = |n|\hbar$. This result was first observed in Ref. [6], where it was found that classical description of one-photon transition in the linear response of one-dimensional (1D) Morse oscillator will give exact result if

$\Delta = \hbar$, and $\Delta = 2\hbar$ for two-photon transition. Indeed, let us show that the classical expression

$$R_C^{(1)}(t) = \sum_n \frac{\imath}{\hbar}|\alpha_n|^2 e^{\imath n\omega t}\Big|_{J=J_0-n\hbar/2} - \sum_n \frac{\imath}{\hbar}|\alpha_n|^2 e^{\imath n\omega t}\Big|_{J=J_0+n\hbar/2} \tag{3.15}$$

gives the exact result for 1D Morse oscillator. We consider the simplest case of linear polarization operator $\alpha = b + b^+$ which has the following classical limit for the Morse oscillator [6]:

$$\alpha_c = \frac{2}{\chi_e\sqrt{1/\chi_e - 1}}\left(\frac{\chi_e^2 J^2}{\hbar^2} - \frac{\chi_e J}{\hbar}\right)^{1/2}\cos(\varphi), \tag{3.16}$$

where $\varphi = [1 - (2\chi_e J/\hbar)]\omega_0 t + \varphi_0$ and $\omega_0 = \sqrt{2D\beta^2/\mu}$ with $\chi_e = \hbar\beta/\sqrt{8D\mu}$ are the parameters for the Morse potential. Polarization (3.16) has only two Fourier components, therefore

$$\begin{aligned} R_C^{(1)}(t) &= -\frac{\imath}{\hbar}|\alpha_{-1}|^2 e^{-\imath\omega t}\Big|_{J=J_0-\hbar/2} + \frac{\imath}{\hbar}|\alpha_1|^2 e^{\imath\omega t}\Big|_{J=J_0-\hbar/2} \\ &\quad -\frac{\imath}{\hbar}|\alpha_{-1}|^2 e^{-\imath\omega t}\Big|_{J=J_0+\hbar/2} + \frac{\imath}{\hbar}|\alpha_1|^2 e^{\imath\omega t}\Big|_{J=J_0+\hbar/2} \\ &= \frac{2}{(1-\chi_e)\hbar}\{(v+1)(1-\chi_e(v+1))\sin[(1-2\chi_e(v+1))\omega_0 t] \\ &\quad - v(1-\chi_e v)\sin[(1-2\chi_e v)\omega_0 t]\}, \end{aligned} \tag{3.17}$$

where the quantization condition $J_0 = (v + 1/2)$ was used. The last expression coincides with the quantum result [6].

3.2.2 Two-dimensional System

Next, we examine the classical response function for the two-dimensional system (coupled oscillators). By analogy to Eq. (3.8) the expression for the classical response function is

$$R_C^{(1)} = -\oint d\varphi_{0x} d\varphi_{0y} dJ_x dJ_y \alpha(t)\left(\frac{\partial\alpha(0)}{\partial\varphi_{0x}}\frac{\partial\rho(J_x,J_y)}{\partial J_x} - \frac{\partial\alpha(0)}{\partial\varphi_{0y}}\frac{\partial\rho(J_x,J_y)}{\partial J_y}\right), \tag{3.18}$$

where we again use the fact that distribution ρ is uniform in φ_{0x} and φ_{0y}. Fourier decomposition of polarization $\alpha(t) = \sum_{n_x,n_y}\alpha_{n_x,n_y}e^{\imath(n_x\varphi_x + n_y\varphi_y)}$ yields

$$\begin{aligned} R_C^{(1)}(t) &= 4\pi^2\imath\sum_{n_x n_y}\int dJ_x dJ_y |\alpha_{n_x n_y}|^2 e^{\imath(n_x\omega_x + n_y\omega_y)t} \\ &\quad \times\left(n_x\frac{\partial}{\partial J_x} + n_y\frac{\partial}{\partial J_y}\right)\rho(J_x,J_y). \end{aligned} \tag{3.19}$$

Microcanonical distribution function $\rho(J_x, J_y) = (1/4\pi^2)\delta(J_x - J_{x0})\delta(J_y - J_{y0})$, which comes as a limit of quantum mechanical eigenstate, again results in the linear time divergence of the classical response function (3.19). Yet, as in the case of 1D system we may introduce uncertainty $O(\hbar)$ around the trajectory to remove this divergence. First, we notice that our (2D) problem with the transition frequency $n_x\omega_x + n_y\omega_y$ can be converted into 1D problem with one-photon transition on frequency $\widetilde{\omega}_x$ after the change of variables

$$\begin{aligned}
\widetilde{J}_x &= \frac{n_x}{n_x^2+n_y^2}J_x + \frac{n_y}{n_x^2+n_y^2}J_y, \\
\widetilde{J}_y &= \frac{n_y}{n_x^2+n_y^2}J_x - \frac{n_x}{n_x^2+n_y^2}J_y, \\
\widetilde{\omega}_x &= \frac{\partial E}{\partial \widetilde{J}_x} = \frac{\partial E}{\partial J_x}\frac{\partial J_x}{\partial \widetilde{J}_x} + \frac{\partial E}{\partial J_y}\frac{\partial J_y}{\partial \widetilde{J}_x} = \omega_x n_x - \omega_y n_y \\
\widetilde{\omega}_y &= \frac{\partial E}{\partial \widetilde{J}_y} = \frac{\partial E}{\partial J_x}\frac{\partial J_x}{\partial \widetilde{J}_y} + \frac{\partial E}{\partial J_y}\frac{\partial J_y}{\partial \widetilde{J}_y} = \omega_x n_y - \omega_y n_x
\end{aligned} \tag{3.20}$$

The classical response function now becomes

$$R_C^{(1)}(t) = 4\pi^2\imath\sum_{n_x n_y}\int d\widetilde{J}_x d\widetilde{J}_y |\alpha_{n_x n_y}|^2 e^{\imath\widetilde{\omega}_x t}\frac{\partial}{\partial \widetilde{J}_x}\rho(\widetilde{J}_x, \widetilde{J}_y). \tag{3.21}$$

with the microcanonical density $\rho(\widetilde{J}_x, \widetilde{J}_y) = (1/4\pi^2)\delta(\widetilde{J}_x - \widetilde{J}_{x0})\delta(\widetilde{J}_y - \widetilde{J}_{y0})$. Integrating out $\widetilde{J}_y$ we get

$$R_C^{(1)}(t) = \imath\sum_{n_x n_y}\left(\int d\widetilde{J}_x |\alpha_{n_x n_y}|^2 e^{\imath\widetilde{\omega}_x t}\frac{\partial}{\partial \widetilde{J}_x}\delta(\widetilde{J}_x - \widetilde{J}_{x0})\right)\Bigg|_{\widetilde{J}_y=\widetilde{J}_{y0}}, \tag{3.22}$$

which is the same as the one-dimensional linear response function (3.10). As previously we now introduce uncertainty $\Delta = \hbar$, which changes microcanonical distribution density $\delta(\widetilde{J}_x - \widetilde{J}_{x0})$ to the uniform distribution density within the width $\hbar$, $(1/\hbar)\theta((\widetilde{J}_x - \widetilde{J}_{x0}) + \hbar/2)$ $\times\theta(\hbar/2 - (\widetilde{J}_x - \widetilde{J}_{x0}))$. This results in

$$R_C^{(1)}(t) = \sum_{n_x n_y}\frac{\imath}{\hbar}|\alpha_{n_x n_y}|^2 e^{\imath\widetilde{\omega}t}\Bigg|_{\substack{\widetilde{J}_x=\widetilde{J}_{x0}-\hbar/2 \\ \widetilde{J}_y=\widetilde{J}_{y0}}} - \sum_{n_x n_y}\frac{\imath}{\hbar}|\alpha_{n_x n_y}|^2 e^{\imath\widetilde{\omega}t}\Bigg|_{\substack{\widetilde{J}_x=\widetilde{J}_{x0}+\hbar/2 \\ \widetilde{J}_y=\widetilde{J}_{y0}}}, \tag{3.23}$$

or in terms of the old variables $\{J_x, J_y\}$ the classical expression for the linear response function becomes

$$\begin{aligned} R_C^{(1)}(t) &= \sum_{n_x n_y} \frac{\imath}{\hbar} |\alpha_{n_x n_y}|^2 e^{\imath(n_x\omega_x + n_y\omega_y)t} \Bigg|_{\substack{\widetilde{J}_x = \widetilde{J}_{x0} - n_x\hbar/2 \\ \widetilde{J}_y = \widetilde{J}_{y0} - n_y\hbar/2}} \\ &\quad - \sum_{n_x n_y} \frac{\imath}{\hbar} |\alpha_{n_x n_y}|^2 e^{\imath(n_x\omega_x + n_y\omega_y)t} \Bigg|_{\substack{\widetilde{J}_x = \widetilde{J}_{x0} + n_x\hbar/2 \\ \widetilde{J}_y = \widetilde{J}_{y0} + n_y\hbar/2}} , \end{aligned} \tag{3.24}$$

From here it follows that in order to describe the transition on frequency $n_x\omega_x + n_y\omega_y$ in classical language, we need to run the classical trajectory that corresponds to the mean values of actions

$$\begin{aligned} J_x = J_{x0} + n_x\hbar/2 &= \hbar(v_x + 1/2) + n_x\hbar/2 \\ &= (\hbar(v_x + 1/2) + \hbar(v_x + n_x + 1/2))/2 \\ &= (J_{x0} + J_{xf})/2, \\ J_y = J_{y0} + n_y\hbar/2 &= \hbar(v_y + 1/2) + n_y\hbar/2 \\ &= (\hbar(v_y + 1/2) + \hbar(v_y + n_y + 1/2))/2 \\ &= (J_{y0} + J_{yf})/2, \end{aligned} \tag{3.25}$$

where J_{x0} and J_{y0} are action variables of the initial semiclassical state and J_{xf} and J_{yf} are action variables of the excited semiclassical state.

We now generalize the expression for the linear response function to the N-dimensional case (N degrees of freedom). Rotating and scaling N-dimensional action space similar to transformations (3.20) to get $\widetilde{\omega}_1 = \partial E/\partial \widetilde{J}_1 = \sum_i^N \omega_i n_i$ we reduce the N-dimensional problem to 1-dimensional problem with effective action $\tilde{J}_1$ as in Eq. (3.22). Imposing the uncertainty $\hbar$ around $\tilde{J}_1$ and transforming action-space back, we obtain the general expression for the classical linear response function of the system with N degrees of freedom

$$R_C^{(1)}(t) = \sum_{n_1 n_2 \ldots n_N} \frac{i}{\hbar} |\alpha_{n_1 n_2 \ldots n_N}|^2 e^{i(\sum^N n_j \omega_j)\cdot t}\Big|_{\vec{J}=\vec{J}_0 - \vec{n}\hbar/2} - \sum_{n_1 n_2 \ldots n_N} \frac{i}{\hbar} |\alpha_{n_1 n_2 \ldots n_N}|^2 e^{i(\sum^N n_j \omega_j)\cdot t}\Big|_{\vec{J}=\vec{J}_0 + \vec{n}\hbar/2}, \quad (3.26)$$

which means that one should run classical trajectory with mean actions $J_j = (J_{j0} + J_{jf})/2$, $j = 1, \ldots, N$, to find classical spectral amplitude $R_C^{(1)}(\omega)$ of the transition with frequency $\omega = \sum_j^N n_j \omega_j$.

The result in (3.26) reproduces the well-known Heisenberg's correspondence principle [51, 52, 53] between the quantum matrix element $\langle u|\alpha(t)|v\rangle$ and the classical $(u\text{-}v)$th Fourier component of α(t), evaluated along the trajectory with mean action $(J_u + J_v)/2$. This correspondence turns out to be almost exact for several exactly solvable systems such as harmonic and Morse oscillators [51] and explains the coincidence of classical and quantum results noted in Ref.[6] and in previous section.

3.3 Nonlinear Response

The nonlinear response function contains more detailed dynamical information than the linear response function. First, we focus on the lowest order nonlinear response function

$$R^{(2)}(\tau_1, \tau_2) = -\frac{1}{\hbar^2}\langle[[\alpha(t_2), \alpha(t_1)], \alpha(0)]\rangle, \quad (3.27)$$

where $t_2 = \tau_1 + \tau_2, t_1 = \tau_1$. The Fourier-Laplace transform of the second-order response function is defined as

$$\tilde{R}^{(2)}(\tilde{\omega}_1, \tilde{\omega}_2) = \int_0^\infty d\tau_1 \int_0^\infty d\tau_2 R^{(2)}(\tau_1, \tau_2) \exp(i\tilde{\omega}_1\tau_1 + i\tilde{\omega}_2\tau_2). \quad (3.28)$$

It is convenient to work with the symmetrized spectrum [? 49, 58]

$$S(\Omega_1, \Omega_2) = \left|\tilde{R}^{(2)}(\Omega_1, \Omega_1 + \Omega_2) + \tilde{R}^{(2)}(\Omega_2, \Omega_1 + \Omega_2)\right|, \quad (3.29)$$

which contains all the information about $2D$ response in the range of $(\Omega_1 > 0, |\Omega_2| < \Omega_1)$.

In the Heisenberg representation the time dependence of the polarization operator is given by $\alpha(t) = e^{iH_0t/\hbar}\alpha(0)e^{-iH_0t/\hbar}$. The quantum expression for $R^{(2)}(\tau_1, \tau_2)$ can be written as

$$\begin{aligned} R_Q^{(2)}(\tau_1, \tau_2) &= -\frac{1}{\hbar^2}\langle g|[[\alpha(\tau_1+\tau_2), \alpha(\tau_1)], \alpha(0)]|g\rangle \\ &= -\frac{1}{\hbar^2}\sum_v\sum_u \langle g|\alpha(0)|u\rangle\langle u|\alpha(0)|v\rangle\langle v|\alpha(0)|g\rangle \\ &\times [\exp\left(i(E_g - E_u)(\tau_1+\tau_2)/\hbar\right)\exp\left(i(E_u - E_v)\tau_1/\hbar\right) \\ &- \exp\left(i(E_u - E_v)(\tau_1+\tau_2)/\hbar\right)\exp\left(i(E_g - E_u)\tau_1/\hbar\right) \\ &- \exp\left(i(E_u - E_v)(\tau_1+\tau_2)/\hbar\right)\exp\left(i(E_v - E_g)\tau_1/\hbar\right) \\ &+ \exp\left(i(E_v - E_g)(\tau_1+\tau_2)/\hbar\right)\exp\left(i(E_u - E_v)\tau_1/\hbar\right)], \end{aligned} \tag{3.30}$$

where E_k is an energy eigenvalue that corresponds to a specific eigenstate $|k\rangle \equiv |k_1, k_2, ..., k_N\rangle$ of the system with N degrees of freedom. State $|g\rangle$ is the initial state which is not necessary the ground state. As mentioned previously, to obtain the classical limit for the response function we should change quantum commutators to Poisson brackets:

$$R_C^{(2)}(\tau_1, \tau_2) = \langle\{\{\alpha(t_2), \alpha(t_1)\}, \alpha(0)\}\rangle \tag{3.31}$$

Again, we use action-angle variables to describe classical motion. In previous section it was shown that the number of degrees of freedom does not play any important role, therefore we start our considerations with one-dimensional system with coordinates $\{J, \varphi\}$. As shown in Appendix A the nonlinear response function (3.31) will have the following expression

$$R_C^{(2)}(\tau_1, \tau_2) = \int dJ \int_0^{2\pi} d\varphi_0 \left(\frac{\partial\alpha(t_2)}{\partial\varphi_0}\frac{\partial\alpha(t_1)}{\partial J} - \frac{\partial\alpha(t_2)}{\partial J}\frac{\partial\alpha(t_1)}{\partial\varphi_0}\right)\frac{\partial\alpha(0)}{\partial\varphi_0}\frac{\partial\rho}{\partial J} \tag{3.32}$$

Now we make use of the quasi-periodicity of motion to decompose $\alpha(t)$ into fundamental frequencies as we did in Eq. (3.9) for the linear response function $\alpha(t) = \sum_n \alpha_n e^{in(\omega t+\varphi_0)}$. Substituting it into Eq. (3.32) and integrating out φ_0 we get

$$R_C^{(2)}(\tau_1,\tau_2) = i\sum_n\sum_m\left\{\int dJ(n+m)\left(m\alpha_m\frac{\partial\alpha_n}{\partial J}-n\alpha_n\frac{\partial\alpha_m}{\partial J}\right)\alpha_{-n-m}\frac{\partial\rho}{\partial J}\,e^{in\omega t_1+im\omega t_2}\right.$$
$$\left.+imn(m+n)(t_1-t_2)\int\alpha_m\alpha_n\alpha_{-n-m}\frac{\partial\omega}{\partial J}\frac{\partial\rho}{\partial J}e^{in\omega t_1+im\omega t_2}dJ\right\} \qquad (3.33)$$

Microcanonical distribution density $\rho=\frac{1}{2\pi}\delta(J-J_0)$ again leads to the time divergence of the response function (3.33). If we now impose uncertainty $\Delta=O(\hbar)$ with the distribution density given by Eq. (3.12) we will still have time divergence due to the second term in Eq. (3.33). Yet, if $mn=0$ there will be no second term and we may describe spectral peaks (Ω_1,Ω_2)={(0, $m\omega$), ($m\omega$, 0), ($n\omega$, $-n\omega$)} of symmetrized spectrum S(Ω_1,Ω_2) with formula (3.33) using density (3.12); these are transitions that involve only two states. Thus, one can see that by considering single classical trajectory with uncertainty $O(\hbar)$ around it one can correctly describe transitions between two states – the case of linear response function and the case of nonlinear response function for transitions (Ω_1,Ω_2)={(0, $m\omega$), ($m\omega$, 0), ($n\omega$, $-n\omega$)}. The latter explains the non-divergence of the 2nd-order response function with quadratic polarization obtained in Ref. [6]. Indeed, polarization $\alpha=(b+b^+)^2$ results only in spectral peaks $(\Omega_1,\Omega_2)=\{(0,2\omega),(2\omega,0),(2\omega,-2\omega)\}$, therefore phase averaging within uncertainty $2\hbar$ does not lead to the divergence of the classical response function at long times.

3.3.1 One-dimensional Systems

Yet, in general the second-order response function involves transitions between three states (Fig.3.1). Therefore one trajectory is not sufficient. We need to employ multiple trajectories in our method. This will solve one more problem of the quantum-classical correspondence – the correct account of anharmonicity effects on the frequencies of transitions between successive states (Fig.3.1). It was impossible to do so having only one fundamental frequency from single trajectory simulation. Multiple trajectories concept is usually used to calculate stability matrices in the classical expression of the nonlinear response function [3]. Yet, stability matrices diverge. To overcome this difficulty we

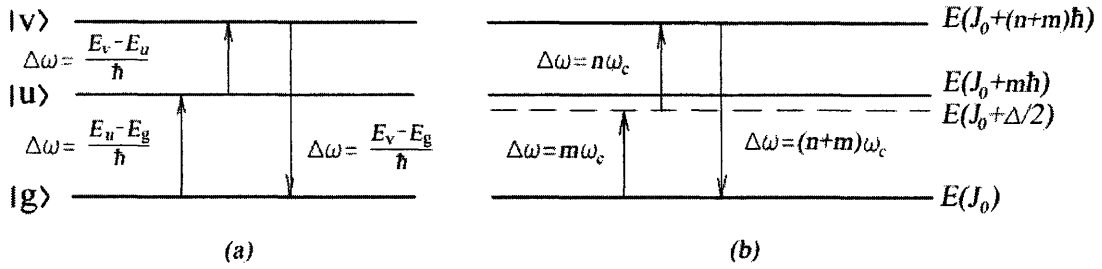

Figure 3.1: The consecutive transitions from the quantum (a) and the classical single-trajectory (b) approaches. The simple classical method on the single trajectory gives only one average frequency $\omega_c = \omega(J_0 + \Delta/2)$, which corresponds to action $J_0+\Delta/2$, and therefore is not able to account for $\Delta\omega(|g\rangle \rightarrow |u\rangle) \neq \Delta\omega(|u\rangle \rightarrow |v\rangle)$.

propose another approach. First, we start with introducing additional variables to the classical expression of the nonlinear response function (3.31) as shown in Appendix B.

$$R_C^{(2)}(\tau_1,\tau_2) = \int \{\{\alpha(J_3,\varphi_3),\alpha(J_2,\varphi_2)\}_3,\alpha(J_1,\varphi_0)\}_3 \times\frac{1}{2\pi}\delta(J_1-J_0)\delta(J_2-J_1)\delta(J_3-J_1)dJ_1dJ_2dJ_3d\varphi_0 \qquad (3.34)$$

where $\varphi_3 = \omega(J_3)t_2 + \varphi_0, \varphi_2 = \omega(J_2)t_1 + \varphi_0$ and brackets $\{\dots\}_3$ are defined as

$$\{A,B\}_3 = \frac{\partial A}{\partial\varphi_0}\left(\frac{\partial}{\partial J_1}+\frac{\partial}{\partial J_2}+\frac{\partial}{\partial J_3}\right)B - \frac{\partial B}{\partial\varphi_0}\left(\frac{\partial}{\partial J_1}+\frac{\partial}{\partial J_2}+\frac{\partial}{\partial J_3}\right)A. \qquad (3.35)$$

Polarizations α in Eq. (3.34) are now evaluated on three separate trajectories, which at this step have the same initial conditions $J_1 = J_2 = J_3 = J_0$, $\varphi_{20} = \varphi_{30} = \varphi_0$. We can also consider Eq.(3.34) in another way - as a trajectory in 4-dimensional space $\{J_1, J_2, J_3, \varphi\}$ with microcanonical distribution density

$$\rho(J_1,J_2,J_3) = \frac{1}{2\pi}\delta(J_1-J_0)\delta(J_2-J_1)\delta(J_3-J_1) \qquad (3.36)$$

As previously our main assumption is that this microcanonical distribution function $\rho(J_1, J_2, J_3)$can be replaced with the uniform distribution function within volume $O(\hbar^2)$ around the trajectory $\{(J_1, J_2, J_3, \varphi) : J_1 = J_2 = J_3 = J_0\}$. In Appendix C such an uncertainty volume is found from the condition of the *nondivergence* (i. e. absence of

derivatives $\partial\alpha(t)/\partial Jj)$ of the classical response function (3.34) (see Fig. 3.2), which is provided by the distribution density

$$\begin{aligned}\rho(J_1,J_2,J_3) &= \frac{1}{2\pi\Delta_1\Delta_2}\theta((J_1-J_0)+\Delta_1/2)\theta((\Delta_1/2)-(J_1-J_0)) \\ &\quad\times\theta\left((J_2-J_1)+\Delta_2/2\right)\theta\left((\Delta_2/2)-(J_2-J_1)\right) \\ &\quad\times\delta\left(J_3+\frac{n}{m}J_2-\frac{n+m}{m}J_1\right)\end{aligned} \tag{3.37}$$

With distribution (3.37) the classical expression for the second-order response function, as shown in Appendix C, becomes

$$R_C^{(2)}(\tau_1,\tau_2)=\sum_{n,m}\frac{-(m+n)m}{\Delta_1\Delta_2} \tag{3.38}$$

$$\times\left\{\begin{array}{l|l}
\alpha_m(J_3)\alpha_n(J_2)\alpha_{-m-n}(J_1)e^{im\omega(J_3)(\tau_1+\tau_2)+in\omega(J_2)\tau_1} & \begin{array}{l}J_1=J_0+\Delta_1/2\\ J_2=J_0+\Delta_2/2+\Delta_1/2\\ J_3=J_0+(\Delta_1-\Delta_2(n/m))/2\end{array} \\
-\alpha_m(J_3)\alpha_n(J_2)\alpha_{-m-n}(J_1)e^{im\omega(J_3)(\tau_1+\tau_2)+in\omega(J_2)\tau_1} & \begin{array}{l}J_1=J_0-\Delta_1/2\\ J_2=J_0+\Delta_2/2-\Delta_1/2\\ J_3=J_0-(\Delta_1+\Delta_2(n/m))/2\end{array} \\
-\alpha_m(J_3)\alpha_n(J_2)\alpha_{-m-n}(J_1)e^{im\omega(J_3)(\tau_1+\tau_2)+in\omega(J_2)\tau_1} & \begin{array}{l}J_1=J_0+\Delta_1/2\\ J_2=J_0-\Delta_2/2+\Delta_1/2\\ J_3=J_0+(\Delta_1+\Delta_2(n/m))/2\end{array} \\
+\alpha_m(J_3)\alpha_n(J_2)\alpha_{-m-n}(J_1)e^{im\omega(J_3)(\tau_1+\tau_2)+in\omega(J_2)\tau_1} & \begin{array}{l}J_1=J_0-\Delta_1/2\\ J_2=J_0-\Delta_2/2-\Delta_1/2\\ J_3=J_0-(\Delta_1-\Delta_2(n/m))/2\end{array}
\end{array}\right\}.$$

Comparing classical result (3.38) with quantum result (3.30) we can see that the forms of the two expressions are the same. As in the case of the linear response function the arbitrariness of the size of the uncertainty volume for the classical nonlinear response function (Fig.3.2) is removed from the requirement of coincidence of quantum and classical expressions, i.e. for $\Delta_1 = |m+n|\hbar$ and $\Delta_2 = |m|\hbar$. With this, the final formula for the classical second-order response function takes the following form

$$R_C^{(2)}(\tau_1,\tau_2) = \sum_{n,m} \frac{-1}{\hbar^2} \tag{3.39}$$

$$\times \left\{ \begin{array}{l|l} \alpha_m(J_3)\alpha_n(J_2)\alpha_{-m-n}(J_1)e^{im\omega(J_3)(\tau_1+\tau_2)+in\omega(J_2)\tau_1} & \\ & J_1=J_0+(n+m)\hbar/2 \\ & J_2=J_0+m\hbar+n\hbar/2 \\ & J_3=J_0+m\hbar/2 \\ -\alpha_m(J_3)\alpha_n(J_2)\alpha_{-m-n}(J_1)e^{im\omega(J_3)(\tau_1+\tau_2)+in\omega(J_2)\tau_1} & \\ & J_1=J_0-(n+m)\hbar/2 \\ & J_2=J_0-n\hbar/2 \\ & J_3=J_0-n\hbar-m\hbar/2 \\ -\alpha_m(J_3)\alpha_n(J_2)\alpha_{-m-n}(J_1)e^{im\omega(J_3)(\tau_1+\tau_2)+in\omega(J_2)\tau_1} & \\ & J_1=J_0+(n+m)\hbar/2 \\ & J_2=J_0+n\hbar/2 \\ & J_3=J_0+n\hbar+m\hbar/2 \\ +\alpha_m(J_3)\alpha_n(J_2)\alpha_{-m-n}(J_1)e^{im\omega(J_3)(\tau_1+\tau_2)+in\omega(J_2)\tau_1} & \\ & J_1=J_0-(n+m)\hbar/2 \\ & J_2=J_0-m\hbar-n\hbar/2 \\ & J_3=J_0-m\hbar/2 \end{array} \right\}.$$

Careful comparison of quantum expression (3.30) and classical expression (3.39) shows that agian each quantum-mechanical propagator $\langle v|\alpha|u\rangle \exp\left(i(E_v - E_u)t/\hbar\right)$ is replaced with the Fourier component $\alpha_{v-u}(J)\exp\left(i(v-u)\omega(J)t\right)|_{J=(J_v+J_u)/2}$ in the classical formula. Therefore, for instance, to calculate the classical second-order response of $1D$-

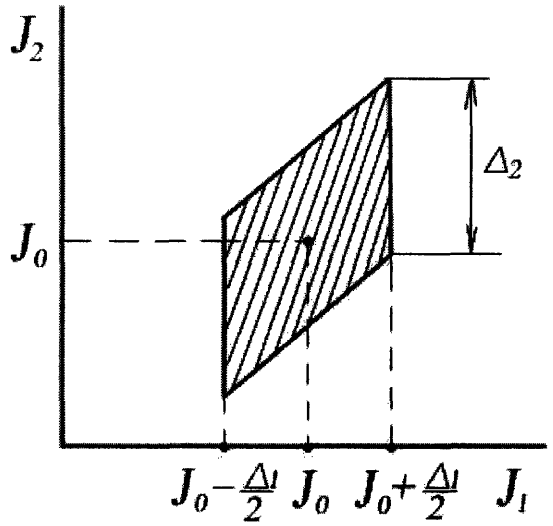

Figure 3.2: Distribution density $\rho(J_1, J_2, J_3)$ for the second-order response function in (J_1, J_2)-plane.

system in the process shown on Fig.3.1a, one should run three classical trajectories $\{J, \varphi_0\}$ with actions $J_0 + n\hbar/2$, $J_0 + n\hbar + m\hbar/2$, $J_0 + (n+m)\hbar/2$ and find fundamental frequencies and spectral components of $\alpha(t)$ along these trajectories. One can check that formula (3.39) reproduces almost exact quantum result for 1-dimensional Morse oscillator with quadratic polarization $\alpha = (b + b^+)^2$, as shown in Ref.[6].

3.3.2 nth-order Response Function for Multidimensional Systems

The result (3.39) can be generalized for the system with N degrees of freedom. As it was shown for the linear response function, by scaling and rotating multidimensional action space we may reduce a N-dimensional problem to one dimensional one. As an example, the second part of Appendix B contains transformations for the second-order response function of two-dimensional systems. The final formula for N-dimensional system have the same result as for one-dimensional system but with vectors instead of scalars (compare Eq.

(3.15) with Eq. (3.26)). The second-order classical response function for N-dimensional system reads

$$R_C^{(2)}(\tau_1,\tau_2)=\sum_{n,m}\frac{-1}{\hbar^2} \tag{3.40}$$

$$\times\left\{\begin{array}{l|l}
\alpha_{\vec{m}}(\vec{J}_3)\alpha_{\vec{n}}(\vec{J}_2)\alpha_{-\vec{m}-\vec{n}}(\vec{J}_1)e^{i\vec{m}\vec{\omega}(\vec{J}_3)(\tau_1+\tau_2)+i\vec{n}\vec{\omega}(J_2)\tau_1} & \vec{J}_1=\vec{J}_0+(\vec{n}+\vec{m})\hbar/2 \\
 & \vec{J}_2=\vec{J}_0+\vec{m}\hbar+\vec{n}\hbar/2 \\
 & \vec{J}_3=\vec{J}_0+\vec{m}\hbar/2 \\
-\alpha_{\vec{m}}(\vec{J}_3)\alpha_{\vec{n}}(\vec{J}_2)\alpha_{-\vec{m}-\vec{n}}(\vec{J}_1)e^{i\vec{m}\vec{\omega}(\vec{J}_3)(\tau_1+\tau_2)+i\vec{n}\vec{\omega}(\vec{J}_2)\tau_1} & \vec{J}_1=\vec{J}_0-(\vec{n}+\vec{m})\hbar/2 \\
 & \vec{J}_2=\vec{J}_0-\vec{n}\hbar/2 \\
 & \vec{J}_3=\vec{J}_0-\vec{n}\hbar-\vec{m}\hbar/2 \\
-\alpha_{\vec{m}}(\vec{J}_3)\alpha_{\vec{n}}(\vec{J}_2)\alpha_{-\vec{m}-\vec{n}}(\vec{J}_1)e^{i\vec{m}\vec{\omega}(\vec{J}_3)(\tau_1+\tau_2)+i\vec{n}\vec{\omega}(\vec{J}_2)\tau_1} & \vec{J}_1=\vec{J}_0+(\vec{n}+\vec{m})\hbar/2 \\
 & \vec{J}_2=\vec{J}_0+\vec{n}\hbar/2 \\
 & \vec{J}_3=\vec{J}_0+\vec{n}\hbar+\vec{m}\hbar/2 \\
+\alpha_{\vec{m}}(\vec{J}_3)\alpha_{\vec{n}}(\vec{J}_2)\alpha_{-\vec{m}-\vec{n}}(\vec{J}_1)e^{i\vec{m}\vec{\omega}(\vec{J}_3)(\tau_1+\tau_2)+i\vec{n}\vec{\omega}(\vec{J}_2)\tau_1} & \vec{J}_1=\vec{J}_0-(\vec{n}+\vec{m})\hbar/2 \\
 & \vec{J}_2=\vec{J}_0-\vec{m}\hbar-\vec{n}\hbar/2 \\
 & \vec{J}_3=\vec{J}_0-\vec{m}\hbar/2
\end{array}\right\}.$$

where $\vec{J}_k=(J_{k_1},J_{k_2},...J_{k_N})$, $\alpha_{\vec{m}}=\alpha_{m_1m_2...m_N}$ and $\vec{m}\vec{\omega}=m_1\omega_1+m_2\omega_2+...+m_N\omega_N$.

Basing on the results for the first- and second-order response functions it becomes possible to find the classical result for the nth order response function. As it was noticed previously the difference between the results for N-dimensional system and for one-dimensional system is that all scalar parameters of the *1-D* system turn to N-component vectors. Therefore, for the purpose of simplicity, we may consider only one-dimensional systems. The classical expression (3.15) for the linear response function can be rewritten in the form

$$R_C^{(1)}(t) = \sum_n \frac{i}{\hbar}\alpha_n(J_1)\alpha_{-n}(J_2)e^{in\omega(J_2)t}\Big|_{\substack{J_1=J_0-n\hbar/2 \\ J_2=J_0-n\hbar/2}} - \sum_n \frac{i}{\hbar}\alpha_n(J_1)\alpha_{-n}(J_2)e^{in\omega(J_2)t}\Big|_{\substack{J_1=J_0+n\hbar/2 \\ J_2=J_0+n\hbar/2}} \tag{3.41}$$

with distribution density within the volume $O(\hbar)$ in 3-dimensional space $\{J_1, J_2, \varphi_0\}$ given by

$$\rho(J_1, J_2) = \frac{1}{2\pi}\frac{1}{|n|\,\hbar}\tilde{\theta}_{|n|\hbar}(J_1 - J_0)\delta(J_2 - J_1), \tag{3.42}$$

where $\tilde{\theta}_\Delta(x) = \theta(x + \Delta/2)\theta(\Delta/2 - x)$ is a square-function of the width Δ. Comparing Eq. (3.42) with Eq. (3.37) it becomes clear, that in order to obtain the non-divergent classical expression for the nth-order nonlinear response function, one should impose uncertainty within the volume $O(\hbar^n)$ around the trajectory in $(n+1)$-dimensional phase space. The uncertainty volume is given for each sequence of transitions $|k_0\rangle \to |k_0+k_1\rangle \to |k_0+k_1+k_2\rangle \to ... \to |k_0+...+k_n\rangle \to |k_0\rangle$ by the distribution density

$$\begin{aligned}
&\rho(J_1, J_2, ..., J_{n+1}) = \frac{1}{2\pi}\frac{1}{|k_1|\,\hbar \times |k_1+k_2|\,\hbar \times |k_1+k_2+k_3|\,\hbar \times ...} \\
&\times\tilde{\theta}_{|k_1|\hbar}(J_1 - J_0) \times \tilde{\theta}_{|k_1+k_2|\hbar}\left(J_2 - \frac{k_1}{k_1}J_1\right) \\
&\times\tilde{\theta}_{|k_1+k_2+k_3|\hbar}\left(J_3 - \frac{k_2}{k_1+k_2}J_2 - \frac{k_1}{k_1+k_2}J_1\right) \\
&\times ... \times \tilde{\theta}_{|k_1+..+k_n|\hbar}\left(J_n - \frac{k_{n-1}}{k_1+k_2+...+k_{n-1}}J_{n-1} - ... - \frac{k_1}{k_1+k_2+...+k_{n-1}}J_1\right) \\
&\times\delta\left(J_{n+1} - \frac{k_n}{k_1+k_2+...+k_n}J_n - ... - \frac{k_1}{k_1+k_2+...+k_n}J_1\right)
\end{aligned} \tag{3.43}$$

Again, distribution functions (3.43) result in the replacement of the quantum mechanical matrix elements $\langle v|\alpha|u\rangle$ with the Fourier coefficients of $\alpha(t)$, evaluated along the classical trajectory with average action $(J_v + J_u)/2$. The latter can be verified by the detailed calculation of the 3rd-order response function $R_C^{(3)}(\tau_1, \tau_2, \tau_3)$ using the distribution density

in Eq.(3.43). It is useful to check that in the limit $\hbar \to 0$ the distribution density (3.43) becomes a microcanonical density in the form of the product of δ-functions as in Eq.(3.36).

3.4 Numerical Calculations

In this section we show how one can numerically implement the above results. We compute the second-order nonlinear response function of the two coupled oscillators and compare its symmetrized spectra $S(\Omega_1, \Omega_2)$ from quantum and classical calculations. We consider Henon-Heiles Hamiltonian [59]

$$H = \frac{1}{2}(p_x^2 + p_y^2 + \omega_x^0 x^2 + \omega_y^0 y^2) + \lambda(xy^2 + \eta \cdot x^3) \tag{3.44}$$

with $\omega_x^0 = 0.7, \omega_y^0 = 1.3, \lambda = -0.1, \eta = 0.1$.

The symmetrized spectrum of the second-order response function is given by equation (3.29). The Fourier-Laplace transform $\tilde{R}^{(2)}(\tilde{\omega}_1, \tilde{\omega}_2)$ of the quantum-mechanical result (3.30) is

$$\begin{aligned} \tilde{R}_Q^{(2)}(\tilde{\omega}_1, \tilde{\omega}_2) \;=\; & -\frac{1}{4\hbar^2} \sum_v \sum_u \langle g|\alpha(0)|u\rangle\langle u|\alpha(0)|v\rangle\langle v|\alpha(0)|g\rangle \\ & \times [\delta\left(\tilde{\omega}_1 - (E_g - E_v)/\hbar\right)\delta\left(\tilde{\omega}_2 - (E_g - E_u)/\hbar\right) \\ & -\delta\left(\tilde{\omega}_1 - (E_g - E_v)/\hbar\right)\delta\left(\tilde{\omega}_2 - (E_u - E_v)/\hbar\right) \\ & -\delta\left(\tilde{\omega}_1 - (E_u - E_g)/\hbar\right)\delta\left(\tilde{\omega}_2 - (E_u - E_v)/\hbar\right) \\ & +\delta\left(\tilde{\omega}_1 - (E_u - E_g)/\hbar\right)\delta\left(\tilde{\omega}_2 - (E_v - E_g)/\hbar\right)] \end{aligned} \tag{3.45}$$

The Hamiltonian in Eq. (3.44) is diagonalized in a local mode basis of 225 harmonic oscillator wave functions and the quantum spectrum (3.45) of the second-order response function is calculated. We consider the polarization operator in the form

$$\alpha = x^2 + y^2. \tag{3.46}$$

The symmetrized spectrum $S_Q(\Omega_1, \Omega_2)$ is plotted on Fig.3.4a. The system is considered to be initially in the state $|g\rangle = |1,1\rangle$. At this energy Henon-Heiles system obeys quasiperiodic motion as seen from numerical calculations.

The classical expression for $\tilde{R}^{(2)}(\tilde{\omega}_1, \tilde{\omega}_2)$ arises from the Fourier-Laplace transform of Eq.(3.40):

$$
\begin{aligned}
R_C^{(2)}(\tilde{\omega}_1, \tilde{\omega}_2) \;=\; & \sum_{n_x, n_y, m_x, m_y} \frac{-1}{4\hbar^2} \\
& \times \Big\{ \alpha_{m_x m_y}(\vec{J}_3)\alpha_{n_x n_y}(\vec{J}_2)\alpha_{-m_x-n_x,-m_y-n_y}(\vec{J}_1) \\
& \quad \times \delta(\tilde{\omega}_1 - \vec{m}\vec{\omega}(\vec{J}_3) - \vec{n}\vec{\omega}(\vec{J}_2))\delta(\tilde{\omega}_2 - \vec{m}\vec{\omega}(\vec{J}_3)) \Big|_{\substack{\vec{J}_1=\vec{J}_0+(\vec{n}+\vec{m})\hbar/2 \\ \vec{J}_2=\vec{J}_0+\vec{m}\hbar+(\vec{n}\hbar/2) \\ \vec{J}_3=\vec{J}_0+\vec{m}\hbar/2}} \\
& - \alpha_{m_x m_y}(\vec{J}_3)\alpha_{n_x n_y}(\vec{J}_2)\alpha_{-m_x-n_x,-m_y-n_y}(\vec{J}_1) \\
& \quad \times \delta(\tilde{\omega}_1 - \vec{m}\vec{\omega}(\vec{J}_3) - \vec{n}\vec{\omega}(\vec{J}_2))\delta(\tilde{\omega}_2 - \vec{m}\vec{\omega}(\vec{J}_3)) \Big|_{\substack{\vec{J}_1=\vec{J}_0-(\vec{n}+\vec{m})\hbar/2 \\ \vec{J}_2=\vec{J}_0-\vec{n}\hbar/2 \\ \vec{J}_3=\vec{J}_0-\vec{n}\hbar-(\vec{m}\hbar/2)}} \\
& - \alpha_{m_x m_y}(\vec{J}_3)\alpha_{n_x n_y}(\vec{J}_2)\alpha_{-m_x-n_x,-m_y-n_y}(\vec{J}_1) \\
& \quad \times \delta(\tilde{\omega}_1 - \vec{m}\vec{\omega}(\vec{J}_3) - \vec{n}\vec{\omega}(\vec{J}_2))\delta(\tilde{\omega}_2 - \vec{m}\vec{\omega}(\vec{J}_3)) \Big|_{\substack{\vec{J}_1=\vec{J}_0+(\vec{n}+\vec{m})\hbar/2 \\ \vec{J}_2=\vec{J}_0+\vec{n}\hbar/2 \\ \vec{J}_3=\vec{J}_0+\vec{n}\hbar+(\vec{m}\hbar/2)}} \\
& + \alpha_{m_x m_y}(\vec{J}_3)\alpha_{n_x n_y}(\vec{J}_2)\alpha_{-m_x-n_x,-m_y-n_y}(\vec{J}_1) \\
& \quad \times \delta(\tilde{\omega}_1 - \vec{m}\vec{\omega}(\vec{J}_3) - \vec{n}\vec{\omega}(\vec{J}_2))\delta(\tilde{\omega}_2 - \vec{m}\vec{\omega}(\vec{J}_3)) \Big|_{\substack{\vec{J}_1=\vec{J}_0-(\vec{n}+\vec{m})\hbar/2 \\ \vec{J}_2=\vec{J}_0-\vec{m}\hbar-(\vec{n}\hbar/2) \\ \vec{J}_3=\vec{J}_0-\vec{m}\hbar/2}} \Big\}
\end{aligned}
\tag{3.47}
$$

where $\vec{J} = (J_x, J_y), \vec{\omega} = (\omega_x, \omega_y), \vec{m} = (m_x, m_y), \vec{n} = (n_x, n_y)$. Given the spectrum of α(t) one can select nonvanishing terms in the above sum. The typical Fourier spectrum of α in the vicinity of the initial state $|1,1\rangle$ is shown in Fig. 3.3. It has 11 significant spectral components: $\alpha_{0,0}$, $\alpha_{1,0}$, $\alpha_{2,0}$, $\alpha_{-1,2}$, $\alpha_{0,2}$, $\alpha_{1,2}$, $\alpha_{-1,0}$, $\alpha_{-2,0}$, $\alpha_{1,-2}$, $\alpha_{0,-2}$, $\alpha_{-1,-2}$, for which

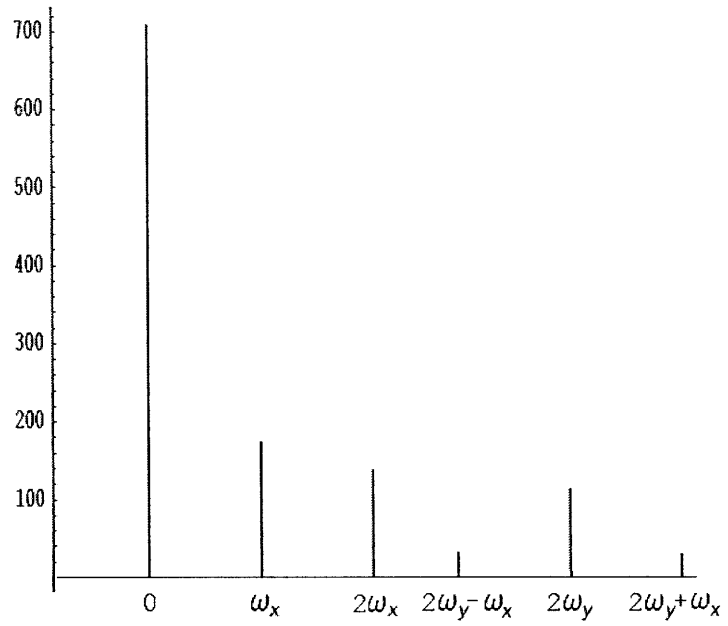

Figure 3.3: Spectral components of $\alpha(t) = x^2 + y^2$ in the region of the initial state $|1,1\rangle$. Representation of the spectral frequencies in terms of the fundamental frequencies $\{\omega_x, \omega_y\}$ leads to decomposition given by Eq. (3.5).

$\alpha_{-n_x,-n_y} = (\alpha_{n_x,n_y})^*$. Therefore classical expression (3.47) will have only those values of $\vec{m} = (m_x, m_y), \vec{n} = (n_x, n_y)$, which satisfy the equality

$$\begin{aligned} &\vec{m} + \vec{n} = \vec{k}, \\ &\vec{m}, \vec{n}, \vec{k} \in \{(0,0),(1,0),(2,0),(-1,2),(0,2),(1,2),(-1,0), \\ &\qquad (-2,0),(1,-2),(0,-2),(-1,-2)\}. \end{aligned} \tag{3.48}$$

In total, there will be 73 such combinations. To calculate the contributions of all the terms in the expression (3.47) we need to run 17 classical trajectories with action variables $J_x = \hbar(N_x + 1/2), J_y = \hbar(N_y + 1/2)$, where mean quantum numbers (N_x, N_y) are

$$\begin{aligned} &(0,1),(0.5,1),(1,1),(1.5,1),(2,1),(2.5,1), \\ &(0,2),(0.5,2),(1,2),(1.5,2),(2,2),(2.5,2), \\ &(0,3),(0.5,3),(1,3),(1.5,3),(2,3). \end{aligned} \tag{3.49}$$

The above 17 trajectories are sufficient for calculating the complete two-dimensional classical spectrum for the system (3.44) with polarization (3.46). To run the above trajectories

we need to find proper initial conditions, which will result in quantum numbers (3.49) according to formula (3.6). It was shown in Ref. [59] that semiclassical spectrum of Henon-Heiles system reasonably agrees with quantum mechanical one if the initial conditions were chosen by selecting J_i from unperturbed Hamiltonian. Thus, we take mean quantum numbers (3.49) for unperturbed actions J_x, J_y and run classical trajectories keeping track of coordinates $x(t)$, $y(t)$ as well as $\alpha(x,y)$. Applying Fourier transform to $x(t)$, $y(t)$ and $\alpha(t)$ evaluated on the same trajectory we select fundamental frequencies $\{\omega_x,\omega_y\}$ from the spectrum of $x(\omega_x,\omega_y)$, $y(\omega_x,\omega_y)$,[55, 56, 57] and find spectral components of α that correspond to these fundamental frequencies (e.g. Fig.3.3). The results of classical simulations and corresponding quantum mechanical results are presented in Table 3.1. The final symmetrized spectrum $S_C(\Omega_1, \Omega_2)$ from the classical calculations is shown on Fig.3.4(b). Both Table 3.1 and Fig.3.4 show good agreement of quantum and classical results. The discrepancy between quantum mechanical and classical calculations may arise from three reasons:(a) the semiclassical quantization does not result in exact quantum mechanical spectrum, (b) the mean-action trajectory does not appropriately approximate the quantum matrix element, (c) the classical initial conditions do not lead to the desired quantized actions (3.6). The main error of the present calculations results from the fact, that in classical simulations we have used initial conditions of the unperturbed Hamiltonian. The latter can be improved by selecting better initial conditions.

3.5 Conclusions and Discussions

In this chapter we have found that the replacement of the microcanonical distribution density with the uniform density within volume $O(\hbar^n)$ in the expanded multidimensional phase space removes the inherent time divergence of the classical linear and nonlinear response functions. Each set of transitions, which corresponds to one term in quantum mechanical formula, defines a particular quantized phase-space uncertainty volume in the classical formula. The form of uncertainty volume is determined by the requirement of non-divergence of classical response function, which restricts the class of distribution func-

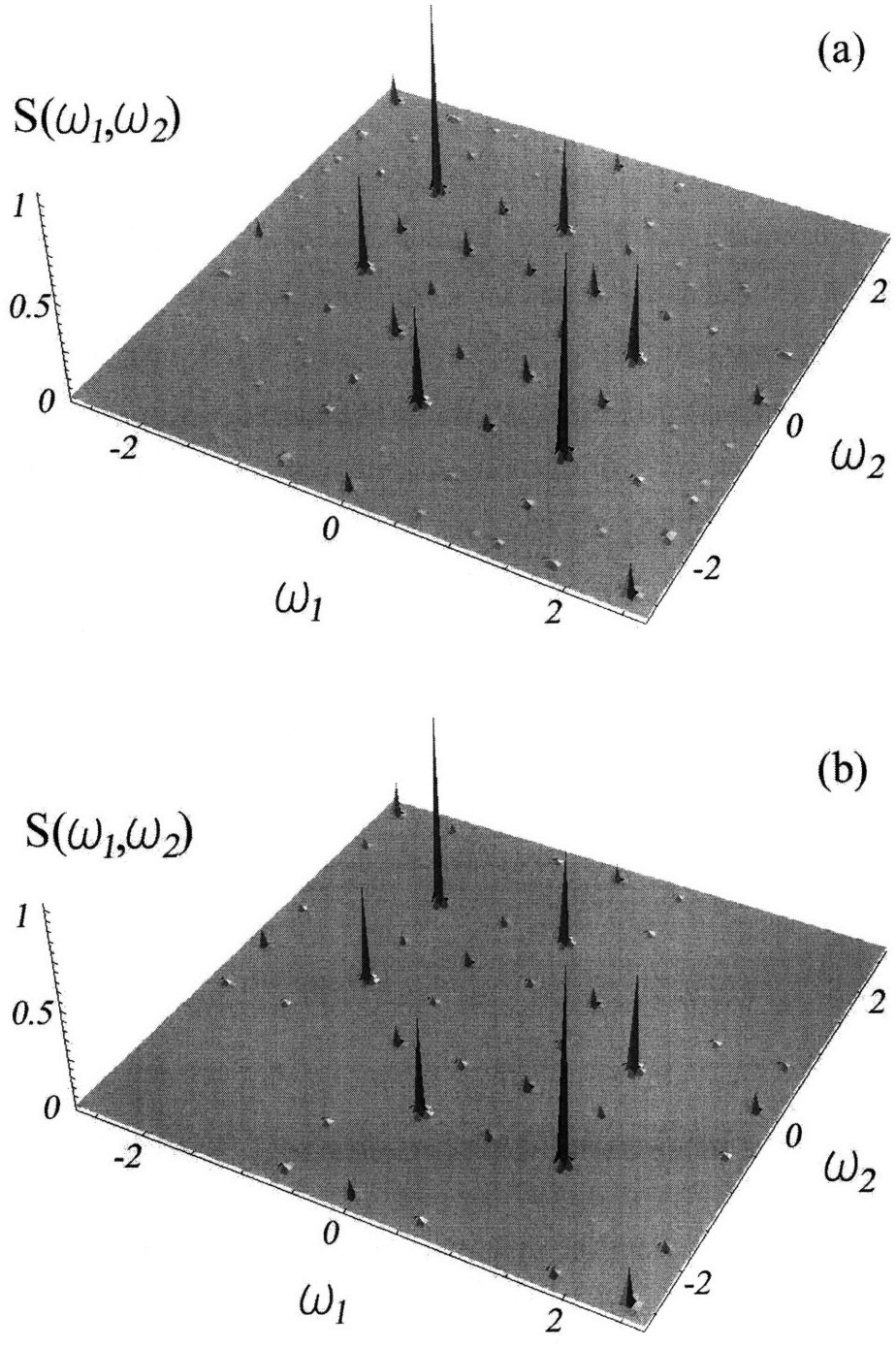

Figure 3.4: Symmetrized 2-D spectrum $S(\omega_1, \omega_2)$ for Henon-Heiles system. (a) Quantum mechanical result (using formula (3.45)); (b) classical result (using formula (3.47)).

tions and their arguments, and the requirement of a discrete spectrum, which selects only theta- and delta-functions in the expression for distribution density. The resulting classical response function is of the same form as the quantum response function for a given initial eigenstate. Classical and quantum expressions have well-defined one-to-one correspondence if the coefficients of the terms in the classical series are the same as those in the quantum formula. Setting these coefficients to be equal, we define the size of uncertainty volume and, in particular, justify the proposed phase-space quantization condition found empirically in Ref. [6]. As a result, we arrive at Heisenberg's correspondence principle, where each matrix element $\langle u|\alpha(t)|v\rangle$ in the quantum formula corresponds to the classical Fourier $(u\text{-}v)$th coefficient of α(t). The same correspondence principle was used in the spectral analysis technique proposed in Ref. [53] and showed good numerical agreement between classical and quantum results. At the same time, for the nonlinear response, we arrive at the multiple trajectories approach, which avoids the divergent interference of classical trajectories.

One may speculate on the possible reasons for the construction of the uncertainty principle in classical response theory. We present a simple physical explanation below. The energy of an isolated quantum mechanical system will not increase, i.e. a system will not respond to the external influence, unless a quantum transition occurs. And if it occurs, the action J, as pointed out by Bohr, changes discontinuously by $\Delta J = n\hbar$ for allowed n-photon transition. Our primary goal is to describe quantum mechanical response with classical dynamics. Yet, in classical mechanics there is no discontinuity – the influence of any force will result in an immediate continuous response of the system, therefore the smallest response of a classical system is zero. How is it possible to describe quantum dynamics, in which the smallest response of the system is $\Delta J = n\hbar$, with continuous theory (classical dynamics), in which the smallest response of the system is $\Delta J = 0$? One possible solution is to introduce the *uncertainty* $n\hbar$ to the latter. This is exactly what we have obtained in the present chapter – to describe a n-photon transition in the response function we need to introduce the uncertainty $n\hbar$ for the classical action. Multiple independent transitions (in the case of nonlinear response) need multiple independent

uncertainties, which results in uncertainty volume in the *expanded* action space. Therefore the expanded action space introduced in our approach is not just a result of algebraic manipulations, but is also based on intuitive physical argument. The latter also turns out to be in agreement with the results mentioned in the Introduction. Indeed, since the nonlinear response function needs a phase space averaging in the expanded phase space then the Boltzmann averaging, which is intrinsically an averaging within the original phase space, fails to converge the classical nonlinear response function for the constant-energy system with quasiperiodic motion. The concept of configurational or thermal averaging has been invoked in several classical and quasi-classical approximations of quantum dynamics, including wave-packet dynamics, non-adiabatic dynamics and centroid dynamics [60, 25, 26, 27, 28, 29, 61, 62, 63]. In the current context, phase space quantization can be generally established for quasiperiodic systems and leads to exact quantum mechanical results for a class of integrable Hamiltonians.

The results of this chapter raise a conceptual question of whether the classical expression for the response function (3.2) is an appropriate limit of the quantum expression (3.1). Indeed, the theory of semiclassical quantization of Poisson brackets [64, 65] establishes the relation between quantum commutator and Poisson brackets in the form $[\hat{f},\hat{g}] = \imath\hbar\widehat{\{f,g\}} + O(\hbar^2)$, where the remainders $O(\hbar^2)$ are power series in whose coefficients are bidifferential operators acting on f and g. The quantization parameter $\hbar$ is considered to be small but finite, thus $O(\hbar^2)$ can be neglected as long as the prefactor of $\hbar^2$ is finite. However, this is not the case in response theory. The expression for quantum response function contains commutators $[\alpha(t_2),\alpha(t_1)]$ of the same dynamical operator $\alpha(t)$ taken at different times. Thus the differential operators in $O(\hbar^2)$ will result in classical divergent derivatives $\partial^n x_k(t_2)/x_j(t_1)^n$ (n-th order stability matrices), which become infinitely large at times $t_2 \to \infty$ and elimination of these terms is not justified. We usually do not face the above problem since most applications of classical mechanics contain Poisson brackets of the functions evaluated at the same moment of time (for example, commutator of dynamical function with Hamiltonian) and therefore we can always take instantaneous coordinates and momenta as system variables avoiding

stability matrices. The $O(\hbar^2)$ is thus finite and can be omitted in the limit of $\hbar \to 0$, resulting in the correspondence principle $[\hat{f}, \hat{g}] \to \imath\hbar \{f, g\}$. Yet, we cannot do the same for the response function and the correct account of the higher order terms in is also impossible. In the present chapter we show that the classical response function can still be calculated as a limit of a quantum expression from the correspondence principle $[\hat{f}, \hat{g}] \to \imath\hbar \{f, g\}$ if we change microcanonical δ-functions to square-functions of the width $O(\hbar)$, $\frac{1}{n\hbar}\theta((J - J_0) + n\hbar/2)\theta(n\hbar/2 - (J - J_0))$. Surprisingly as it may seem, while the replacement of the distribution functions lies within the error of $O(\hbar)$, which is introduced as a result of eliminating higher order terms in the Plank constant, the classical response function changes drastically and becomes very close to quantum result once phase-space is quantized.

3.6 Appendix A: Simplification of Classical Response Functions.

In this Appendix we simplify the expression for the classical response function

$$R_C^{(2)}(\tau_1, \tau_2) = \langle\{\{\alpha(t_2), \alpha(t_1)\}, \alpha(0)\}\rangle = Tr(\{\{\alpha(t_2), \alpha(t_1)\}, \alpha(0)\}\rho). \tag{3.50}$$

Using identity $\mathrm{Tr}[\{A, B\}C] = \mathrm{Tr}[A\{B, C\}]$ we find

$$\begin{aligned} R_C^{(2)}(\tau_1, \tau_2) &= Tr(\{\alpha(t_2), \alpha(t_1)\}, \{\alpha(0), \rho\}) \\ &= \int dJ \int_0^{2\pi} d\varphi_0 \left(\frac{\partial\alpha(t_2)}{\partial\varphi_0}\frac{\partial\alpha(t_1)}{\partial J} - \frac{\partial\alpha(t_2)}{\partial J}\frac{\partial\alpha(t_1)}{\partial\varphi_0} \right) \\ &\quad \times \left(\frac{\partial\alpha(0)}{\partial\varphi_0}\frac{\partial\rho}{\partial J} - \frac{\partial\alpha(0)}{\partial J}\frac{\partial\rho}{\partial\varphi_0} \right) \end{aligned} \tag{3.51}$$

If ρ does not depend on φ, then

$$\begin{aligned} R_C^{(2)}(\tau_1, \tau_2) &= Tr(\{\alpha(t_2), \alpha(t_1)\}, \{\alpha(0), \rho\}) \\ &= \int dJ \int_0^{2\pi} d\varphi_0 \left(\frac{\partial\alpha(t_2)}{\partial\varphi_0}\frac{\partial\alpha(t_1)}{\partial J} - \frac{\partial\alpha(t_2)}{\partial J}\frac{\partial\alpha(t_1)}{\partial\varphi_0} \right) \frac{\partial\alpha(0)}{\partial\varphi_0}\frac{\partial\rho}{\partial J} \end{aligned} \tag{3.52}$$

Another approach used in the text is

$$\begin{aligned} R_C^{(2)}(\tau_1,\tau_2) &= Tr(\{\alpha(t_2),\alpha(t_1)\},\{\alpha(0),\rho\}) \\ &= Tr(\alpha(t_2),\{\alpha(t_1),\{\alpha(0),\rho\}\}) \\ &= \int dJ \int_0^{2\pi} d\varphi_0 \alpha(t_2) \left(\frac{\partial \alpha(t_1)}{\partial \varphi_0} \frac{\partial}{\partial J} \left(\frac{\partial \alpha(0)}{\partial \varphi_0} \frac{\partial \rho}{\partial J} \right) \right. \\ &\quad \left. - \frac{\partial \alpha(t_1)}{\partial J} \frac{\partial}{\partial \varphi_0} \left(\frac{\partial \alpha(0)}{\partial \varphi_0} \frac{\partial \rho}{\partial J} \right) \right) \end{aligned} \tag{3.53}$$

which is obtained by successive applications of identity $\mathrm{Tr}[\{A,B\}C] = \mathrm{Tr}[A\{B,C\}]$.

3.7 Appendix B: Expanded Phase Space

3.7.1 A. One-dimensional System

In this Appendix we introduce additional variables into the expression for the classical second-order response function and thus effectively increase the dimensionality of phase space. Using identity $\alpha(J_1) = \int \alpha(J_2)\delta(J_2 - J_1)dJ_2$ we introduce variables J_2 and J_3 into the expression (3.31)

$$\begin{aligned} R_C^{(2)}(\tau_1,\tau_2) &= \int \{\{\alpha(J_1,\varphi_0,t_2),\alpha(J_1,\varphi_0,t_1)\},\alpha(J_1,\varphi_0,0)\} \frac{1}{2\pi}\delta(J_1 - J_0)dJ_1 d\varphi_0 \\ &= \int \left\{ \left(\frac{\partial \left(\int \alpha_3(J_3)\delta(J_3 - J_1)dJ_3 \right)}{\partial \varphi_0} \frac{\partial \left(\int \alpha_2(J_2)\delta(J_2 - J_1)dJ_2 \right)}{\partial J_1} \right. \right. \\ &\quad \left. \left. - \frac{\partial \left(\int \alpha_3(J_3)\delta(J_3 - J_1)dJ_3 \right)}{\partial J_1} \frac{\partial \left(\int \alpha_2(J_2)\delta(J_2 - J_1)dJ_2 \right)}{\partial \varphi_0} \right), \alpha_1(J_1) \right\} \\ &\quad \times \frac{1}{2\pi}\delta(J_1 - J_0)dJ_1 d\varphi_0 \\ &= \int \left\{ \left(\frac{\partial \alpha_3(J_3)}{\partial \varphi_0}\delta(J_3 - J_1) \cdot \alpha_2(J_2) \frac{\partial \delta(J_2 - J_1)}{\partial J_1} \right. \right. \\ &\quad \left. \left. - \alpha_3(J_3) \frac{\partial \delta(J_3 - J_1)}{\partial J_1} \frac{\partial \alpha_2(J_2)}{\partial \varphi_0}\delta(J_2 - J_1) \right), \alpha_1(J_1) \right\} \\ &\quad \times \frac{1}{2\pi}\delta(J_1 - J_0)dJ_1 dJ_2 dJ_3 d\varphi_0 \end{aligned} \tag{3.54}$$

Using $\frac{\partial\delta(J_2-J_1)}{\partial J_1} = -\frac{\partial\delta(J_2-J_1)}{\partial J_2}$ and integrating by parts over J_3 and J_2 the terms in Eq. (3.54), we obtain

$$\begin{aligned} R_C^{(2)}(\tau_1,\tau_2) &= \int\left\{\left(\frac{\partial}{\partial\varphi_0}\left(\frac{\partial\alpha_3(J_3)}{\partial\varphi_0}\frac{\partial\alpha_2(J_2)}{\partial J_2} - \frac{\partial\alpha_3(J_3)}{\partial J_3}\frac{\partial\alpha_2(J_2)}{\partial\varphi_0}\right)\frac{\partial\alpha_1(J_1)}{\partial J_1}\right.\right. \\ &\quad \left.\left. - \left[\left(\frac{\partial}{\partial J_2}+\frac{\partial}{\partial J_3}\right)\left(\frac{\partial\alpha_3(J_3)}{\partial\varphi_0}\frac{\partial\alpha_2(J_2)}{\partial J_2} - \frac{\partial\alpha_3(J_3)}{\partial J_3}\frac{\partial\alpha_2(J_2)}{\partial\varphi_0}\right)\right]\frac{\partial\alpha_1(J_1)}{\partial\varphi_0}\right\} \\ &\quad \times\frac{1}{2\pi}\delta(J_1-J_0)\delta(J_2-J_1)\delta(J_3-J_1)dJ_1dJ_2dJ_3d\varphi_0 \end{aligned} \tag{3.55}$$

which is equivalent to

$$\begin{aligned} R_C^{(2)}(\tau_1,\tau_2) &= \int\{\{\alpha_3(J_3),\alpha_2(J_2)\}_3,\alpha_1(J_1)\}_3 \\ &\quad \times\frac{1}{2\pi}\delta(J_1-J_0)\delta(J_2-J_1)\delta(J_3-J_1)dJ_1dJ_2dJ_3d\varphi_0 \end{aligned} \tag{3.56}$$

where $\{A,B\}_3 = \frac{\partial A}{\partial\varphi_0}\left(\frac{\partial}{\partial J_1}+\frac{\partial}{\partial J_2}+\frac{\partial}{\partial J_3}\right)B - \frac{\partial B}{\partial\varphi_0}\left(\frac{\partial}{\partial J_1}+\frac{\partial}{\partial J_2}+\frac{\partial}{\partial J_3}\right)A$.

3.7.2 B. Two-dimensional System (Two Degrees of Freedom)

Repeating the same steps (3.54) - (3.55) for the system with two degrees of freedom $\{J_x,$ $J_y,$ $\varphi_x,$ $\varphi_y\}$ we will get the same expression as (3.55) but with vectors $\vec{J} = (J_x, J_y)$ and $\vec{\varphi}_0 = (\varphi_{0x}, \varphi_{0y})$ instead of scalars J and φ_0. Substituting Fourier decomposition of α

$$\begin{aligned} \alpha_j(\vec{J_j},\vec{\varphi}_j) &= \sum_{n_xn_y}\alpha^{(j)}_{n_xn_y}e^{(i(n_x\omega_x^{(j)}+n_y\omega_y^{(j)})\cdot t+i(n_x\varphi_{0x}+n_y\varphi_{0y}))} \\ &\equiv \sum_{\vec{n}}\tilde{\alpha}^{(j)}_{\vec{n}}, \end{aligned} \tag{3.57}$$

the classical second-order response function for the system with two degrees of freedom takes the form

$$
\begin{aligned}
&R_C^{(2)}(\tau_1,\tau_2) \\
&= \sum_{\vec{n}_1\vec{n}_2\vec{n}_3} \int \left\{ \left(i \left(i\tilde{\alpha}^{(3)}_{\vec{n}_3} \left[n_{3x}\frac{\partial}{\partial J_{2x}} + n_{3y}\frac{\partial}{\partial J_{2y}} \right] \tilde{\alpha}^{(2)}_{\vec{n}_2} - i\tilde{\alpha}^{(2)}_{\vec{n}_2} \left[n_{2x}\frac{\partial}{\partial J_{3x}} + n_{2y}\frac{\partial}{\partial J_{3y}} \right] \tilde{\alpha}^{(3)}_{\vec{n}_3} \right) \right. \\
&\times \left[(n_{3x}+n_{2x})\frac{\partial}{\partial J_{1x}} + (n_{3y}+n_{2y})\frac{\partial}{\partial J_{1y}} \right] \tilde{\alpha}^{(1)}_{\vec{n}_1} \\
&-i\tilde{\alpha}^{(1)}_{\vec{n}_1} \left[(n_{3x}+n_{2x}) \left(\frac{\partial}{\partial J_{2x}} + \frac{\partial}{\partial J_{3x}} \right) + (n_{3y}+n_{2y}) \left(\frac{\partial}{\partial J_{2y}} + \frac{\partial}{\partial J_{3y}} \right) \right] \\
&\times \left. \left(i\tilde{\alpha}^{(3)}_{\vec{n}_3} \left[n_{3x}\frac{\partial}{\partial J_{2x}} + n_{3y}\frac{\partial}{\partial J_{2y}} \right] \tilde{\alpha}^{(2)}_{\vec{n}_2} - i\tilde{\alpha}^{(2)}_{\vec{n}_2} \left[n_{2x}\frac{\partial}{\partial J_{3x}} + n_{2y}\frac{\partial}{\partial J_{3y}} \right] \tilde{\alpha}^{(3)}_{\vec{n}_3} \right) \right\} \\
&\times \frac{1}{4\pi^2}\delta(\vec{J}_1-\vec{J}_0)\delta(\vec{J}_2-\vec{J}_1)\delta(\vec{J}_3-\vec{J}_1)d\vec{J}_1 d\vec{J}_2 d\vec{J}_3 d\vec{\varphi}_0
\end{aligned}
\tag{3.58}
$$

where we have used the condition $\vec{n}_1 + \vec{n}_2 + \vec{n}_3 = 0$ for non-vanishing value of the integral over φ_0.

Now we make transformations in 6-dimensional space $\{J_{1x},\ J_{1y},\ J_{2x},\ J_{2y},\ J_{3x},\ J_{3y}\}$ and introduce new variables $\tilde{\vec{J}}_j = \vec{f}_j(\vec{J}_1, \vec{J}_2, \vec{J}_3)$, j = 1,2,3. For the particular case of $n_{3x}n_{2y} \neq n_{2x}n_{3y}$ we take such variables $\tilde{\vec{J}}_j$ that

$$
\begin{aligned}
\frac{\partial}{\partial \tilde{J}_{1x}} &= (n_{3x}+n_{2x})\frac{\partial}{\partial J_{1x}} + (n_{3y}+n_{2y})\frac{\partial}{\partial J_{1y}} \\
\frac{\partial}{\partial \tilde{J}_{2x}} &= n_{3x}\left(\frac{\partial}{\partial J_{2x}} + \frac{\partial}{\partial J_{3x}} \right) + n_{3y}\left(\frac{\partial}{\partial J_{2y}} + \frac{\partial}{\partial J_{3y}} \right) \\
\frac{\partial}{\partial \tilde{J}_{3x}} &= n_{2x}\left(\frac{\partial}{\partial J_{2x}} + \frac{\partial}{\partial J_{3x}} \right) + n_{2y}\left(\frac{\partial}{\partial J_{2y}} + \frac{\partial}{\partial J_{3y}} \right)
\end{aligned}
\tag{3.59}
$$

With this, expression (3.58) becomes

$$
\begin{aligned}
R_C^{(2)}(\tau_1,\tau_2) \;=\; & \sum_{\vec{n}_1\vec{n}_2\vec{n}_3} \int \left\{ \left(i \left(i\tilde{\alpha}^{(3)}_{\vec{n}_3} \frac{\partial}{\partial \tilde{J}_{2x}} \tilde{\alpha}^{(2)}_{\vec{n}_2} - i\tilde{\alpha}^{(2)}_{\vec{n}_2} \frac{\partial}{\partial \tilde{J}_{3x}} \tilde{\alpha}^{(3)}_{\vec{n}_3} \right) \frac{\partial}{\partial \tilde{J}_{1x}} \tilde{\alpha}^{(1)}_{\vec{n}_1} \right. \right. \\
& \left. -i\tilde{\alpha}^{(1)}_{\vec{n}_1} \left(\frac{\partial}{\partial \tilde{J}_{2x}} + \frac{\partial}{\partial \tilde{J}_{3x}} \right) \left(i\tilde{\alpha}^{(3)}_{\vec{n}_3} \frac{\partial}{\partial \tilde{J}_{2x}} \tilde{\alpha}^{(2)}_{\vec{n}_2} - i\tilde{\alpha}^{(2)}_{\vec{n}_2} \frac{\partial}{\partial \tilde{J}_{3x}} \tilde{\alpha}^{(3)}_{\vec{n}_3} \right) \right\} \\
& \times \frac{1}{4\pi^2}\delta(\vec{J}_1(\tilde{\vec{J}}_1) - \vec{J}_0)\delta(\vec{J}_2(\tilde{\vec{J}}_2, \tilde{\vec{J}}_3) - \vec{J}_1(\tilde{\vec{J}}_1)) \\
& \times \delta(\vec{J}_3(\tilde{\vec{J}}_2, \tilde{\vec{J}}_3) - \vec{J}_1(\tilde{\vec{J}}_1)) \left| \frac{\partial \vec{J}}{\partial \tilde{\vec{J}}} \right| d\tilde{\vec{J}}_1 d\tilde{\vec{J}}_2 d\tilde{\vec{J}}_3 d\vec{\varphi}_0
\end{aligned}
\tag{3.60}
$$

which after integrating out $\tilde{J}_{1y}, \tilde{J}_{2y}, \tilde{J}_{3y}$ has the same form as one-dimensional expression (3.55). The cases $n_{3x}n_{2y} = n_{2x}n_{3y}$ can be considered separately as well. Thus, each

set of transitions $|g_1, g_2, .., g_N\rangle \rightarrow |u_1, u_2, ..., u_N\rangle \rightarrow |v_1, v_2, ..., v_N\rangle \rightarrow |g_1, g_2, ..., g_N\rangle$ can be described by the appropriate series of transitions in one-dimensional system $|\tilde{g}_1\rangle \rightarrow |\tilde{u}_1\rangle \rightarrow |\tilde{v}_1\rangle \rightarrow |\tilde{g}_1\rangle$.

3.8 Appendix C: Uncertainty Distribution Density for Two-time Response

In this Appendix we derive an explicit expression for the distribution density $\rho(J_1, J_2, J_3)$ that does not lead to the divergence of the classical expression for the second-order non-linear response function

$$\begin{aligned} R_C^{(2)}(\tau_1, \tau_2) &= \int \{\{\alpha(J_3, \varphi_3), \alpha(J_2, \varphi_2)\}_3, \alpha(J_1, \varphi_0)\}_3 \\ &\quad \times \rho(J_1, J_2, J_3) dJ_1 dJ_2 dJ_3 d\varphi_0 \end{aligned} \tag{3.61}$$

Performing integration by parts we get

$$\begin{aligned} R_C^{(2)}(\tau_1, \tau_2) &= \int dJ_1 dJ_2 dJ_3 d\varphi_0 \\ &\quad \times \alpha(J_3, \varphi_3)\{\alpha(J_2, \phi_2), \{\alpha(J_1, \varphi_0), \rho(J_1, J_2, J_3)\}_3\}_3 \end{aligned} \tag{3.62}$$

Our goal is to find such function $\rho(J_1, J_2, J_3)$, that will not result in divergent derivatives $\partial\alpha(t)/\partial Jj$, and at the same time will not have derivatives $\partial^n\rho/\partial J^n$ higher than first-order ones. The latter is necessary to have discrete spectrum of $R_C^{(2)}(\Omega_1, \Omega_2)$, i.e. in the form of δ-functions. One may notice that the derivative $\left(\frac{\partial}{\partial J_1} + \frac{\partial}{\partial J_2} + \frac{\partial}{\partial J_3}\right)$ in brackets $\{A, B\}_3$ does not influence a multiplier of the form $f(aJ_1 + bJ_2 + cJ_3)$, if $a + b + c = 0$. Therefore it is reasonable to look for the expression of $\rho(J_1, J_2, J_3)$ in the form

$$\rho(J_1, J_2, J_3) = f_1(J_1) f_2(a_1 J_1 + b_1 J_2) f_3(a_2 J_1 + b_2 J_2 + c_2 J_3) \tag{3.63}$$

where $a_1 + b_1 = 0$, $a_2 + b_2 + c_2 = 0$. Substituting this into Eq. (3.62) we get

$$
\begin{aligned}
R_C^{(2)}(\tau_1,\tau_2) &= \int \left(\alpha_3 \frac{\partial \alpha_2}{\partial \varphi_0} \left[\frac{\partial}{\partial J_1} \left(\frac{\partial \alpha_1}{\partial \varphi_0} f_1'(J_1) \right) f_2(a_1 J_1 + b_1 J_2) f_3(a_2 J_1 + b_2 J_2 + c_2 J_3) \right] \right. \\
&\left. -\alpha_3 \frac{\partial \alpha_2}{\partial J_2} \left[\frac{\partial^2 \alpha_1}{\partial \varphi_0^2} f_1'(J_1) f_2(a_1 J_1 + b_1 J_2) f_3(a_2 J_1 + b_2 J_2 + c_2 J_3) \right] \right) dJ_1 dJ_2 dJ_3 d\varphi_0 \\
&= \int \left(-\alpha_3 \frac{\partial \alpha_2}{\partial \varphi_0} \frac{\partial \alpha_1}{\partial \varphi_0} f_1'(J_1) \frac{\partial}{\partial J_1} \left(f_2(a_1 J_1 + b_1 J_2) f_3(a_2 J_1 + b_2 J_2 + c_2 J_3) \right) \right. \\
&\left. +\alpha_3 \alpha_2 \frac{\partial^2 \alpha_1}{\partial \varphi_0^2} f_1'(J_1) \frac{\partial}{\partial J_2} \left(f_2(a_1 J_1 + b_1 J_2) f_3(a_2 J_1 + b_2 J_2 + c_2 J_3) \right) \right) dJ_1 dJ_2 dJ_3 d\varphi_0
\end{aligned} \tag{3.64}
$$

where in the last step integration by parts was used. After substituting Fourier decomposition $\alpha(J_j, \varphi_j) = \sum_n \alpha_n(J_j) e^{in\varphi_j}$ and integrating out φ_0, the last expression in (3.64) becomes

$$
\begin{aligned}
R_C^{(2)}(\tau_1,\tau_2) \quad &= \sum_{n,m} \int dJ_1 dJ_2 dJ_3 2\pi \alpha_m(J_3) \alpha_n(J_2) \alpha_{-m-n}(J_1) (-m-n) f_1'(J_1) \\
&\times \left(\left(n \frac{\partial}{\partial J_1} + (m+n) \frac{\partial}{\partial J_2} \right) \left(f_2(a_1 J_1 + b_1 J_2) f_3(a_2 J_1 + b_2 J_2 + c_2 J_3) \right) \right) \\
&\times \exp(im\omega(J_3) t_2 + in\omega(J_2) t_1)
\end{aligned} \tag{3.65}
$$

We now find such coefficients a_2, b_2, c_2 and a_1, b_1 that $na_2 + (n+m)b_2 = 0$. These coefficients can be chosen as $a_2 = -(n+m), b_2 = n, c_2 = m, a_1 = -1, b_1 = 1$. Finally the distribution density and the response function take the following form

$$
\rho(J_1, J_2, J_3) = f_1(J_1) f_2(J_2 - J_1) f_3(mJ_3 + nJ_2 - (n+m)J_1) \tag{3.66}
$$

$$
\begin{aligned}
R_C^{(2)}(\tau_1,\tau_2) \quad &= \quad 2\pi \sum_{n,m} \int dJ_1 dJ_2 dJ_3 \\
&\times \alpha_m(J_3) \alpha_n(J_2) \alpha_{-m-n}(J_1) (-m-n) m \\
&\times f_1'(J_1) f_2'(J_2 - J_1) f_3(mJ_3 + nJ_2 - (n+m)J_1) \\
&\exp(im\omega(J_3) t_2 + in\omega(J_2) t_1)
\end{aligned} \tag{3.67}
$$

For the microcanonical distribution density $\rho(J_1, J_2, J_3)$, functions $f_1(J_1)$ and $f_2(J_2 - J_1)$ would be δ-functions $\delta(J_1 - J_0)$ and $\delta(J_2 - J_1)$ correspondently, which lead to the

divergence of the classical response function (3.67). Yet, we may impose two uncertainties to the functions $f_1(J_1)$ and $f_2(J_2 - J_1)$ replacing δ-functions with the step-functions of the width Δ

$$
\begin{aligned}
f_1(J_1) &= \frac{1}{\Delta_1}\theta((J_1 - J_0) + \Delta_1/2)\theta(\Delta_1/2 - (J_1 - J_0)) \\
f_2(J_2 - J_1) &= \frac{1}{\Delta_2}\theta((J_2 - J_1) + \Delta_2/2)\theta(\Delta_2/2 - (J_2 - J_1))
\end{aligned}
\tag{3.68}
$$

This removes the divergence of the classical response function since no derivatives of δ-function appears in $R_C^{(2)}(\tau_1, \tau_2)$. The normalized uncertainty distribution density then has the following form

$$
\begin{aligned}
\rho(J_1, J_2, J_3) \;=\; & \frac{1}{2\pi\Delta_1\Delta_2}\theta((J_1 - J_0) + \Delta_1/2)\theta((\Delta_1/2) - (J_1 - J_0)) \\
& \times\theta\left((J_2 - J_1) + \Delta_2/2\right)\theta\left((\Delta_2/2) - (J_2 - J_1)\right) \\
& \times\delta\left(J_3 + \frac{n}{m}J_2 - \frac{n+m}{m}J_1\right)
\end{aligned}
\tag{3.69}
$$

and the classical response function (3.67) becomes

$$
\begin{aligned}
R_C^{(2)}(\tau_1, \tau_2) &= \sum_{n,m}\frac{-(m+n)m}{\Delta_1\Delta_2} \\
&\times\left\{\begin{array}{l|l}
\alpha_m(J_3)\alpha_n(J_2)\alpha_{-m-n}(J_1)e^{im\omega(J_3)(\tau_1+\tau_2)+in\omega(J_2)\tau_1} & \\
 & J_1=J_0+\Delta_1/2 \\
 & J_2=J_0+\Delta_2/2+\Delta_1/2 \\
 & J_3=J_0+(\Delta_1-\Delta_2(n/m))/2 \\
-\alpha_m(J_3)\alpha_n(J_2)\alpha_{-m-n}(J_1)e^{im\omega(J_3)(\tau_1+\tau_2)+in\omega(J_2)\tau_1} & \\
 & J_1=J_0-\Delta_1/2 \\
 & J_2=J_0+\Delta_2/2-\Delta_1/2 \\
 & J_3=J_0-(\Delta_1+\Delta_2(n/m))/2
\end{array}\right.
\end{aligned}
\tag{3.70}
$$

$$-\alpha_m(J_3)\alpha_n(J_2)\alpha_{-m-n}(J_1)e^{im\omega(J_3)(\tau_1+\tau_2)+in\omega(J_2)\tau_1}$$

$$J_1=J_0+\Delta_1/2$$

$$J_2=J_0-\Delta_2/2+\Delta_1/2$$

$$J_3=J_0+(\Delta_1+\Delta_2(n/m))/2$$

$$+\alpha_m(J_3)\alpha_n(J_2)\alpha_{-m-n}(J_1)e^{im\omega(J_3)(\tau_1+\tau_2)+in\omega(J_2)\tau_1}$$

$$\left.\begin{array}{l} J_1=J_0-\Delta_1/2 \\ J_2=J_0-\Delta_2/2-\Delta_1/2 \\ J_3=J_0-(\Delta_1-\Delta_2(n/m))/2 \end{array}\right\}.$$

Table 3.1: Quantum matrix elements and correspondent classical Fourier components for the two-dimensional Henon-Heiles system.

$\langle u_x u_y \vert\alpha(0)\vert v_x v_y\rangle^a$	$\vert\langle u_x u_y \vert\alpha(0)\vert v_x v_y\rangle\vert^a$	$\omega_Q{}^b$	$\alpha_{n_x n_y}(N_x, N_y)^c$	$\vert\alpha_{n_x n_y}(N_x, N_y)\vert^c$	$\omega_C{}^d$
$\langle 0,1\vert\alpha\vert 0,1\rangle$	2.00	0	$\alpha_{0,0}(0,1)$	2.08	0
$\langle 0,0\vert\alpha\vert 0,2\rangle$	0.54	2.552	$\alpha_{0,2}(0,1)$	0.62	2.558
$\langle 0,1\vert\alpha\vert 0,3\rangle$	0.93	2.526	$\alpha_{0,2}(0,2)$	1.03	2.527
$\langle 0,2\vert\alpha\vert 0,2\rangle$	2.94	0	$\alpha_{0,0}(0,2)$	3.12	0
$\langle 0,3\vert\alpha\vert 0,3\rangle$	3.98	0	$\alpha_{0,0}(0,3)$	4.32	0
$\langle 0,2\vert\alpha\vert 0,4\rangle$	1.32	2.498	$\alpha_{0,2}(0,3)$	1.36	2.497
$\langle 0,0\vert\alpha\vert 1,2\rangle$	0.100	3.221	$\alpha_{1,2}(0.5,1)$	0.102	3.225
$\langle 0,1\vert\alpha\vert 1,1\rangle$	0.62	0.680	$\alpha_{1,0}(0.5,1)$	0.59	0.679
$\langle 0,2\vert\alpha\vert 1,0\rangle$	0.12	1.861	$\alpha_{-1,2}(0.5,1)$	0.12	1.868
$\langle 0,1\vert\alpha\vert 1,3\rangle$	0.18	3.182	$\alpha_{1,2}(0.5,2)$	0.16	3.175
$\langle 0,2\vert\alpha\vert 1,2\rangle$	0.98	0.668	$\alpha_{1,0}(0.5,2)$	0.79	0.663
$\langle 1,1\vert\alpha\vert 0,3\rangle$	0.22	1.846	$\alpha_{-1,2}(0.5,2)$	0.23	1.848
$\langle 0,3\vert\alpha\vert 1,3\rangle$	1.36	0.655	$\alpha_{1,0}(0.5,3)$	1.38	0.652
$\langle 0,2\vert\alpha\vert 1,4\rangle$	0.27	3.140	$\alpha_{1,2}(0.5,3)$	0.22	3.137
$\langle 0,4\vert\alpha\vert 1,2\rangle$	0.32	1.830	$\alpha_{-1,2}(0.5,3)$	0.31	1.833
$\langle 1,1\vert\alpha\vert 1,1\rangle$	3.55	0	$\alpha_{0,0}(1,1)$	3.60	0
$\langle 0,1\vert\alpha\vert 2,1\rangle$	1.03	1.357	$\alpha_{2,0}(1,1)$	0.82	1.354
$\langle 1,1\vert\alpha\vert 1,3\rangle$	0.88	2.501	$\alpha_{0,2}(1,2)$	0.91	2.504
$\langle 1,2\vert\alpha\vert 1,2\rangle$	4.59	0	$\alpha_{0,0}(1,2)$	4.65	0
$\langle 0,2\vert\alpha\vert 2,2\rangle$	1.04	1.332	$\alpha_{2,0}(1,2)$	0.98	1.327
$\langle 1,3\vert\alpha\vert 1,3\rangle$	5.72	0	$\alpha_{0,0}(1,3)$	5.87	0
$\langle 1,2\vert\alpha\vert 1,4\rangle$	1.24	2.472	$\alpha_{0,2}(1,3)$	0.94	2.474
$\langle 0,3\vert\alpha\vert 2,3\rangle$	1.06	1.306	$\alpha_{2,0}(1,3)$	0.96	1.300
$\langle 1,1\vert\alpha\vert 2,1\rangle$	1.08	0.676	$\alpha_{1,0}(1.5,1)$	0.89	0.675
$\langle 1,1\vert\alpha\vert 2,3\rangle$	0.25	3.152	$\alpha_{1,2}(1.5,2)$	0.24	3.154
$\langle 2,1\vert\alpha\vert 1,3\rangle$	0.30	1.825	$\alpha_{-1,2}(1.5,2)$	0.21	1.830
$\langle 1,2\vert\alpha\vert 2,2\rangle$	1.61	0.664	$\alpha_{1,0}(1.5,2)$	1.25	0.662
$\langle 1,3\vert\alpha\vert 2,3\rangle$	2.18	0.650	$\alpha_{1,0}(1.5,3)$	2.12	0.648
$\langle 1,2\vert\alpha\vert 2,4\rangle$	0.38	3.107	$\alpha_{1,2}(1.5,3)$	0.32	3.106
$\langle 2,2\vert\alpha\vert 1,4\rangle$	0.43	1.808	$\alpha_{-1,2}(1.5,3)$	0.46	1.810
$\langle 1,1\vert\alpha\vert 3,1\rangle$	1.78	1.349	$\alpha_{2,0}(2,1)$	1.65	1.346
$\langle 2,1\vert\alpha\vert 2,1\rangle$	5.15	0	$\alpha_{0,0}(2,1)$	5.18	0
$\langle 2,2\vert\alpha\vert 2,2\rangle$	6.27	0	$\alpha_{0,0}(2,2)$	6.30	0
$\langle 1,3\vert\alpha\vert 3,3\rangle$	1.83	1.295	$\alpha_{2,0}(2,3)$	1.47	1.292
$\langle 2,3\vert\alpha\vert 2,3\rangle$	7.52	0	$\alpha_{0,0}(2,3)$	7.61	0
$\langle 2,2\vert\alpha\vert 2,4\rangle$	1.16	2.443	$\alpha_{0,2}(2,3)$	1.03	2.447
$\langle 2,1\vert\alpha\vert 3,1\rangle$	1.59	0.672	$\alpha_{1,0}(2.5,1)$	1.24	0.669
$\langle 2,2\vert\alpha\vert 3,2\rangle$	2.26	0.659	$\alpha_{1,0}(2.5,2)$	2.06	0.658
$\langle 2,1\vert\alpha\vert 3,3\rangle$	0.31	3.120	$\alpha_{1,2}(2.5,2)$	0.30	3.123
$\langle 3,1\vert\alpha\vert 2,3\rangle$	0.35	1.803	$\alpha_{-1,2}(2.5,2)$	0.34	1.808

[a] Matrix elements of the polarization operator in the eigenbasis of (3.44).

[b] Frequencies of transition between quantum states in the first column, $\omega_Q = |E_u - E_v|/\hbar$

[c] Fourier components of α(t) calculated along the classical trajectories $J_x = \hbar(N_x + 1/2)$, $J_y = \hbar(N_y + 1/2)$ (each quantum mechanical matrix element $\langle v_x, v_y|\alpha|v_x + n_x, v_y + n_y\rangle$ corresponds to Fourier coefficient $\alpha_{n_n n_y}$ evaluated on the classical trajectory $J_x = \hbar(v_x + (n_x/2) + 1/2)$, $J_y = \hbar(v_y + (n_y/2) + 1/2)$).

[d] Frequencies of the Fourier components in the fifth column, $\tilde{\omega}_{n_x n_y} = n_x\omega_x(N_x, N_y) + n_y\omega_y(N_x, N_y)$.

Chapter 4

Semiclassical Wigner Approximation

4.1 Introduction

Applications of multidimensional spectroscopy to large molecules and condensed phase systems have motivated the calculation of response functions using classical dynamics.[8, 3, 6, 5, 44, 45, 50] Classical evaluation of response functions usually employs the simple correspondence rule between the quantum commutator $[\widehat{A}, \widehat{B}]$ and the classical Poisson bracket $\imath\hbar\{A, B\}$. However the classical response theory has several problems. Van Kampen cautioned the validity of the application of classical perturbation theory to the calculation of a system's response.[10] Recent numerical and analytical results demonstrate the divergence of both linear and non-linear classical response functions at long times.[3, 5, 11] Yet, while the quantum response function is well defined and can be rigorously calculated, the problems appear after the classical limit is taken. The key question is whether the classical limit is taken appropriately. In the present chapter we follow the derivation of the classical limit from the phase space representation of quantum mechanics to show that the simple classical limit of the response function in terms of Poisson brackets is not valid at long times. The upper time limit for the quantum-classical agreement, i.e., the crossover time, is found to be inversely proportional to system's anharmonicity.

The nonlinear response $P^{(n)}(t)$ to the n-th order in the applied field $E(t)$ is described

by

$$P^{(n)}(t) = \int_0^\infty dt_n ... \int_0^\infty dt_1 \times E(t-t_n)...E(t-t_1-...t_n)R^{(n)}(t_n,...,t_1), \quad (4.1)$$

with the n-th order response function $R^{(n)}$ [1]

$$R^{(n)}(t_n,...,t_1) = \left(\frac{\imath}{\hbar}\right)^n \langle[[...[\widehat{\alpha}(\tau_n),\widehat{\alpha}(\tau_{n-1})],...,\widehat{\alpha}(\tau_1)],\widehat{\alpha}(0)]\rangle, \quad (4.2)$$

where $\tau_n = \sum_{i=1}^n t_i$ and the operator $\widehat{\alpha}(\widehat{\mathbf{x}}(t),\widehat{\mathbf{p}}(t))$ stands for the polarization operator or the dipole operator. The classical expression for the response function is obtained by replacing quantum commutators with Poisson brackets and neglecting the higher order terms in the Planck constant ($\hbar \to 0$)

$$R_c^{(n)}(t_n,...,t_1) = (-1)^n\langle\{\{...\{\alpha(\tau_n),\alpha(\tau_{n-1})\},...,\alpha(\tau_1)\},\alpha(0)\}\rangle, \quad (4.3)$$

where $\{...\}$ are Poisson brackets. But can we neglect higher order terms? To answer this question we examine the classical expansion of quantum mechanics.

4.2 Wigner Representation of Quantum Mechanics

We begin with the Weyl-Wigner-Moyal symbol-calculus approach,[66, 67, 68] which introduces Weyl transforms (scalar functions) instead of operators and the Wigner function instead of the state vector using the rule

$$symb(\widehat{A}) \equiv a_\hbar(\mathbf{p},\mathbf{q}) = \int d\mathbf{v} e^{(\imath/\hbar)\mathbf{p}\cdot\mathbf{v}}\langle\mathbf{q}-\frac{1}{2}\mathbf{v}|\widehat{A}|\mathbf{q}+\frac{1}{2}\mathbf{v}\rangle \quad (4.4)$$

The non-commutative Moyal product that corresponds to non-commutative product of quantum operators follows directly from the definition of the Weyl transform

$$symb(\widehat{A}\widehat{B}) \equiv a_\hbar * b_\hbar = a_\hbar \exp\left(\frac{\imath\hbar}{2}\left[\frac{\overleftarrow{\partial}}{\partial\mathbf{q}}\frac{\overrightarrow{\partial}}{\partial\mathbf{p}} - \frac{\overleftarrow{\partial}}{\partial\mathbf{p}}\frac{\overrightarrow{\partial}}{\partial\mathbf{q}}\right]\right) b_\hbar, \quad (4.5)$$

where the arrows indicate the direction of operation of the derivative. The quantum commutator $[\widehat{A}, \widehat{B}]$ in the phase space representation then corresponds to Moyal brackets

$$\begin{aligned}
\{a_\hbar, b_\hbar\}_\hbar &= a_\hbar * b_\hbar - b_\hbar * a_\hbar \\
&= 2\imath a_\hbar \sin\left(\frac{\hbar}{2}\left[\frac{\overleftarrow{\partial}}{\partial \mathbf{q}}\frac{\overrightarrow{\partial}}{\partial \mathbf{p}} - \frac{\overleftarrow{\partial}}{\partial \mathbf{p}}\frac{\overrightarrow{\partial}}{\partial \mathbf{q}}\right]\right) b_\hbar \\
&= \imath\hbar\left(\frac{\partial a_\hbar}{\partial \mathbf{q}}\frac{\partial b_\hbar}{\partial \mathbf{p}} - \frac{\partial a_\hbar}{\partial \mathbf{p}}\frac{\partial b_\hbar}{\partial \mathbf{q}}\right) \\
&- \frac{\imath\hbar^3}{24} a_\hbar \left(\frac{\overleftarrow{\partial}}{\partial \mathbf{q}}\frac{\overrightarrow{\partial}}{\partial \mathbf{p}} - \frac{\overleftarrow{\partial}}{\partial \mathbf{p}}\frac{\overrightarrow{\partial}}{\partial \mathbf{q}}\right)^3 b_\hbar + ... \qquad (4.6)
\end{aligned}$$

where the first term is the classical Poisson brackets multiplied by $\imath\hbar$. Hence, an appropriate phase space representation of the quantum response function takes the form

$$\begin{aligned}
&R^{(n)}(t_n, ..., t_1) = \left(\frac{\imath}{\hbar}\right)^n \int d\mathbf{p}d\mathbf{q}\rho_\hbar(\mathbf{p}, \mathbf{q}) \\
&\times\{\{...\{\alpha_\hbar(\tau_n), \alpha_\hbar(\tau_{n-1})\}_\hbar, ..., \alpha_\hbar(\tau_1)\}_\hbar, \alpha_\hbar(0)\}_\hbar. \qquad (4.7)
\end{aligned}$$

Eq.(4.7) and Eq.(4.2) are equivalent expressions of quantum response functions.

The evaluation of the classical limit of Eq.(4.7) can be illustrated for quasiperiodic systems. We introduce the semiclassical wave function[69, 70, 71, 72, 46, 62, 47] correspondent to eigenvalue $E_\mathbf{n} = H(\mathbf{J}_n = \mathbf{n}\hbar + \boldsymbol{\beta}\hbar)$:

$$\langle\boldsymbol{\varphi}|\mathbf{n}\rangle = (2\pi)^{-N/2} e^{\imath\mathbf{n}\boldsymbol{\varphi}}, \qquad (4.8)$$

where N is the dimensionality of the system and $\boldsymbol{\beta}$ is the Maslov index. We use semiclassical wave function (4.8) to express the Weyl transform in action-angle basis $(\mathbf{J}, \boldsymbol{\varphi})$, [72, 69, 70, 71]

$$\begin{aligned}
a_\hbar(\mathbf{J}_n, \boldsymbol{\varphi}) &= \int_{-\pi}^{\pi} d\boldsymbol{\xi} e^{\imath\mathbf{n}\cdot\boldsymbol{\xi}} \langle\boldsymbol{\varphi} - \frac{1}{2}\boldsymbol{\xi}|\widehat{A}|\boldsymbol{\varphi} + \frac{1}{2}\boldsymbol{\xi}\rangle \\
&= \sum_\mathbf{k} a_\mathbf{k}(\mathbf{J}_n) e^{\imath\mathbf{k}\boldsymbol{\varphi}}. \qquad (4.9)
\end{aligned}$$

The latter is just a Fourier decomposition of the classical function

$$a(\mathbf{J}, \boldsymbol{\varphi}) = \sum_\mathbf{k} a_\mathbf{k}(\mathbf{J}) e^{\imath\mathbf{k}\boldsymbol{\varphi}}. \qquad (4.10)$$

Thus, the Weyl symbols in semiclassical representation (4.8) are *classical functions* with quantized actions $\mathbf{J}$. Angle variables $\boldsymbol{\varphi}$ obey classical dynamics as required by WKB approximation (4.8). The expression (4.7) thus reads

$$R_s^{(n)}(t_n,...,t_1) = \left(\frac{\imath}{\hbar}\right)^n \sum_{\mathbf{k}} \int d\boldsymbol{\varphi}\rho(\mathbf{J}_k,\boldsymbol{\varphi})$$
$$\times\{\{...\{\alpha(\tau_n),\alpha(\tau_{n-1})\}_\hbar,...,\alpha(\tau_1)\}_\hbar,\alpha(0)\}_\hbar \tag{4.11}$$

which differs from the classical expression (4.3) in the use of the Moyal bracket

$$\{a,b\}_\hbar = 2\imath a \sin\left(\frac{\hbar}{2}\left[\frac{\overleftarrow{\partial}}{\partial\boldsymbol{\varphi}}\frac{\overrightarrow{\partial}}{\partial\mathbf{J}} - \frac{\overleftarrow{\partial}}{\partial\mathbf{J}}\frac{\overrightarrow{\partial}}{\partial\boldsymbol{\varphi}}\right]\right)b. \tag{4.12}$$

The classical limit of the Moyal bracket $\{...,...\}_\hbar$ follows directly from Eq.(4.6) by omitting the higher order terms in the Planck constant and preserving only the first (Poisson-bracket) term: $\lim_{\hbar\to 0}\{...,...\}_\hbar = \imath\hbar\{...,...\}$. Yet, this simple limit is not valid for response theory. The higher order terms in the expansion (4.6) can be omitted only if the prefactor of $\hbar^n$ is finite. However, this is not the case in response theory. The expression for the response function contains commutators of the same operator $\hat{\alpha}(t)$ evaluated at different times $[\hat{\alpha}(t),\hat{\alpha}(0)]$. The expansion (4.6) of the Moyal bracket $\{\alpha(t),\alpha(0)\}_\hbar$ thus leads to the n-th order stability matrix

$$M^{(n)} = \frac{\partial^n\mathbf{q}(t)}{\partial\mathbf{q}(0)^{n-k}\partial\mathbf{p}(0)^k} \tag{4.13}$$

in each $\hbar^n$-term. For the classical motion, stability matrices diverge as $O(t^n)$ for integrable systems and exponentially for chaotic ones. Every $\hbar^n$ term in the series of $\{\alpha(t),\alpha(0)\}_\hbar$ in Eq.(4.6) carries a time-divergent factor which becomes infinitely large as $t\to\infty$, implying that at sufficiently long times a small $\hbar^n$ will be compensated by large t^n. Thus, time divergence of the classical response function arises from the simple limit in the form (4.3) neglecting terms which can be larger than the leading term at long times. Strictly speaking, taking the usual classical limit $\hbar\to 0$ we interchange the limits $\lim_{t\to\infty}$ and $\lim_{\hbar\to 0}$ which are *non-commuting*. The noncommutativity of the limits $t\to\infty$ and $\hbar\to 0$ was pointed out by Berry in [73]. The response function (4.7) is well-defined for any moment of time, but the exchange of the two limits and the subsequent elimination of

higher order terms of Moyal bracket expansion (4.6) lead to the well-known problem of time-divergence.[10, 5, 8, 6, 11] It is worth noting that we do not meet the same difficulties with the limit $\{a,b\}_\hbar \to \imath\hbar\{a,b\}$ (and thus with the correspondence principle $[\widehat{A},\hat{B}] \leftrightarrow \imath\hbar\{a,b\}$) in equilibrium applications where the commutators are evaluated at the same moment of time. Without the presence of stability matrices, the elimination of the higher order terms in $\hbar$ is justified.

4.3 The Convergence of Semiclassical Series

Our main argument is that response functions can be systematically evaluated with classical observables by calculating higher order terms of Moyal expansion (4.6). Resummation of the infinite terms in the Moyal bracket expansion converges to a semi-classical result which has one-to-one correspondence to the quantum response function.

We demonstrate the above argument by first establishing the convergence of series for $\{a(t_2),b(t_1)\}_\hbar$ in Eq. (4.11) for regular systems. Fourier decomposition (4.10) reduces expression (4.12) to

$$\begin{aligned}\{a(t_2),b(t_1)\}_\hbar \quad &= \sum_{\mathbf{n},\mathbf{m}} \left\{ e^{\frac{\hbar\mathbf{m}}{2}\frac{\partial}{\partial\mathbf{J}}} \left(a_\mathbf{n} e^{\imath\mathbf{n}\boldsymbol{\varphi}(t_2)}\right)\right\}\left\{ e^{-\frac{\hbar\mathbf{n}}{2}\frac{\partial}{\partial\mathbf{J}}} \left(b_\mathbf{m} e^{\imath\mathbf{m}\boldsymbol{\varphi}(t_1)}\right)\right\} \\ &\quad - \sum_{\mathbf{n},\mathbf{m}} \left\{ e^{-\frac{\hbar\mathbf{m}}{2}\frac{\partial}{\partial\mathbf{J}}} \left(a_\mathbf{n} e^{\imath\mathbf{n}\boldsymbol{\varphi}(t_2)}\right)\right\}\left\{ e^{\frac{\hbar\mathbf{n}}{2}\frac{\partial}{\partial\mathbf{J}}} \left(b_\mathbf{m} e^{\imath\mathbf{m}\boldsymbol{\varphi}(t_1)}\right)\right\}, \qquad (4.14)\end{aligned}$$

where $\boldsymbol{\varphi}(t) = \boldsymbol{\omega}t + \boldsymbol{\varphi}_0$ with $\boldsymbol{\omega} = \partial E/\partial\mathbf{J}$. Suppose $\{a,b\}_\hbar$ is taken at a particular value of the quantized action $\mathbf{J} = \mathbf{J_j}$, the translational operator $\exp\left(\boldsymbol{\Delta}\frac{\partial}{\partial\mathbf{J}}\right)$ in Eq.(4.14) leads to

$$\begin{aligned}&\{a(t_2),b(t_1)\}_\hbar|_{\mathbf{J}=\mathbf{J_j}} \\ &= \sum_{\mathbf{n},\mathbf{m}} \left(a_\mathbf{n} e^{\imath\mathbf{n}\boldsymbol{\varphi}(t_2)}|_{\mathbf{J}=\mathbf{J}_j+\frac{\hbar\mathbf{m}}{2}}\right)\left(b_\mathbf{m} e^{\imath\mathbf{m}\boldsymbol{\varphi}(t_1)}|_{\mathbf{J}=\mathbf{J}_j-\frac{\hbar\mathbf{n}}{2}}\right) \\ &\quad - \sum_{\mathbf{n},\mathbf{m}} \left(a_\mathbf{n} e^{\imath\mathbf{n}\boldsymbol{\varphi}(t_2)}|_{\mathbf{J}=\mathbf{J}_j-\frac{\hbar\mathbf{m}}{2}}\right)\left(b_\mathbf{m} e^{\imath\mathbf{m}\boldsymbol{\varphi}(t_1)}|_{\mathbf{J}=\mathbf{J}_j+\frac{\hbar\mathbf{n}}{2}}\right) \qquad (4.15)\end{aligned}$$

where the summation over $\mathbf{n}$ or $\mathbf{m}$ can be truncated for a given precision. In particular,

considering the quantum matrix element $\langle \mathbf{v}|[\hat{a}(t_2), \hat{b}(t_1)]|\mathbf{v}\rangle$

$$\begin{aligned}\langle \mathbf{v}|[\hat{a}(t_2), \hat{b}(t_1)]|\mathbf{v}\rangle &= \sum_{\mathbf{n}} \Big(\langle \mathbf{v}|\hat{a}(t_2)|\mathbf{v}+\mathbf{n}\rangle \langle \mathbf{v}+\mathbf{n}|\hat{b}(t_1)|\mathbf{v}\rangle \\ &- \langle \mathbf{v}|\hat{b}(t_1)|\mathbf{v}+\mathbf{n}\rangle \langle \mathbf{v}+\mathbf{n}|\hat{a}(t_2)|\mathbf{v}\rangle \Big), \end{aligned} \tag{4.16}$$

it follows from Eq.(4.15) that its classical correspondence takes the form

$$\begin{aligned} &\int \sum_{\mathbf{n}} \{a(t_2), b(t_1)\}_{\hbar} \frac{\delta_{\mathbf{nj}}}{(2\pi)^N} d\boldsymbol{\varphi}_0 \\ &= \sum_{\mathbf{n}} \left(a_{\text{-}\mathbf{n}} e^{-\imath \mathbf{n}\omega t_2}|_{\mathbf{J}=\mathbf{J}_v+\frac{\hbar \mathbf{n}}{2}} \right) \left(b_{\mathbf{n}} e^{\imath \mathbf{n}\omega t_1}|_{\mathbf{J}=\mathbf{J}_v+\frac{\hbar \mathbf{n}}{2}} \right) \\ &- \sum_{\mathbf{n}} \left(a_{\mathbf{n}} e^{\imath \mathbf{n}\omega t_2}|_{\mathbf{J}=\mathbf{J}_v+\frac{\hbar \mathbf{n}}{2}} \right) \left(b_{\text{-}\mathbf{n}} e^{-\imath \mathbf{n}\omega t_1}|_{\mathbf{J}=\mathbf{J}_v+\frac{\hbar \mathbf{n}}{2}} \right), \end{aligned} \tag{4.17}$$

which *does not* lead to a time divergence. As a result, the semi-classical response function Eq. (4.11) maps to the quantum response function (4.2) through the Heisenberg's correspondence principle [52, 74] between the quantum matrix element and classical Fourier component: $\langle v+n|\hat{\alpha}(t)|v\rangle \leftrightarrow \alpha_n e^{\imath n\omega t}|_{J_v+n\hbar/2}$. We recently used phase space quantization to arrive at the same quantum-classical correspondence and generalized the correspondence principle to non-linear response functions.[6, 75] Surprisingly, the semiclassical expression (4.11) or equivalently Eq.(4.17) still leads to exact quantum results for several exactly solvable systems including the harmonic oscillator and Morse oscillator discussed later.[6, 75]

4.4 The Crossover Time

Let us estimate crossover time when the quantum mechanical effects in the $\hbar$-expansion of Moyal brackets $\{\alpha(t), \alpha(0)\}_{\hbar}$ start to play a significant role. For a $1D$ system the first two terms of the Moyal bracket expansion (4.12) are

$$\begin{aligned} \{\alpha(t), \alpha(0)\}_{\hbar} &= \imath\hbar \left(\frac{\partial \alpha(t)}{\partial \varphi_0} \frac{\partial \alpha(0)}{\partial J} - \frac{\partial \alpha(t)}{\partial J} \frac{\partial \alpha(0)}{\partial \varphi_0} \right) \\ &- \frac{\imath\hbar^3}{24} \alpha(t) \left(\frac{\overleftarrow{\partial}}{\partial \varphi_0} \frac{\overrightarrow{\partial}}{\partial J} - \frac{\overleftarrow{\partial}}{\partial J} \frac{\overrightarrow{\partial}}{\partial \varphi_0} \right)^3 \alpha(0) + ... \end{aligned} \tag{4.18}$$

With Fourier decomposition (4.10), the derivatives $\partial\alpha(t)/\partial J$ in the above expression results in time-divergent terms $t\imath n\frac{\partial\omega}{\partial J}\alpha_n e^{\imath n\omega t+\imath n\varphi_0}$. At long times, the first term (Poisson-bracket term) in (4.18) is of the order of the divergent derivative $|\frac{\partial\alpha(t)}{\partial J}| \sim t|\alpha_{max}\frac{\partial\omega}{\partial J}|$, the second is of the order of its highest divergent derivative $|\frac{\partial^3\alpha(t)}{\partial J^3}| \sim t^3|\alpha_{max}\left(\frac{\partial\omega}{\partial J}\right)^3|$, where $|\alpha_{max}|$ is the largest spectral component in the decomposition (4.10). Obviously the second term becomes significant when it is of the same magnitude as the first term $\hbar t|\alpha_{max}|^2\frac{\partial\omega}{\partial J} \simeq \hbar^3 t^3|\alpha_{max}|^2\left(\frac{\partial\omega}{\partial J}\right)^3$, giving the crossover time

$$t^* \simeq \frac{1}{\hbar|\frac{\partial\omega}{\partial J}|}. \tag{4.19}$$

For the harmonic systems $\partial\omega/\partial J = 0$ the crossover time (4.19) is infinite, implying that the response functions of harmonic systems can be successfully calculated using the single Poisson-brackets term. Eq.(4.19) justifies the known-equivalence of quantum and classical response functions for harmonic systems. However, any anharmonicity $\partial\omega/\partial J \neq 0$ leads to the finite value of the crossover time t^* (4.19), and the crossover time decreses with anharmonicity.[76] Beyond the critial time, $t > t^*$, one should expect the failure of the correspondence principle $[\hat{\alpha}(t), \hat{\alpha}(0)] \leftrightarrow \imath\hbar\{\alpha(t), \alpha(0)\}$ and thus the need to include higher order terms in the expansion of the Moyal product.

We illustrate the above arguments with the linear response function of constant-energy Morse oscillator with the Hamiltonian $\hat{H} = -\frac{\hbar^2}{2\mu}\frac{d^2}{dq^2} + D\left(1-e^{-\sigma q}\right)^2$. In Ref.[6], we introduced the one-photon polarization operator $\hat{\alpha} = (b + b^+)$ with its classical analog [6] $\alpha(J,\varphi) = 2\sqrt{\frac{\chi_e(J/\hbar)^2-(J/\hbar)}{1-\chi_e}}\cos(\varphi)$, where $\varphi = \left(1-\frac{2\chi_e J}{\hbar}\right)\omega_0 t + \varphi_0$, $\omega_0 = \sqrt{2D\sigma^2/\mu}$ and $\chi_e = \hbar\sigma/\sqrt{8D\mu}$. The quantum linear response function for a given energy state E_v is then

$$\begin{aligned} R^{(1)}(t) &= \left(\frac{\imath}{\hbar}\right)\langle v|[\hat{\alpha}(t), \hat{\alpha}(0)]|v\rangle \\ &= \frac{2}{(1-\chi_e)\hbar}\left(v+1-\chi_e(v+1)^2\right)\sin\left\{(1-2\chi_e(v+1))\omega_0 t\right\} \\ &- \frac{2}{(1-\chi_e)\hbar}\left(v-\chi_e v^2\right)\sin\left\{(1-2\chi_e v)\omega_0 t\right\}. \end{aligned} \tag{4.20}$$

The semiclassical expression (4.11)-(4.17) gives exactly the same result, when the quantization condition $J_v = \hbar(v+1/2)$ was used. The simple classical limit in Eq. (4.3)

yields

$$
\begin{aligned}
R_c^{(1)}(t) &= -\int \{\alpha(t), \alpha(0)\} \frac{\delta(J - J_v)}{2\pi} dJ d\varphi_0 \\
&= \frac{2}{(1-\chi_e)\hbar} (1 - \chi_e(2v+1)) \sin\{(1 - \chi_e(2v+1))\omega_0 t\} \\
&- \frac{\omega_0 t}{(1-\chi_e)\hbar} \left(1 - (1 - (2v+1)\chi_e)^2\right) \sin\{(1 - \chi_e(2v+1))\omega_0 t\}, \quad (4.21)
\end{aligned}
$$

which diverges linearly in time. The dependence of the semiclassical result (4.11) on the number of terms in the Moyal bracket expansion is shown on Fig.4.1 for the one-dimensional Morse oscillator with parameters $\omega_0 = 5$, $\chi_e = 0.005, \hbar = 1$ and linear polarization operator. The agreement between quantum (4.2) and classical (4.3) linear response functions indeed starts to fail after time $t^* = 1/(\hbar \left|\frac{\partial \omega}{\partial J}\right|) = 1/(2\chi_e\omega_0) = 20$ (Fig.4.1a). As we systematically include higher order terms of Moyal bracket expansion the agreement with the quantum result extends to longer times. The account of all terms of Moyal bracket expansion gives the exact quantum result.

Let us estimate the crossover time t^* for real systems, liquids CS_2 and Xe. The curvature of Morse potential $V_M(r) = \left(\epsilon \left(e^{\sigma(1-r/r_e)} - 1\right)^2 - \epsilon\right)$ coinsides well with Lennard-Jones potential $V_{LJ} = 4\epsilon\left((\xi/r)^{12} - (\xi/r)^6\right)$ for $\sigma = 6$ with $r_e = \sqrt[6]{2}\xi$.[77] For CS_2 molecule with $\mu = 76$ a.u. and mean Lennard-Jones radius $\xi \simeq 3.5\mathring{A}$ we have $t^* = 1/2\chi_e\omega_0 = \mu(\sqrt[6]{2}\xi)^2/\hbar\sigma^2 \simeq 5$ ps. For Xe, $\mu = 131$ a.u. and $\xi = 3.91\mathring{A}$, thus $t^* \simeq 10$ ps. Both times are on the same order of the time scales of the reported experiments and MD simulations [44, 50]. However, MD simulations of real systems do not observe the divergence of the response functions. It was demonstrated in [43] that the response functions for irregular dynamics may convergence. Research is being continued to find the quantum-classical correspondence for chaotic and dissipative systems. Yet, the crossover time t^* derived in this chapter remains a good estimation for the time interval of the validity of the classical approximation to the exact quantum results in response theory.

We have shown that the problem of the time divergence of the classical response function stems from the interchange of non-commuting limits $\hbar \to 0$ and $t \to \infty$, which results in the elimination of the higher order terms of the Weyl transform of quantum commutator $[\hat{A}(t), \hat{B}(0)]$. The proposed semiclassical expression (4.11) removes the clas-

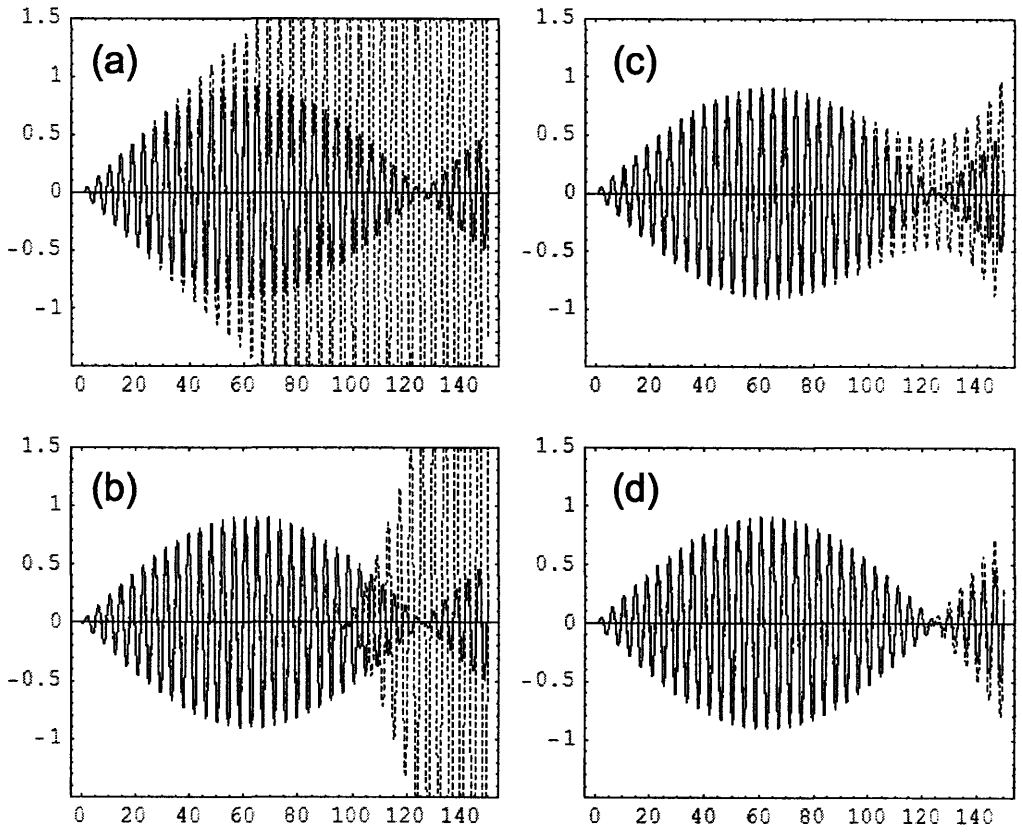

Figure 4.1: Linear response functions of constant-energy Morse oscillator. The solid lines represent quantum results from Eq.(4.2) and the dashed lines represent semiclassical result from Eq.(4.11) for the case of: (a) single Poisson-bracket term in the expansion of Moyal bracket; (b) two lowest order terms of the expansion ($\hbar$-term and $\hbar^3$-term); (c) three lowest order terms ($\hbar, \hbar^3, \hbar^5$-terms); (d) four lowest terms ($\hbar, \hbar^3, \hbar^5, \hbar^7$-terms).

sical divergence. The accuracy of classical dynamics can be systematically improved by incorporating higher order corrections beyond the crossover time.

4.5 Application of Semiclassical Corrections to Restore Quantum Recurrence of Momentum- momentum Correlation Function

In the present section we use the same idea of semiclassical representation in action-angle variables stated above to show how semiclassical corrections of the higher-order in the Planck constant restore quantum recurrence of a correlation function. In an early paper, Deutch, Kinsey, and Silbey compared classical and quantum momentum autocorrelation functions of a particle in a one-dimensional box.[78] They found that the classical autocorrelation function decays irreversibly whereas the quantum function displays recurrence, a signature of phase coherence. The classical autocorrelation function is the simple $\hbar \to 0$ limit of the quantum result, however, an analytic expansion of the quantum autocorrelation function in terms of $\hbar$ has not been obtained. The non-analytic nature of the quantum correlation function is related to the time-divergence in classical response theory.[3, 5, 6, 11, 75, 79] Specifically, the reported divergence arises from the interchange of non-commuting limits of $\hbar \to 0$ and $t \to \infty$. A semiclassical analysis of microcanonical response functions leads to the phase-space quantization,[75] which removes the classical divergence and results in a correspondence between quantum transitions and classical trajectories. In this section, we derive a semiclassical $\hbar$ expansion of the canonical correlation function using the Weyl-Wigner symbol-calculus approach and resum the expansion to obtain non-perturbative expression which captures the quantum recurrence in canonical correlation functions.

Following Ref.[78] we adopt the symmetrized quantum mechanical correlation function

$$C(t) = \frac{1}{2}\mathrm{Tr}\left[\hat{\rho}_{eq}\left(\hat{p}(t)\hat{p} + \hat{p}\hat{p}(t)\right)\right], \tag{4.22}$$

where $\hat{\rho}_{eq}$ is the Boltzmann operator. $C(t)$ is often used in literature because of its Fourier

relation with the imaginary part $\chi''(\omega)$ of the response function, $C(\omega) = \hbar \coth(\beta\hbar\omega/2)\chi''(\omega)$. For a particle in one-dimensional box, the autocorrelation function (4.22) is given by [78]

$$\begin{aligned} C(t) &= \left(\frac{\hbar^2\sqrt{\pi}}{\zeta^3 L^2 Z}\right) \sum_{k=-\infty}^{+\infty} \sum_{n=-\infty}^{+\infty} \\ &\times \exp\left[-\left((2k+1)\frac{T}{2} - \frac{n\pi}{\zeta}\right)^2\right] \\ &\times \left\{\left[\frac{2}{(2k+1)^2} - \frac{4}{(2k+1)^2}\left((2k+1)\frac{T}{2} - \frac{n\pi}{\zeta}\right)^2\right]\right. \\ &\times \cos\left((2k+1)^2\frac{T\zeta}{2}\right) - \frac{4\zeta}{(2k+1)}\left((2k+1)\frac{T}{2} - \frac{n\pi}{\zeta}\right) \\ &\times \left.\sin\left((2k+1)^2\frac{T\zeta}{2}\right)\right\} \end{aligned} \tag{4.23}$$

where $T = t\sqrt{2\pi^2/\mu\beta L^2}$, $\zeta = \hbar\sqrt{\beta\pi^2/2\mu L^2}$ and $Z = \sum_{n=1}^{\infty} \exp(-n^2\zeta^2)$ is the partition function. The quantum correlation functions (4.23) plotted on Fig.4.2 for two different temperatures show the recurrence, a characteristic of the quantum autocorrelation function. However, as shown in Ref.[78], the simple classical limit of $C(t)$

$$\begin{aligned} C_{cl}(t) &= \langle p(t)p(0)\rangle \\ &= \int_0^L dq \int_{-\infty}^{\infty} dp \rho_{eq}(p) p p(t) \end{aligned} \tag{4.24}$$

has a monotonically decaying profile (Fig.4.3).

To systematically examine the classical limit of Eq.(4.22) we use the Weyl-Wigner symbol-calculus approach. Using the property $\mathrm{Tr}(\hat{A}\hat{B}) = (2\pi\hbar)^{-N} \int dpdq a_\hbar(p,q) b_\hbar(p,q)$, the expression (4.22) takes the form

$$\begin{aligned} C(t) &= \int dpdq \rho_\hbar(p,q) \\ &\times \left\{p_\hbar(p,q,t) \cos\left[\frac{\hbar}{2}\left(\frac{\overleftarrow{\partial}}{\partial q}\frac{\overrightarrow{\partial}}{\partial p} - \frac{\overleftarrow{\partial}}{\partial p}\frac{\overrightarrow{\partial}}{\partial q}\right)\right] p_\hbar(p,q)\right\}. \end{aligned} \tag{4.25}$$

The Weyl symbol $p_\hbar(p,q)$ in coordinates $\{p,q\}$ is the phase space momentum p, which follows directly from the expression (4.4) written in $|p\rangle$ basis. However, $p_\hbar(p,q,t)$ does not have a simple classical correspondence.[66] For this reason we switch to action-angle

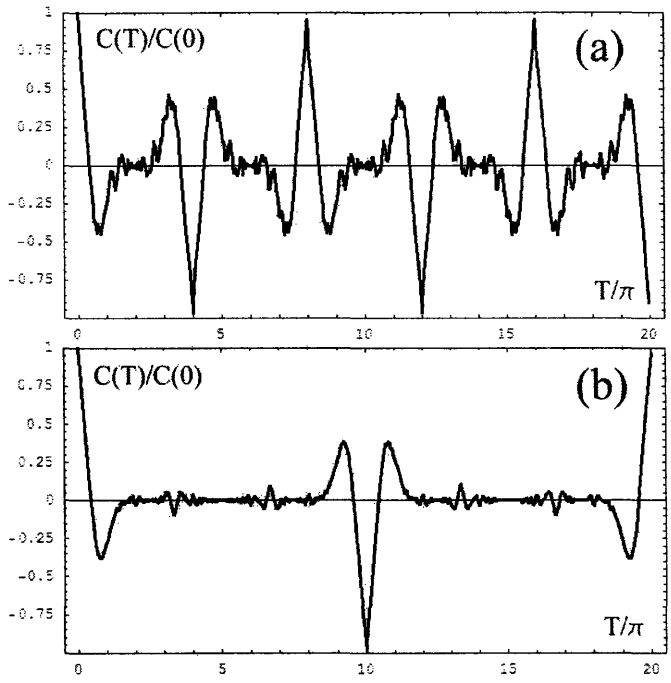

Figure 4.2: Quantum momentum autocorrelation functions for (a) $\zeta = 0.5$ and (b) $\zeta = 0.2$

variables $\{J, \varphi\}$ and express the Weyl transform (4.4) in $|\varphi\rangle$ basis. The Weyl symbols $p_\hbar(J, \varphi, t)$ and $\rho_\hbar(J, \varphi)$ for momentum and density operators in action-angle variables are

$$\begin{aligned} p_\hbar(J_n, \varphi, t) &= p[J_n, \varphi(t)] \\ &= \sum_k p_k(J_n) e^{ik(\omega t + \varphi_0)} \end{aligned} \tag{4.26}$$

$$\begin{aligned} \rho_\hbar(J_n, \varphi) &= \rho(J_n, \varphi) \\ &= \frac{1}{2\pi Z} \sum_m e^{-\beta E(J_m)} \delta_{n,m}, \end{aligned} \tag{4.27}$$

where Z is the partition function.

Substituting (4.26) and (4.27) into Eq.(4.25) we get the semiclassical expression

$$\begin{aligned} C(t) &= \sum_n \int d\varphi_0 \left(\frac{1}{2\pi Z} \sum_m e^{-\beta E(J_m)} \delta_{n,m} \right) \\ &\times \left\{ p(J, \varphi(t)) \cos\left[\frac{\hbar}{2} \left(\frac{\overleftarrow{\partial}}{\partial \varphi_0} \frac{\overrightarrow{\partial}}{\partial J} - \frac{\overleftarrow{\partial}}{\partial J} \frac{\overrightarrow{\partial}}{\partial \varphi_0} \right) \right] p(J, \varphi(0)) \right\} \\ &= \langle p(t) p(0) \rangle_Q - \frac{\hbar^2}{8} \left\langle p(t) \hat{\mathrm{D}}^2 p(0) \right\rangle_Q + \frac{\hbar^4}{384} \left\langle p(t) \hat{\mathrm{D}}^4 p(0) \right\rangle_Q + \ldots \end{aligned} \tag{4.28}$$

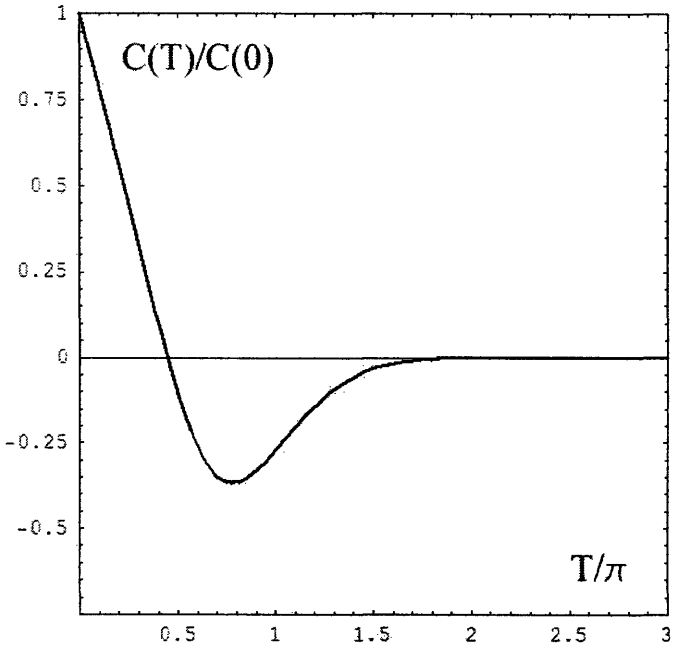

Figure 4.3: Classical momentum autocorrelation function (which is independent of temperature in scaled time coordinates)

where $\hat{\mathrm{D}} = \left(\frac{\overleftarrow{\partial}}{\partial\varphi_0}\frac{\overrightarrow{\partial}}{\partial J} - \frac{\overleftarrow{\partial}}{\partial J}\frac{\overrightarrow{\partial}}{\partial\varphi_0}\right)$ and the average $\langle ... \rangle_Q$ is taken over the phase density (4.27) with quantized actions. The phase space averaging $\langle ... \rangle_Q$ is related to the averaging $\langle ... \rangle$ over continuous phase space. Indeed, the summation over the discrete variable can be converted to an integration over the continuous variable using delta-functions [78]

$$\sum_{n=1}^{\infty} = \int dJ \sum_{n=1}^{\infty} \delta(J - n\hbar) \tag{4.29}$$

We know that for $J > 0$

$$\sum_{n=1}^{\infty} \delta(J - n\hbar) = \sum_{n=-\infty}^{\infty} \delta(J - n\hbar) = \frac{1}{\hbar} + \frac{2}{\hbar}\sum_{m=1}^{\infty} \cos\left(2\pi m J/\hbar\right). \tag{4.30}$$

Combining (4.29) with (4.30) we have

$$\langle f \rangle_Q = \frac{A}{Z\hbar}\langle f \rangle + \frac{2A}{Z\hbar}\left\langle \sum_{m=1}^{\infty} f \cos(2\pi m J/\hbar) \right\rangle. \tag{4.31}$$

where $A = \int_0^{\infty} e^{-\beta E(J)} dJ$. The WKB approximation [80, 47, 71] (4.8) assumes that motion occurs mainly in the region of $J \gg \hbar$ implying that the temperature is sufficiently high

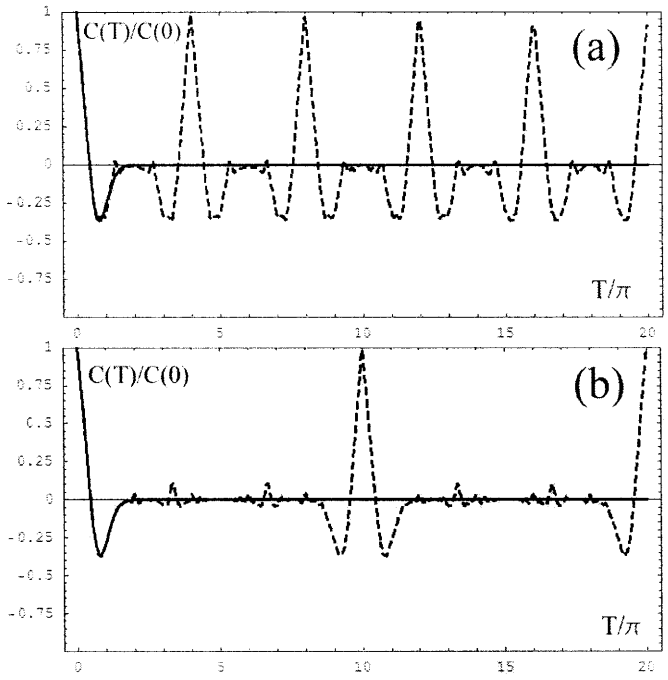

Figure 4.4: Classical momentum autocorrelation functions with averaging over continuous (solid line) and quantized (dashed line) phase space for (a) $\zeta = 0.5$ and (b) $\zeta = 0.2$

$1/\beta \gg \hbar^2\pi^2/2\mu L^2$. Thus $A/Z\hbar \simeq 1$ as shown in Ref.[78] and we may skip the overall factor $(A/Z\hbar)$ from further considerations.

The momentum autocorrelation function (4.25) thus reads

$$\begin{aligned} C(t) &= \langle p(t)p(0)\rangle + 2\sum_{m=1}^{\infty}\left\langle p(t)p(0)\cos\left(\frac{2\pi mJ}{\hbar}\right)\right\rangle \\ &- \frac{\hbar^2}{8}\left\langle p(t)\hat{\mathrm{D}}^2p(0)\right\rangle - \frac{\hbar^2}{4}\sum_{m=1}^{\infty}\left\langle \left(p(t)\hat{\mathrm{D}}^2p(0)\right)\cos\left(\frac{2\pi mJ}{\hbar}\right)\right\rangle + \ldots \end{aligned} \quad (4.32)$$

The first term in the expression (4.32) is the classical correlation function $C_{cl}(t)$ and the remaining terms are quantum corrections expressed as phase space averages of classical functions. We note that in the usual classical limit, the $\hbar^{2n}$-terms in Eq. (4.32) or (4.25) are omitted. However, every $\hbar^{2n}$-term in (4.25) has time-divergent derivatives (stability matrix) $\partial p(t)/\partial J$, which grows linearly in time for integrable systems and exponentially for chaotic systems. The small value of the factor $\hbar^{2n}$ can be always compensated by the large value of t. Thus the omission of these terms is not justified and leads to the well-known problem of time-divergence of the classical response functions [3, 5, 79].

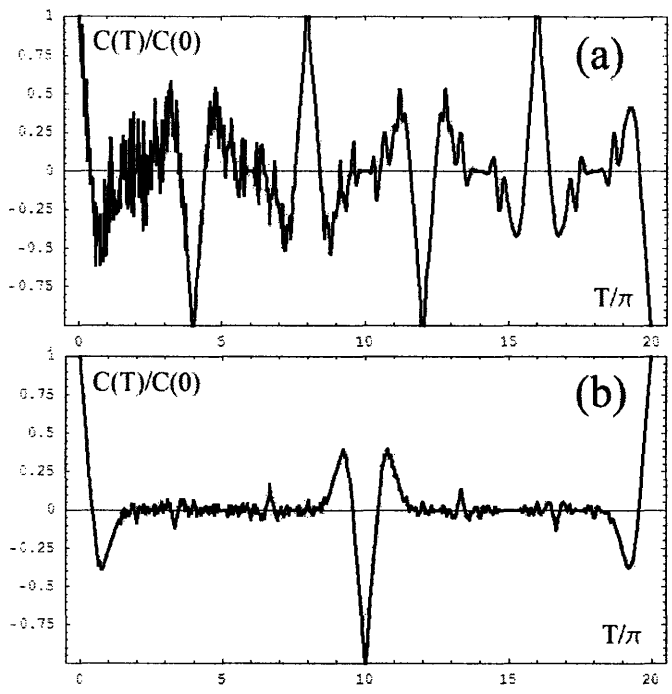

Figure 4.5: Semiclassical momentum autocorrelation functions calculated from Eq.(4.36) for (a) $\zeta = 0.5$ and (b) $\zeta = 0.2$

The above argument can be supported by calculating $C(t)$ with $\hbar^{2n}$-terms omitted. The results from the evaluation of the first two terms in Eq.(4.32): $C_{cl}(t)$ and its correction for phase space quantization, are plotted in Fig.4.4. Comparing Fig.4.2 and Fig.4.4 one can see that phase space quantization restores quantum recurrence but yet with wrong sings and thus higher-order terms in $\hbar$ are needed.

The convergence of series (4.32) can be shown analytically for the system under consideration. Substituting (4.26) and (4.31) into (4.25) we have

$$\begin{aligned} C(t) &= \int dJd\varphi_0 \left(1 + 2\sum_{m=1}^{\infty} \cos(2\pi mJ/\hbar)\right) \frac{1}{\hbar Z} e^{-\beta E(J)} \\ &\times \left\{ \sum_k p_k(J) e^{\imath k(\omega t + \varphi_0)} \cos\left[\frac{\hbar}{2}\left(\imath k \frac{\overrightarrow{\partial}}{\partial J} - \frac{\overleftarrow{\partial}}{\partial J}\imath n\right)\right] \sum_n p_n(J) e^{\imath n \varphi_0} \right\} \end{aligned} \quad (4.33)$$

Since $\exp\left(\Delta J \frac{\partial}{\partial J}\right) f(J) = f(J + \Delta J)$, then

$$C(t) = \frac{1}{\hbar Z}\int dJ \left(1+2\sum_{m=1}^{\infty}\cos(2\pi m J/\hbar)\right) e^{-\beta E(J)} \times \sum_{n=-\infty}^{\infty}\left(|p_n|^2\cos(n\omega t)\right)\Big|_{J-n\hbar/2} \quad (4.34)$$

For a particle in one-dimensional box $p_{2k+1}(J) = 2J/(2k+1)L$, $\omega = \partial E/\partial J = \pi^2 J/\mu L^2$ and

$$C(t) = \frac{1}{\hbar Z}\int dJ \left(1+2\sum_{m=1}^{\infty}\cos(2\pi m J/\hbar)\right) e^{-\beta\frac{\pi^2 J^2}{2\mu L^2}} \times \sum_{k=-\infty}^{\infty}\frac{4}{(2k+1)^2 L^2}\left(J-\frac{\hbar(2k+1)}{2}\right)^2 \cos\left\{\frac{n\pi^2 t}{\mu L^2}\left(J-\frac{\hbar(2k+1)}{2}\right)\right\} \quad (4.35)$$

The straightforward integration of the expression (4.35) gives the semiclassical expression

$$\begin{aligned} C(t) = & \left(\frac{\hbar^2\sqrt{\pi}}{\zeta^3 L^2 Z}\right)\sum_{k=-\infty}^{+\infty}\sum_{m=-\infty}^{+\infty} \\ & \times \exp\left[-\left((2k+1)\frac{T}{2}-\frac{m\pi}{\zeta}\right)^2\right] \\ & \times \left\{\left[\frac{2}{(2k+1)^2}-\frac{4}{(2k+1)^2}\left((2k+1)\frac{T}{2}-\frac{m\pi}{\zeta}\right)^2+\zeta^2\right]\right. \\ & \times \cos\left((2k+1)^2\frac{T\zeta}{2}\right)-\frac{4\zeta}{(2k+1)}\left((2k+1)\frac{T}{2}-\frac{m\pi}{\zeta}\right) \\ & \times \left.\sin\left((2k+1)^2\frac{T\zeta}{2}\right)\right\}. \end{aligned} \quad (4.36)$$

The semiclassical result (4.36) reproduces the quantum expression (4.23) almost exactly except for a constant term $\zeta^2 = \beta\hbar^2\pi^2/2L^2\mu$, which is negligible in the high temperature regime required for the semiclassical analysis leading to Eq.(4.36).

In this section we have studied the classical limit of the quantum autocorrelation function. The semiclassical expression for the momentum autocorrelation function of a particle in a one-dimensional box is obtained. The Weyl-Wigner symbol-calculus approach allows to find the explicit expressions for the semiclassical corrections to the classical momentum correlation function. Resummation of the derived semiclassical series results in an almost exact quantum formula. Because of the semiclassical nature of the analysis,

the agreement between quantum and semiclassical results improves at higher temperatures (compare Fig.4.5 with Fig.4.2).

Chapter 5

The influence of dissipation on the quantum-classical correspondence in response theory

5.1 Introduction

In the previous chapters the concept of quantum-classical correspondence was discussed for isolated systems. Yet, all real systems are open and subject to the influence of noise from surrounding. The influence of noise is especially important in chemistry, where the coupling between molecules and thermal bath is responsible for fluctuations in the structure and energy levels of a molecule, the flow of energy into and out of molecules, and thermally activated processes.

Coupling of quantum system to the surrounding results in the loss of quantum coherence in the system of interest [81, 82]. Many theoretical and experimental works have demonstrated that decoherence plays an essential role in quantum-classical correspondence and that in the presence of decoherence the quantum dynamics behaves more classically than in the absence of decoherence [83, 84, 85, 86]. This suggests that the agreement between the quantum and the classical response functions will agree better if coupling to bath is introduced. Quantitatively, we expect that the crossover time t^* (de-

fined in the previous chapter as the time interval for the classical-like behavior of quantum system) will increase if the effects of dissipation are included.

Dissipative systems are often defined as systems coupled linearly to a harmonic bath [87]. The classical dynamics of these systems is described by generalized Langevin equation (GLE), which is obtained as a continuum limit of an infinite number of bath oscillators. In this limit, the bath degrees of freedom are collectively accounted for by the addition of friction term and random-force terms to the Newton's equations of motion of the system of interest, thus resulting in a Langevin equation [87]. GLE has been a convenient analytical tool in describing all the effects of dissipation.

The semiclassical approach to the quantum-classical correspondence in response theory developed in previous chapters employs propagation along the classical trajectories as a starting point to calculation of higher order quantum corrections. Thus, it is straightforward to extend this approach to the case of dissipative classical trajectories. The idea of using classical Langevin trajectories in semiclassical calculations of the dynamics of quantum systems coupled linearly to harmonic bath was also developed in Refs. [88, 89]. It was shown [89] that in the continuum limit of the semiclassical initial value representation the path integral over system paths includes only classical GLE paths.

5.2 The Model of Dissipative System

Many condensed phase systems can be characterized by the system of interest coupled to a harmonic bath. The harmonic bath turns to be a convenient approximation since it allows an analytical description and leads to the derivation of GLE. In this section we consider a Morse oscillator linearly coupled to a harmonic bath. The system-bath Hamiltonian with system potential $V(q) = D(1 - \exp(-\sigma q))^2$ has the following form

$$H = \frac{p^2}{2} + V(q) + \frac{1}{2}\sum_{j=1}^{N}\left(p_j^2 + \omega_j^2\left(x_j - \frac{c_j}{\omega_j^2}q\right)^2\right), \tag{5.1}$$

where ω_j is a bath mode harmonic frequency and c_j is a coupling strength. The equation of motion for the system coordinate q takes the GLE form [87]

$$\ddot{q} + \frac{dV(q)}{dq} + \int_0^t dt' \gamma(t-t')\dot{q}(t) = \xi(t), \tag{5.2}$$

with the friction kernel

$$\gamma(t) = \sum_{j=1}^{N} \frac{c_j^2}{\omega_j^2} \cos(\omega_j t) \tag{5.3}$$

and random force

$$\xi(t) = \sum_{j=1}^{N} c_j \left(\left(x_j - \frac{c_j}{\omega_j^2} q(0) \right) \cos(\omega_j t) + \frac{p_j}{\omega_j} \sin(\omega_j t) \right). \tag{5.4}$$

The friction kernel is related to the correlation of random force via fluctuation-dissipation theorem

$$\langle \xi(t)\xi(t') \rangle = kT\gamma(t-t'), \tag{5.5}$$

where T is the temperature of the bath. For simplification, in the present analysis we use delta-correlated random force with friction kernel $\gamma(t-t') = \gamma\delta(t-t')$, i.e. white noise. The Langevin equation thus becomes

$$\ddot{q} + \frac{dV(q)}{dq} + \gamma\dot{q}(t) = \xi(t), \tag{5.6}$$

The semiclassical response function that we have introduced in the previous chapter has the following form

$$\begin{aligned} R_s^{(n)}(t_n, ..., t_1) &= \left(\frac{\imath}{\hbar}\right)^n \sum_{\mathbf{k}} \int d\boldsymbol{\varphi} \rho(\mathbf{J}_k, \boldsymbol{\varphi}) \\ &\times \{\{...\{\alpha(\tau_n), \alpha(\tau_{n-1})\}_\hbar, ..., \alpha(\tau_1)\}_\hbar, \alpha(0)\}_\hbar \end{aligned} \tag{5.7}$$

where $\alpha(t)$'s are classical observables evaluated along the classical trajectories and $\{...\}_\hbar$ is the Moyal bracket written in terms of classical action-angle variables

$$\{a,b\}_\hbar = 2\imath a \sin\left(\frac{\hbar}{2}\left[\frac{\overleftarrow{\partial}}{\partial\boldsymbol{\varphi}}\frac{\overrightarrow{\partial}}{\partial\mathbf{J}} - \frac{\overleftarrow{\partial}}{\partial\mathbf{J}}\frac{\overrightarrow{\partial}}{\partial\boldsymbol{\varphi}}\right]\right)b. \tag{5.8}$$

This representation was shown to be almost exact for Morse oscillator [79, 75], square-well potential [90] and is exact for harmonic potential. It is interesting that quantum corrections to the classical Poisson-bracket term in representation (5.7) come as higher order derivatives of classical functions propagated along the classical trajectories. It is straightforward to extend our semiclassical approach to the case of dissipative systems replacing Newtonian classical trajectories with Langevin classical trajectories. As mentioned in the Introduction, an argument in support of the validity of this extension is the possibility of similar replacement of classical dynamics in the initial value representation semiclassical approach discussed in Refs. [89, 88].

Due to the simplicity of the form of semiclassical corrections in the representation (5.7), which are just functions of higher order derivatives $\partial^n\alpha(t)/\partial J^n$, it is now relatively easy to study the effects of dissipation on quantum-classical correspondence. To proceed, in the next section, we derive the equations of time-evolution of stability matrix elements $\partial Q(t)/Q(0)$, $(Q = \{q,p\})$ from the Langevin equation (5.6).

5.3 Time Evolution of Stability Matrix Elements in the Presence of Dissipation

We return to the two-dimensional form of the Langevin equation (5.6)

$$\begin{aligned}\frac{dq}{dt} &= p \\ \frac{dp}{dt} &= -\left.\frac{\partial V}{\partial q}\right|_{q=q(t)} - \gamma p + \xi(t)\end{aligned} \tag{5.9}$$

Considering initial conditions $q(0), p(0)$ as parameters, we take the partial derivative of the equations (5.9) with respect to $q(0)$ and $p(0)$ to get the system of equations for the first

order stability matrix elements $M_q^q = \partial q(t)/\partial q(0)$, $M_q^p = \partial p(t)/\partial q(0)$, $M_p^q = \partial q(t)/\partial p(0)$ and $M_p^p = \partial p(t)/\partial p(0)$

$$\begin{aligned}
\frac{d}{dt}M_q^q &= M_q^p \\
\frac{d}{dt}M_q^p &= -V''(q)M_q^q - \gamma M_q^p - \gamma\delta(t) \\
\frac{d}{dt}M_p^q &= M_p^p \\
\frac{d}{dt}M_p^p &= -V''(q)M_p^q - \gamma M_p^p
\end{aligned} \tag{5.10}$$

where $V''(q) \equiv \partial^2 V/\partial q^2$. Technically speaking, the derivatives of stochastic process (5.9) are not defined. To resolve this issue, we perform differentiation with respect to $q(0)$ and $p(0)$ before taking the continuum limit of infinite number of bath oscillators [87], i.e. we get use of equations (5.3) and (5.4):

$$\begin{aligned}
\frac{\partial\xi(t)}{\partial q(0)} &= \frac{\partial}{\partial q(0)}\sum_{j=1}^{N} c_j\left(\left(x_j - \frac{c_j}{\omega_j^2}q(0)\right)\cos(\omega_j t) + \frac{p_j}{\omega_j}\sin(\omega_j t)\right) \\
&= -\sum_{j=1}^{N}\frac{c_j^2}{\omega_j^2}\cos(\omega_j t) \\
&= -\gamma(t) \\
\frac{\partial\xi(t)}{\partial p(0)} &= \frac{\partial}{\partial p(0)}\sum_{j=1}^{N} c_j\left(\left(x_j - \frac{c_j}{\omega_j^2}q(0)\right)\cos(\omega_j t) + \frac{p_j}{\omega_j}\sin(\omega_j t)\right) \\
&= 0
\end{aligned} \tag{5.11}$$

In the continuum limit of infinite number of bath oscillators, friction kernel $\gamma(t)$ is defined by spectral density function, which in our case corresponds to the white noise with $\gamma(t) = \gamma\delta(t)$. This results in the simple expression for $\partial\xi(t)/\partial q(0)$ in the form of delta-term $\gamma\delta(t)$, which appears in Eq. (5.10).

Considering equations (5.10) one can notice that, different from the original equations of motion (5.9), equations (5.10) do not have explicit stochastic terms. The only source of stochasticity comes through the stochastic behavior of $q(t)$ which is contained in the anharmonic terms of $V(q)$, i.e. in the derivative $V''(q)$ (thus, for instance, for harmonic

potential, equations (5.10) are analytical and do not contain any source of stochastisity). It is thus expected that the effect of thermal fluctuations on time behavior of stability matrices is smaller for systems with lower anharmonicities. Since time behavior of stability matrix elements explicitly influences the time behavior of quantum corrections, which stand for quantum coherence effects [79, 90], then we expect that the influence of the bath temperature on quantum decoherence in response theory will be smaller for systems with lower anharmonicity. The latter agrees with the well-known fact that an ensemble of harmonic oscillators linearly coupled to a harmonic solvent dephases only through energy loss and not through pure dephasing process [91, 92, 93, 94].

The effect of energy relaxation comes into equations (5.10) in the form of friction terms γM_p^p and γM_q^p. To better illustrate the role of these terms on the process of dephasing one may combine, for instance, the last two equations in (5.10) to get

$$\ddot{M}_p^q + \gamma \dot{M}_p^q + V''(q) M_p^q = 0. \tag{5.12}$$

The analogy between Eq.(5.12) and a damped driven harmonic oscillator can be seen representing $V''(q)$ with the leading harmonic and anharmonic terms, i.e. $V''(q) = \omega_0^2 + fq(t) \approx \omega_0^2 + fA\cos(\omega t)$, where ω_0 is the bottom-well harmonic frequency, f is the cubic anharmonicity and $q(t) = A(t)\cos(\omega t)$ is the time dependence of system's coordinate at the current value of energy. Substituting this into the expression (5.12) we get a simple picture

$$\ddot{M}_p^q + \gamma \dot{M}_p^q + \omega_0^2 M_p^q = fA(t)\cos(\omega t) M_p^q. \tag{5.13}$$

From here one can see that in the absence of friction γ and anharmonicity f, the stability matrix element M_p^q does not diverge and oscillates periodically. In the presence of anharmonicity, the amplitude of oscillations of matrix element M_p^q increases due to the driving "force" on the right side of the equation. This divergent behavior corresponds to the preservation of coherence in the original system between the two classical trajectories launched from the infinitely close initial points in phase space (since M_p^q represents the

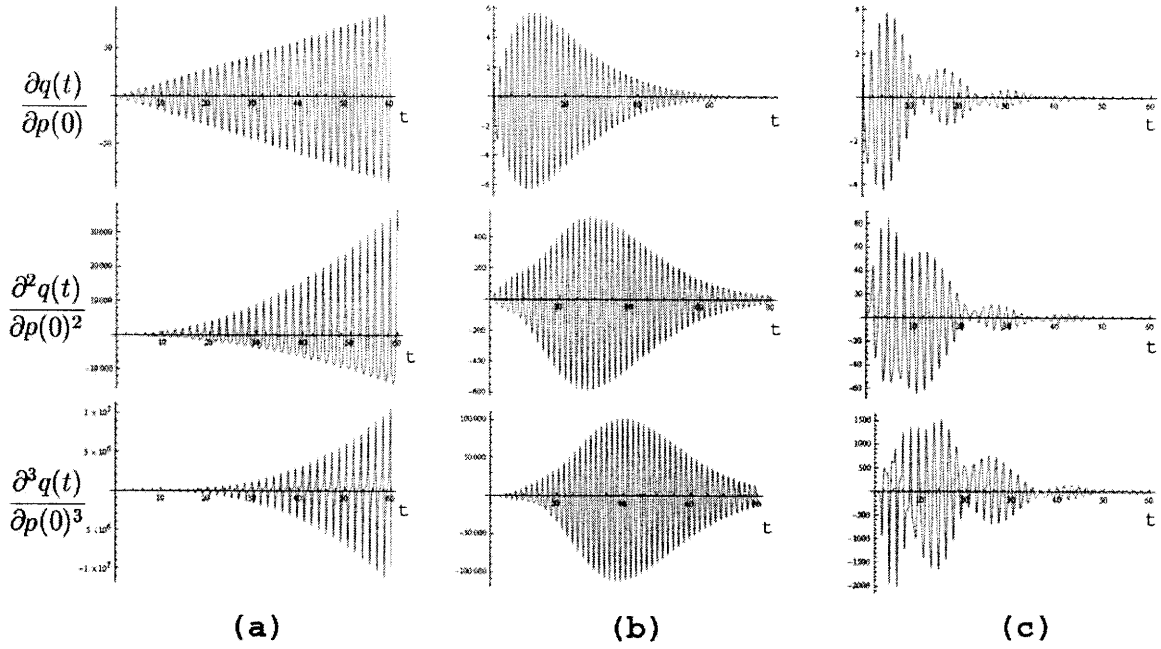

Figure 5.1: The behavior of stability derivatives for Morse oscillator in the presence of dissipation. (a) isolated Morse oscillator; (b) dissipative motion with non-zero friction γ and zero temperature; (c) non-zero friction γ and temperature T.

derivative of $q(t)$ over the initial condition $p(0)$). The introduction of friction term $\gamma \dot{M}_p^q$ kills the divergence indicating the loss of coherence between the two classical trajectories.

The equations of motion for higher order stability derivatives $\partial^n q(t)/\partial q(0)^k \partial p(0)^{n-k}$, $\partial^n p(t)/\partial q(0)^k \partial p(0)^{n-k}$ can be obtained in the same way as Eq.(5.10) by subsequent differentiation of Langevin equation (5.9) over initial conditions. Similar to the behavior of the first-order stability derivatives in the presence of dissipation, the growth of higher-order stability derivatives will be reduced due to the friction γ and the decoherence from the stochastisity of $q(t)$. The latter corresponds to dephasing due to energy relaxation and pure dephasing.

What is more important to our purposes is that because of the damping (see for instance Eq.(5.13)) the amplitude of oscillations of stability matrix elements reaches a maximum value (see Fig.5.1). This amplitude becomes smaller as the ratio f/γ of the amplitude of the "driving" force f, i.e. anharmonicity, and the damping coefficient γ decreases (this dephasing corresponds to energy relaxation) or if the phase of the "driving"

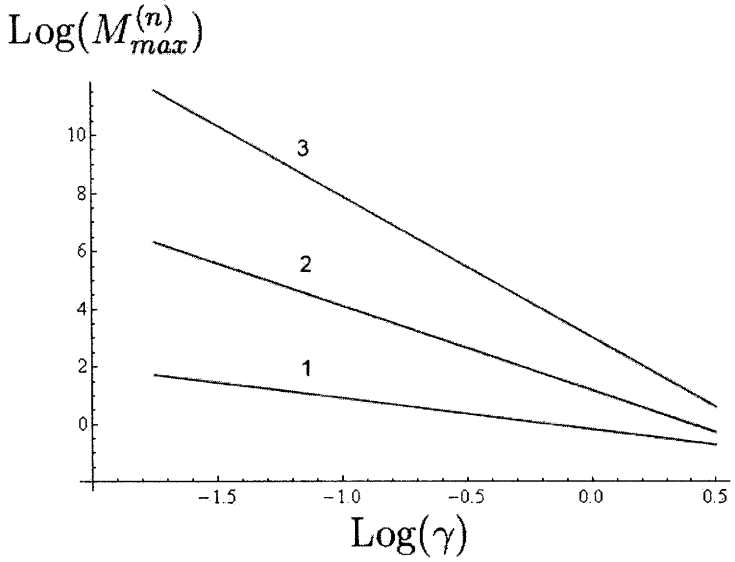

Figure 5.2: Dependence of maximum value of $M^{(n)} = \partial^n q(t)/\partial p(0)^n$, $M^{(n)}_{max} \equiv \max_t [\partial^n q(t)/\partial p(0)^n]$, on friction strength γ for a Morse oscillator at zero temperature. Numbers from 1 to 3 label $M^{(1)}_{max}$, $M^{(2)}_{max}$ and $M^{(3)}_{max}$, respectively. The decay of $M^{(n)}_{max}$ is $1/\gamma^n$.

force becomes more and more random (this corresponds to pure dephasing). At longer times the amplitude of oscillations of stability derivatives decays to zero. The higher order stability derivatives are more sensitive to dephasing (see Fig.5.2) than the lower-order derivatives, which has clear physical explanation - it is much easier to destroy the collective coherence of n classical trajectories as n increases, thus since stability derivatives $\partial^n q(t)/\partial^k q(0)\partial^{n-k} p(0)$ reflect the coherence between the n classical trajectories, their sensitivity to classical dephasing increases with n. For example, see Fig.5.2, the maximum value of $\partial q(t)/\partial q(0)$ depends on friction as $1/\gamma$, the maximum value of $\partial^2 q(t)/\partial q(0)^2$ is proportional to $1/\gamma^2$, the maximum value of $\partial^3 q(t)/\partial q(0)^3$ is proportional to $1/\gamma^3$. Thus, at some values of bath parameters γ and temperature T the higher order stability derivatives become smaller than the first-order stability derivative, indicating that higher order semiclassical corrections become less important than the first-order classical Poisson-bracket term. At these and greater values of γ and T the dynamic behavior of system of interest can be considered purely classical.

5.4 The criterion for classical behavior

In the presence of friction γ, the approximate behavior of the amplitude of $\partial^n q(t)/\partial q(0)^n$ is proportional to $t^n \exp(-\gamma t/2)$ (see Fig.5.2), which is a product of the regular divergent behavior of the n-th order stability derivative $O(t^n)$, discussed in chapter 4, and an exponential decay due to the friction. Thus, similarly to the discussion in section 4.2, in the presence of friction the Poisson-bracket term of the Moyal bracket $\{\alpha(t), \alpha(0)\}$ behaves as $\hbar \left(\frac{\partial \omega}{\partial J}\right) t \exp(-\gamma t/2)$ and the second term, $\hbar^3$-term, behaves as $\hbar^3 \left(\frac{\partial \omega}{\partial J}\right) t^3 \exp(-\gamma t/2)$. The maximum value of the Poisson-bracket term is $\sim \hbar \left(\frac{\partial \omega}{\partial J}\right) \frac{1}{\gamma}$ and the maximum value of the first correction ($\hbar^3$-term) is $\sim \hbar^3 \left(\frac{\partial \omega}{\partial J}\right)^3 \frac{1}{\gamma^3}$. The Poisson-bracket term dominates over the first correction term if

$$\hbar \left(\frac{\partial \omega}{\partial J}\right) \frac{1}{\gamma} > \hbar^3 \left(\frac{\partial \omega}{\partial J}\right)^3 \frac{1}{\gamma^3}, \tag{5.14}$$

i.e. when

$$\frac{1/\hbar(\partial \omega/\partial J)}{1/\gamma} > 1. \tag{5.15}$$

The expression in the numerator is the crossover time $t^* = 1/\hbar(\partial \omega/\partial J)$ from Eq. (4.19) and the expression in the denominator is on the order of the classical dephasing time $t_{deph} = 2/\gamma$ due to energy relaxation. The above inequality can be thus rewritten in the form

$$\frac{t^*}{t_{deph}} > 1. \tag{5.16}$$

Equation (5.16) sets a criterion on when a dissipative quantum dynamics can be considered classical. According to this inequality, quantum corrections to classical dynamics become unnecessary if classical dephasing is faster than the deviation of classical dynamics from quantum dynamics, which means that the semiclassical $\hbar^n$-terms from the Moyal bracket expansion should decay (with the characteristic time scale t_{deph}) before they become important at $t = t^*$.

Inclusion of bath temperature T will modify the above dephasing time in the well-known form [2]

$$\frac{1}{t_{deph}} = \frac{1}{2\tau_{rlx}} + \frac{1}{\tau_{p.deph.}}, \tag{5.17}$$

where τ_{rlx} is the dephasing time due to energy relaxation and $\tau_{p.deph.}$ is a pure dephasing time. For the potential with cubic anharmonicity f, i.e. $U(q) = \frac{1}{2}m\omega_0^2 q^2 + \frac{1}{6}fq^3$, coupled linearly to thermal bath with temperature T and friction kernell $\gamma(t)$, the dephasing time can be found as [93]

$$\frac{1}{t_{deph}} = \frac{Re[\widetilde{\gamma}(\imath\omega_0)]}{2} + \frac{f^2(kT)}{4m^3\omega_0^6}\widetilde{\gamma}(0), \tag{5.18}$$

where

$$\widetilde{\gamma}(s) = \int_0^\infty \gamma(t')e^{-st'}dt' \tag{5.19}$$

is a Laplace transform of the kernel. For a Morse oscillator $f = 6\alpha^3 D = 3m\omega_0\sqrt{2m\chi_e\omega_0/\hbar}$, and upon substitution of (5.19) and (4.19) into (5.16) we get the following criterion for the validity of classical description of quantum dynamics in a dissipative Morse oscillator

$$\frac{t^*}{t_{deph}} = \frac{Re[\widetilde{\gamma}(\imath\omega_0)]}{4\chi_e\omega_0} + \frac{9}{4}\frac{\widetilde{\gamma}(0)kT}{\hbar\omega_0^2} > 1 \tag{5.20}$$

5.5 Numerical Results

We can compare (5.20) with the quantum calculations of a dissipative Morse oscillator done by Miller and co-workers, in which the effects of dissipation on the propagation of the wave packet was studied using the semiclassical initial value representation technique [95]. The spectral density of the bath was in the Ohmic form

$$J(\omega) = (\eta_e m\omega_0)\omega e^{-\omega/\omega_c}, \tag{5.21}$$

with the cut off frequency ω_c well below the system oscillation frequency ω_0. The latter means the absence of the energy relaxation contribution to the process of dephasing. The ratio t^*/t_{deph} in this case is

$$\frac{t^*}{t_{deph}} = \frac{9}{4}\frac{\eta_e kT}{\hbar\omega_0}. \tag{5.22}$$

We compare the magnitude of this ratio for different values of T and η_e with the numerical simulations from the Ref. [95], see Fig.5.3. One can see that quantum effects disappear as the value of t^*/t_{deph} approaches to 1.

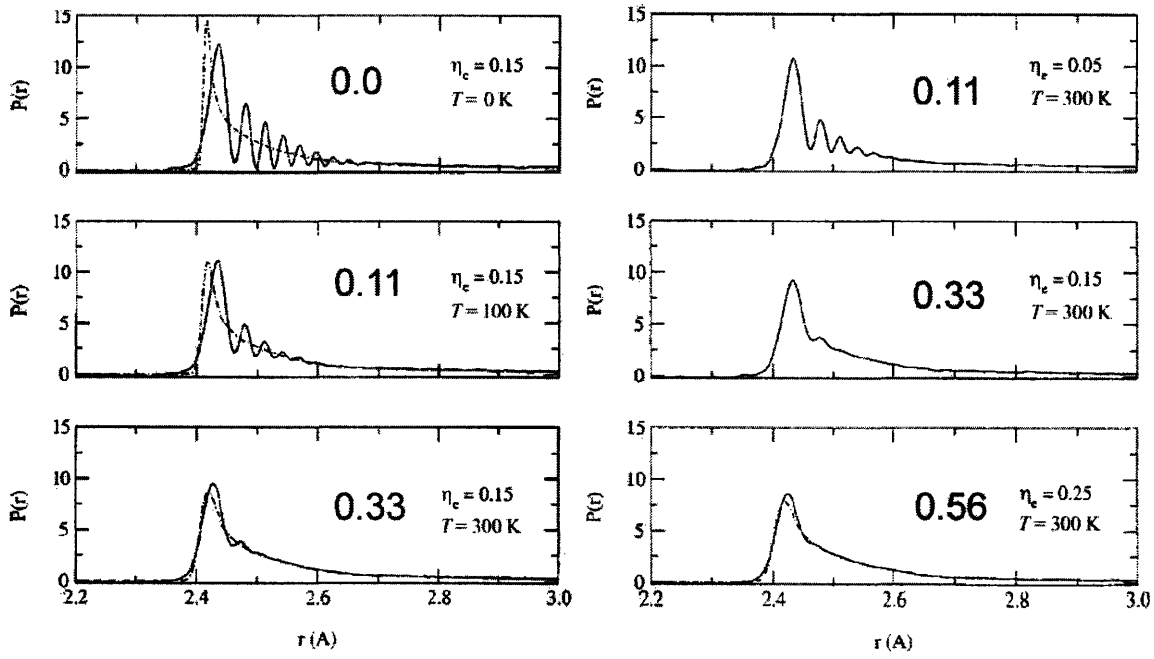

Figure 5.3: Effect of coupling strength on the time-dependent probability distribution $P(r)$ of vibrational coordinate of Morse oscillator. The numerical results were taken from JCP 114, 2562 (2000). Solid line was obtained using Forward-Backward Initial Value Representation method, and the dashed line was obtained using Linear Semiclassical Initial Value Representation method, which is a classical Wigner model. The values of ratio t^*/t_{deph} calculated from Eq.(5.22) are shown in each picture in bold for the corresponding values of η_e and T.

We have also calculated the linear response function of Morse oscillator with one-photon polarization operator $\hat{\alpha} = b+b^+$ (the same as in section 4.4) using the semiclassical representation (4.7) in the case when the bath cutoff frequency ω_c is greater than system frequency ω_0. To calculate semiclassical corrections up to the $\hbar^5$-term we calculated the time-dependence of stability derivatives up to the 5-th order. The equations of motion of the latter were derived by differentiating the Langevin equation (5.9) similarly to the ones given by (5.10). Since neither of the differential equations for stability matrix elements explicitly contains stochastic terms, we can use the regular Runge-Kutta scheme. The stochastic equation (5.9) for $q(t)$ and $p(t)$ was solved with Euler integration scheme. The initial conditions for the Morse oscillator were taken from the microcanonical distribution at the energy $D/10$, where D is the dissociation energy, with the same equilibrium temperature of the bath $D/10$. The results of simulations are shown in Fig.5.4 for the different values of friction strengths γ. One can see that the contribution from the higher order correction terms become less and less important as the friction strength γ increases. We also compare the latter results with the criterion (5.20), which in the case of large ω_c can be written in the form

$$\frac{t^*}{t_{deph}} = \frac{\eta_e}{2\chi_e} + \frac{9}{4}\frac{\eta_e kT}{\hbar\omega_0} > 1 \tag{5.23}$$

and see (Fig.5.4) that classical and semiclassical results start to coincide at $\frac{t^*}{t_{deph}} \sim 1$.

5.6 Discussion

In this chapter we discussed the effects of dissipation on the behavior of semiclassical corrections in the Moyal expansion (4.18). We have shown that the divergence of these corrections, and thus their contributions to the summation in (4.18), can be significantly reduced by introducing the effects of dissipation. At values of bath frication and temperature, given by the criterion (5.20), the contribution of higher-order $\hbar^n$-terms to the semiclassical series (4.18) is much smaller than the contribution from the classical Poisson-bracket term and, therefore, at these and higher values of friction and temperature the dynamics of system can be considered classical.

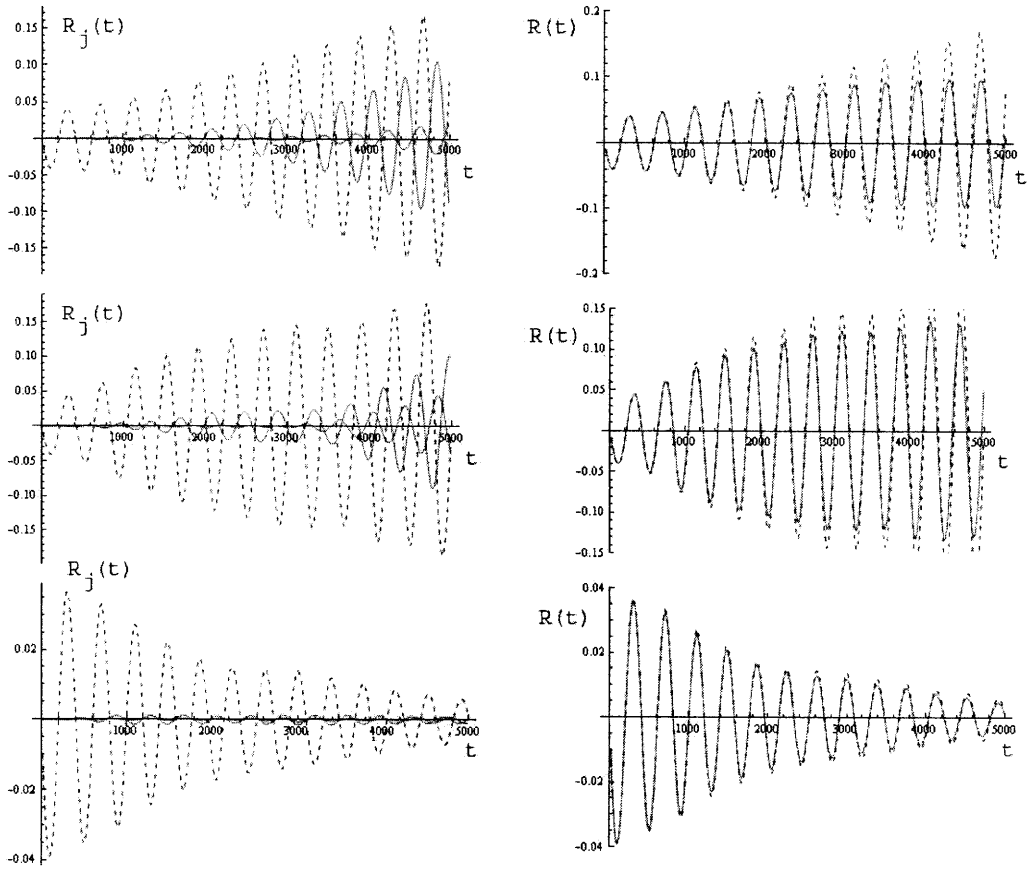

Figure 5.4: The convergence of semiclassical series for the expression of the linear response function of the Morse oscillator with one-photon polarization as a function of friction strength. Left column represents the time-dependence of the semiclassical $R_1(t), R_2(t)$ and $R_3(t)$ correction terms: dashed line represents the classical first-order term $R_1(t)$; solid lines represent semiclassical $\hbar^3$- and $\hbar^5$-terms, $R_2(t)$ and $R_3(t)$, respectively. The column on the right side corresponds to the overall semiclassical linear response function $R_1(t) + R_2(t) + R_3(t)$ shown with solid lines and is compared to the classical form of the linear response function $R_1(t)$ shown in dashed line. The strength of friction γ increases from top to bottom with zero-value for the top two pictures and maximal value for the bottom two pictures.

Criterion (5.20) sets simple limits of when the dynamics of quantum system can be described in terms of classical mechanics - one needs to compare the anharmonicity of a system with the parameters of bath and if they satisfy inequality (5.20), then the dynamics of system is classical. The underlying physics of the criterion is that decoherence effects from dissipation destroy the spreading of the quantum wave packet, which is due to anharmonicity. As long as quantum wave packet remains localized we can associate a classical particle with it. In the absence of dissipation this characteristic time of wave packet spreading/delocalization is the crossover time t^* that we found in chapter 4, which increases in the presence of dissipation.

Chapter 6

Suppression of photon echo as a signature of chaos

6.1 Introduction

A great deal of theoretical work has been devoted a decade ago to study the signatures of chaos in quantum systems [96, 97, 98, 99, 100, 101, 102]. It has been shown that systems with regular dynamics possess Poisson energy level statistics, while systems with chaotic dynamics possess GOE statistics. Obtaining level statistics from experimental spectrum has several difficulties [103, 104], thus it is interesting to find the effect of different level statistics on the time-domain signal, i.e. quantum signature of chaos in the time domain. Single time-domain experiments provide an opportunity to find the signature of chaos without necessity to resolve level statistics.

The basic idea in searching for a time-domain signature of level statistics lies in averaging over the ensemble of time-dependent superposition states. Consider a quantum state $|\psi\rangle$, which is a superposition of two system's eigenstates $|n_1\rangle$ and $|n_2\rangle$ that correspond to eigenvalues E_{n_1} and E_{n_2} respectively, then after coherent excitation of $|\psi\rangle$, it will dephase due to the factor $\exp\{\imath(E_{n_1} - E_{n_2})t/\hbar\}$. The average over ensemble of states $|\psi(t)\rangle$ in some cases is equivalent to the average over level spacings $E_{n_1} - E_{n_2}$, resulting in different time-domain signals for different level spacing statistics. Pechukas was

the first to propose the idea that the average survival probability $P(t) = |\langle\psi(0)|\psi(t)\rangle|^2$ behaves differently for systems with chaotic and regular dynamics [105]. This idea was further developed by Wilkie and Brumer [106, 107] to show that the time resolved fluorescence depends on the average survival probability and therefore carries signatures of quantum chaos. The main difficulty of the approach proposed by Wilkie and Brumer is the necessity to extract information about chaos from the exponential decay of fluorescence signal. In fact, the time-resolution of fluorescence experiment is on the order of the time-scale of a correlation dip that carries the information about underlying chaotic motion. Correlation dip appears at $t_{corr} = h/N\langle\Delta E\rangle$ [106], where N is the number of eigenstates involved in a superposition state and $\langle\Delta E\rangle$ is the average nearest neighbor spacing between the corresponding eigenvalues. To resolve level spacing $\langle\Delta E\rangle$ one needs to have level widths smaller than $\langle\Delta E\rangle$, which means that the life time of levels should be greater than $t_{life} = h/\langle\Delta E\rangle$. Thus, the average time t_{life} that is needed for the excited state to "produce" a signal is always greater than the characteristic time of interest t_{corr} of this signal. To better resolve the time scale t_{corr} we can perform instead an ultrafast time-resolved spectroscopic experiment.

In the present chapter we develop further the idea stated in [106] and to show how to employ ultrafast spectroscopic techniques, in particular, the photon-echo technique, to study nuclear level statistics on the excited electronic state surface. Consideration of non-linear experiment is also interesting because so far the effect of chaos in non-linear spectroscopy has been studied only in classical perspective. It was shown by Mukamel and co-workers that classical non-linear response functions are good indicators of chaotic dynamics, since they incorporate stability matrices that diverge linearly in time for systems with quasi-periodic dynamics and exponentially for systems with chaotic dynamics. Chernyak and co-workers have recently shown [108] that classical non-linear signal for chaotic motion shows instability in frequency domain which can be an indicator of chaos. In present chapter we employ the difference in energy level statistics for Hamiltonians with regular and chaotic motion to study quantum effect of chaos on the photon-echo signal.

The dynamics (either regular or chaotic) which underlies particular energy level statistics is of interest to chemical physicists. Thus, the model we consider is a multiatomic molecule with two electronic states. Nuclear energy levels of the excited electronic state obey either Poisson or GOE statistics, implying that nuclear dynamics in the excited electronic state is either regular or chaotic. Nuclear dynamics in the ground electronic state is assumed to be harmonic with frequency Ω_0, which means that system has at least N ground vibrational levels equally spaced with distance $\hbar\Omega_0$; in section 6.4 we extend our results to the case when ground electronic state has Poisson statistics of nuclear energy levels, which better describes real polyatomic molecules [?].

When the system is radiated by a short laser pulse of duration τ, each nuclear level in the ground electronic state will coherently excite a bandwidth $\Delta\Omega \sim 1/\tau$ of vibrational levels in the excited electronic state. The condition to excite two or more vibrational states in the upper electronic state is $\Delta\Omega > \langle\Delta E\rangle/\hbar$ or equivalently $\tau\langle\Delta E\rangle/\hbar < 1$, where $\langle\Delta E\rangle$ is the average level spacing in the excited electronic state. If this condition is satisfied, then each of N ground vibrational states will produce one superposition $|\psi(t)\rangle$ state in the excited electronic state. It will be clarified in Section 6.2 that such group excitation from N ground states results in the averaging over $N\langle\Delta E\rangle/\hbar\Omega_0$ eigenstates in the upper electronic state, which will thus incorporate energy level statistics of the excited electronic state.

In paper [106] by Wilkie and Brumer the excitation by partially coherent multimode laser pulses from a single ground state was proposed as a way to incorporate energy level statistics of the excited electronic state, in this proposal a single ground vibrational state is irradiated by N laser pulses which are incoherent with each other. This approach is rather difficult to implement experimentally since the number of modes N should be significant ($N > 100$) and also incoherent to each other. Instead, in the present chapter, we note that one can incoherently populate N ground states and then use a single-mode laser pulse. For this reason, we initially randomly populate N vibrational states of the ground electronic state using any available experimental techniques. The initial density matrix for non-linear spectroscopy experiment will thus be $\rho_g = \sum_{n=1}^{N} a_n |g_n\rangle\langle g_n|$, where

a_n is a population of the n-th vibrational level $|g_n\rangle$ of the ground electronic state.

In section 6.2 we describe the non-linear experiment in detail and analytically derive the expression for the third-order polarization. In section 6.3 we consider the differences in photon-echo signal for systems with regular and irregular dynamics. In section 6.4 we extend our results to the case of Poisson statistics of nuclear levels in the ground electronic state. In section 6.5 we discuss the suppression of photon-echo signal at time $\tau_1 = 4\tau$ for chaotic systems.

6.2 The Theory

We consider a system with two electronic states - ground $|g\rangle$ and excited $|e\rangle$. The adiabatic Hamiltonian of the system is given by

$$H = |g\rangle H_g \langle g| + |e\rangle (H_e + \omega_{eg}) \langle e|, \tag{6.1}$$

where H_g is the nuclear Hamiltonian on the ground electronic potential surface; H_e is the nuclear Hamiltonian on the excited electronic potential surface; ω_{eg} is the electronic gap between the minima of both potentials (Fig.6.1). The nuclear dynamics of interest (either regular or chaotic) corresponds to Hamiltonian H_e, and thus the statistics of nuclear energy levels in the excited electronic state is assumed to be either random (Poisson Ensemble) or correlated (Gaussian Orthogonal Ensemble). Physically, only particular areas of energy level spectrum of H_e obey particular level statistics - at low energies nuclear dynamics is mostly quasiperiodic and thus the corresponding level statistics should be that of Poisson Ensemble, while at high energies it can be chaotic with corresponding statistics of GOE. By changing the carrier frequency of the excitation pulse we can select the energy region of interest.

The most common technique in non-linear spectroscopy is a three-pulse photon-echo experiment. In this experiment the system is irradiated with three subsequent pulses with delay periods τ_1 and τ_2 between them. The measurement is done at time t after the third

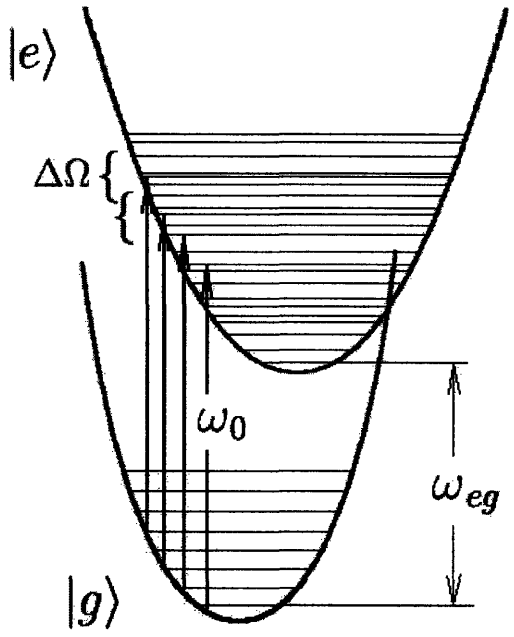

Figure 6.1: The molecular level scheme for a two level system

pulse (Fig.6.2). The electric field acting on the system is

$$\begin{aligned} E(\mathbf{r},t) &= E_1(t+\tau_2+\tau_1)\exp(i\mathbf{k}_1\mathbf{r}-i\omega_1 t)+E_2(t+\tau_2)\exp(i\mathbf{k}_2\mathbf{r}-i\omega_2 t) \\ &+ E_3(t)\exp(i\mathbf{k}_3\mathbf{r}-i\omega_3 t), \end{aligned} \tag{6.2}$$

where ω_j and $\mathbf{k}_j$ are frequencies and wave-vectors of the incident waves correspondingly, $E_j(t)$ denotes the temporal envelope. We assume that all three pulses have the same frequencies $\omega_1=\omega_2=\omega_3=\omega_0$ and temporal envelopes $E(t)=E_0\exp(-t^2/2\tau^2)$, although they have different orientation of $\mathbf{k}_j$. Photon-echo signal is measured in the direction $\mathbf{k}_s=\mathbf{k}_3+\mathbf{k}_2-\mathbf{k}_1$ [1]. The corresponding non-linear polarization is given by [1]

$$\begin{aligned} P^{(3)} &\quad (\mathbf{k}_s=\mathbf{k}_3+\mathbf{k}_2-\mathbf{k}_1,t) \\ &= \left(\frac{i}{\hbar}\right)^3\int_0^\infty dt_3\int_0^\infty dt_2\int_0^\infty dt_1[R_2(t_3,t_2,t_1)+R_3(t_3,t_2,t_1)] \\ &\times E_3(t-t_3)E_2(t+\tau_2-t_3-t_2)E_1^*(t+\tau_1+\tau_2-t_3-t_2-t_1) \\ &\times \exp[i(\omega_0-\omega_{eg})(t_3-t_1)], \end{aligned} \tag{6.3}$$

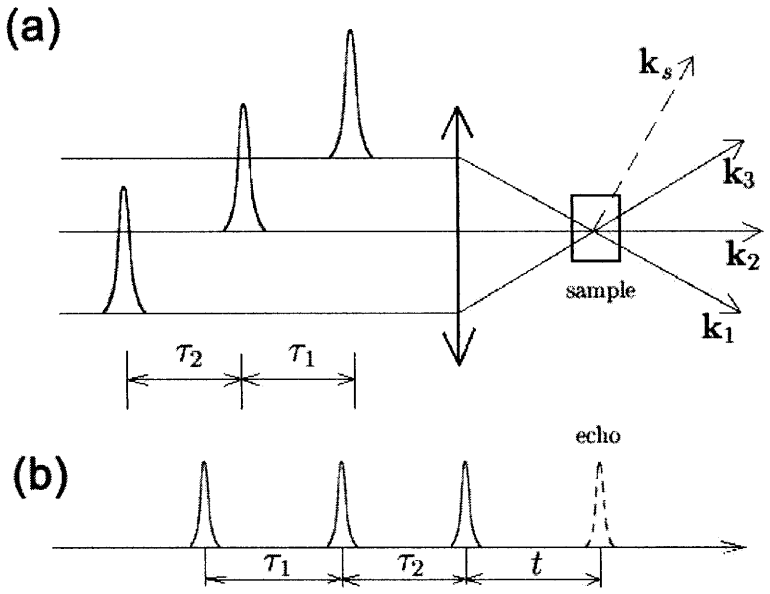

Figure 6.2: Three-pulse photon echo experiment in (a) space and (b) time [1].

where the two response terms in the photon-echo signal are

$$\begin{aligned} R_2(t_3,t_2,t_1) = \quad & \left\langle \hat{\mu} \exp\left[\frac{\imath}{\hbar} H_e(t_1+t_2)\right] \hat{\mu} \exp\left[\frac{\imath}{\hbar} H_g t_3\right] \hat{\mu} \right. \\ & \left. \times \exp\left[-\frac{\imath}{\hbar} H_e(t_2+t_3)\right] \hat{\mu} \exp\left[-\frac{\imath}{\hbar} H_g t_1\right] \rho_g \right\rangle \qquad (6.4) \\ R_3(t_3,t_2,t_1) = \quad & \left\langle \hat{\mu} \exp\left[\frac{\imath}{\hbar} H_e t_1\right] \hat{\mu} \exp\left[\frac{\imath}{\hbar} H_g(t_2+t_3)\right] \hat{\mu} \right. \\ & \left. \times \exp\left[-\frac{\imath}{\hbar} H_e t_3\right] \hat{\mu} \exp\left[-\frac{\imath}{\hbar} H_g(t_1+t_2)\right] \rho_g \right\rangle . \qquad (6.5) \end{aligned}$$

Here, $\hat{\mu}$ is the electronic dipole moment operator, $\rho_g = \sum_{n=1}^{N} a_n |g_n\rangle\langle g_n|$ is the ground state nuclear density operator, with a_n the population of the n-th vibrational level $|g_n\rangle$ of the ground electronic state and N the total number of initially populated ground vibrational states.

Assuming that pulses do not overlap, i.e. $t, \tau_2, \tau_1 > \tau$ (which is actually the necessary condition in deriving Eq.(6.3)) we can set the lower limit for the integrals in (6.3) to $-\infty$.

Using the completeness relation $\sum |n\rangle\langle n| = 1$ in (6.4) and (6.5) repeatedly we obtain

$$R_2(t_3,t_2,t_1) = \sum_{n,k,u,v} \langle g_n|\hat{\mu}|e_u\rangle \exp\left[\frac{\imath}{\hbar}E_u^e(t_1+t_2)\right] \langle e_u|\hat{\mu}|g_k\rangle \exp\left[\frac{\imath}{\hbar}E_k^g t_3\right] \langle g_k|\hat{\mu}|e_v\rangle$$
$$\times \exp\left[-\frac{\imath}{\hbar}E_v^e(t_2+t_3)\right] \langle e_v|\hat{\mu}|g_n\rangle \exp\left[-\frac{\imath}{\hbar}E_n^g t_1\right] \exp[-\beta E_n^g] \qquad (6.6)$$

$$R_2(t_3,t_2,t_1) = \sum_{n,k,u,v} \langle g_n|\hat{\mu}|e_u\rangle \exp\left[\frac{\imath}{\hbar}E_u^e t_1\right] \langle e_u|\hat{\mu}|g_k\rangle \exp\left[\frac{\imath}{\hbar}E_k^g(t_2+t_3)\right] \langle g_k|\hat{\mu}|e_v\rangle$$
$$\times \exp\left[-\frac{\imath}{\hbar}E_v^e t_3\right] \langle e_v|\hat{\mu}|g_n\rangle \exp\left[-\frac{\imath}{\hbar}E_n^g(t_1+t_2)\right] \exp[-\beta E_n^g]. \qquad (6.7)$$

Plugging (6.6)-(6.7) into (6.3) and performing integrations we get

$$P^{(3)}(t) = \left(\frac{\imath}{\hbar}\right)^3 (\sqrt{2\pi}\tau E_0)^3 \sum_{n,k,u,v} a_n \langle g_n|\hat{\mu}|e_u\rangle\langle e_u|\hat{\mu}|g_k\rangle\langle g_k|\hat{\mu}|e_v\rangle\langle e_v|\hat{\mu}|g_n\rangle$$
$$\times \; e^{-(\varepsilon_k-\varepsilon_v)^2\tau^2/2} e^{-(\varepsilon_n-\varepsilon_u)^2\tau^2} e^{(\varepsilon_k-\varepsilon_n)(\varepsilon_u-\varepsilon_v)\tau^2}$$
$$\times \; \left\{e^{\imath(\varepsilon_u-\varepsilon_v)\tau_2} + e^{\imath(\varepsilon_k-\varepsilon_n)\tau_2}\right\} e^{\imath(\varepsilon_k-\varepsilon_v)t} e^{\imath(\varepsilon_u-\varepsilon_n)\tau_1}, \qquad (6.8)$$

where we denote

$$\varepsilon_n \equiv E_n^g/\hbar$$
$$\varepsilon_k \equiv E_k^g/\hbar$$
$$\varepsilon_u \equiv (E_u^e/\hbar) - (\omega_0 - \omega_{eg})$$
$$\varepsilon_v \equiv (E_v^e/\hbar) - (\omega_0 - \omega_{eg}). \qquad (6.9)$$

Here, E_n^g and $|g_n\rangle$ are the n-th eigenvalues and the n-th eigenstates of the Hamiltonian $\hat{H}_g$, respectively; E_v^e and $|e_v\rangle$ are the v-th eigenvalue and the v-th eigenstate of $\hat{H}_e$.

Matrix elements $\langle e_i|\hat{\mu}|g_j\rangle$ can be positive or negative depending on i and j. For systems with chaotic classical limit the distribution of matrix elements is shown to be Gaussian and centered around zero [109, 110]. Here we assume that $\langle e_i|\hat{\mu}|g_j\rangle$ are symmetrically distributed around zero, with the mean value much smaller than the width of distribution. The result of summation (6.8) is therefore determined by terms that contain squares of coefficients $\langle e_i|\hat{\mu}|g_j\rangle$, i.e. by terms with $\{k=n, v\neq u\}$, $\{v=u, k\neq n\}$ and $\{k=n, v=u\}$. Let us consider the three cases separately, denoting contributions from each of them $P_a^{(3)}(t)$, $P_b^{(3)}(t)$ and $P_c^{(3)}(t)$, respectively. The contribution from summation $\{k=n, v\neq u\}$

is:

$$P_a^{(3)}(t) = \left(\frac{\imath}{\hbar}\right)^3 (\sqrt{2\pi}\tau E_0)^3 \sum_{n=1}^{N} a_n \sum_{u,v}{}' \quad |\langle g_n|\hat{\mu}|e_u\rangle|^2 |\langle g_n|\hat{\mu}|e_v\rangle|^2$$
$$\times \quad e^{-(\varepsilon_n-\varepsilon_v)^2\tau^2/2} e^{-(\varepsilon_n-\varepsilon_u)^2\tau^2}$$
$$\times \quad \left\{e^{\imath(\varepsilon_u-\varepsilon_v)\tau_2}+1\right\} e^{\imath(\varepsilon_n-\varepsilon_v)t} e^{\imath(\varepsilon_u-\varepsilon_n)\tau_1}, \quad (6.10)$$

where $\sum'$ indicates the exclusion of terms with $u = v$.

In the Condon approximation, matrix elements $\langle g_n|\hat{\mu}|e_u\rangle$ can be represented as a product of electronic dipole matrix element $\mu_0 \equiv \langle g|\hat{\mu}|e\rangle$, which is a constant, and a multidimensional Franck-Condon factor $S_{nu} \equiv |\langle g, \nu_n|e, \nu_u\rangle|$, which is the overlap between multidimensional nuclear wave functions. We expect no correlation between energy spectrum $(\varepsilon_j - \varepsilon_i)$ and multidimensional Franck-Condon factors S_{ij}. Therefore summation (6.10), which is the average $\sum^M ... = M\langle ...\rangle$, will result in the product of averages $\langle f(S_{ij})g(\varepsilon_i - \varepsilon_j)\rangle = \langle f(S_{ij})\rangle\langle g(\varepsilon_i - \varepsilon_j)\rangle$:

$$P_a^{(3)}(t) = \left(\frac{\imath}{\hbar}\right)^3 (\sqrt{2\pi}\tau E_0)^3 \mu_0^2 \langle S_{nu}^2 S_{nv}^2\rangle'$$
$$\times \sum_{n=1}^{N} a_n \sum_{u,v}{}' e^{-(\varepsilon_n-\varepsilon_v)^2\tau^2/2} e^{-(\varepsilon_n-\varepsilon_u)^2\tau^2} \left\{e^{\imath(\varepsilon_u-\varepsilon_v)\tau_2}+1\right\} e^{\imath(\varepsilon_n-\varepsilon_v)t} e^{\imath(\varepsilon_u-\varepsilon_n)\tau_1} \quad (6.11)$$

where $\langle S_{nu}^2 S_{nv}^2\rangle'$ is the average of products of squared Franck-Condon factors for the vertical transitions from the N ground vibrational states, $u \neq v$. Now we take a look at populations a_n - by the construction populations a_n are uncorrelated with the energy spectrum ε_n (for instance, populations from Boltzmann distribution $a_n = \exp(-\beta\varepsilon_n)/\mathrm{Tr}[\exp(-\beta\varepsilon_n)]$ would definitely result in correlation between a_n and ε_n, which we do not want). Therefore, in summation over n, which is equivalent to the averaging over N ground states, we can average a_n and ε_n separately, giving

$$P_a^{(3)}(t) = \left(\frac{\imath}{\hbar}\right)^3 (\sqrt{2\pi}\tau E_0)^3 \mu_0^2 \langle S_{nu}^2 S_{nv}^2\rangle'$$
$$\times \langle a_n\rangle \sum_{u,v}{}' \sum_{n=1}^{N} e^{-(\varepsilon_n-\varepsilon_v)^2\tau^2/2} e^{-(\varepsilon_n-\varepsilon_u)^2\tau^2} \left\{e^{\imath(\varepsilon_u-\varepsilon_v)\tau_2}+1\right\} e^{\imath(\varepsilon_n-\varepsilon_v)t} e^{\imath(\varepsilon_u-\varepsilon_n)\tau_1} \quad (6.12)$$

The last summation over n in the above equation can be performed by replacing it with the integral $\sum_n = \int dn$. Since, as discussed above, the first N ground vibrational levels

are assumed to be harmonic (equally spaced) then $\varepsilon_n = n\Omega_0$ and thus integration over n gives

$$\begin{aligned} P_a^{(3)}(t) &= \left(\frac{\imath}{\hbar}\right)^3 (\sqrt{2\pi}\tau E_0)^3 \mu_0^2 \langle S_{nu}^2 S_{nv}^2 \rangle' \langle a_n \rangle \sqrt{\frac{\pi}{6}} \frac{1}{\tau\Omega_0} e^{-\frac{(t-\tau_1)^2}{6\tau^2}} \\ &\times \sum_v \sum_{r=\pm,1\pm2,\ldots} e^{-\frac{\Delta_r^2\tau^2}{3}} e^{\frac{\imath\Delta_r}{3}(2t+\tau_1)} \left\{e^{\imath\Delta_r\tau_2} + 1\right\} \qquad (6.13) \\ &\times \left(\mathrm{erf}\left[\imath\frac{t-t_1}{\sqrt{6}\tau} + \frac{2}{\sqrt{6}}\Delta_r\tau + \frac{3}{\sqrt{6}}\varepsilon_v\tau\right] - \mathrm{erf}\left[\imath\frac{t-\tau_1}{\sqrt{6}\tau} + \frac{2}{\sqrt{6}}\Delta_r\tau + \frac{3}{\sqrt{6}}(\varepsilon_v - N\omega_0)\tau\right]\right), \end{aligned}$$

where we have introduced new variable $\Delta_r \equiv \Delta_{u-v} = \varepsilon_u - \varepsilon_v$, which stands for the distance between nearest r levels (r-th nearest neighbor distance). The error functions in (6.13) defines the interval of nonzero terms in summation over ε_v, i.e. $\varepsilon_v \in \{0, N\Omega_0\}$. The difference of these two error functions is 2 on the interval $\varepsilon_v \in \{0, N\Omega_0\}$ and 0 outside. We can neglect non-constant behavior of error functions (boundary effects) in the very small region $\varepsilon_v \in \{-2\pi/\tau, 2\pi/\tau\}$ and $\varepsilon_v \in \{N\Omega_0 - 2\pi/\tau, N\Omega_0 + 2\pi/\tau\}$ and consider the superposition of two error functions in (6.13) as a step function, which equals 2 on the interval $\varepsilon_v \in \{0, N\Omega_0\}$ and 0 outside. This results in a restricted summation over v from 0 to $N_v = N\Omega_0\hbar/\langle\Delta E\rangle$, where $\langle\Delta E\rangle$ is the average level spacing in the excited electronic state. Equation (6.13) thus takes the form:

$$\begin{aligned} P_a^{(3)}(t) &= \left(\frac{\imath}{\hbar}\right)^3 (\sqrt{2\pi}\tau E_0)^3 \mu_0^2 \langle S_{nu}^2 S_{nv}^2 \rangle' \langle a_n \rangle \sqrt{\frac{\pi}{6}} \frac{1}{\tau\Omega_0} e^{-\frac{(t-\tau_1)^2}{6\tau^2}} \\ &\times 2\frac{N\Omega_0}{\langle\Delta E\rangle} \sum_{r=\pm,1\pm2,\ldots} \left\langle e^{-\frac{\Delta_r^2\tau^2}{3}} e^{\frac{\imath\Delta_r}{3}(2t+\tau_1)} \left\{e^{\imath\Delta_r\tau_2} + 1\right\} \right\rangle, \qquad (6.14) \end{aligned}$$

where the last averaging is due to the summation over v. Obviously, Δ_r is a function of ε_v, therefore averaging over v results in an average over Δ_r - we will have $N_r = ((N\Omega_0\hbar/\langle\Delta E\rangle) - r) \approx N\Omega_0\hbar/\langle\Delta E\rangle$ spacings (values of Δ_r) to average over, which is actually a very good statistics, that becomes even better if $\langle\Delta E\rangle \ll \hbar\Omega_0$. Averaging over Δ_r, on the other hand, can be done using nearest-neighbor distribution functions,

which are known functions for both Poisson and GOE statistics [106]. Thus we have

$$\sum_{r=\pm1,\pm2,\ldots} \left\langle e^{-\frac{\Delta_r^2\tau^2}{3}} e^{\frac{\imath\Delta_r}{3}(2t+\tau_1)} \left\{ e^{\imath\Delta_r\tau_2} + 1 \right\} \right\rangle$$
$$= 2\int_0^\infty e^{-\frac{\Delta^2\tau^2}{3}} \left\{ \cos\left[\Delta\left(\frac{2t+\tau_1}{3}+\tau_2\right)\right] + \cos\left[\Delta\left(\frac{2t+\tau_1}{3}\right)\right] \right\}$$
$$\times \sum_{r=1,2,\ldots} \rho_r(\Delta) d\Delta. \tag{6.15}$$

For now we postpone further consideration of expression (6.15) until the next section and continue with the remaining contributions $P_b^{(3)}(t)$ and $P_c^{(3)}(t)$. Denoting expression (6.15) with $F(t)$, we get the final expression for $P_a^{(3)}(t)$ in the form

$$P_a^{(3)}(t) = Ce^{-\frac{(t-\tau_1)^2}{6\tau^2}} F(t), \tag{6.16}$$

where $C = \left(\frac{\imath}{\hbar}\right)^3 (\sqrt{2\pi}\tau E_0)^3 \mu_0^2 \langle S_{nu}^2 S_{nv}^2\rangle' \langle a_n\rangle \sqrt{\frac{\pi}{6}} \frac{2N\hbar}{\tau\langle\Delta E\rangle}$ is a constant.

Let us now consider $P_b^{(3)}(t)$, it reads

$$P_b^{(3)}(t) = \left(\frac{\imath}{\hbar}\right)^3 (\sqrt{2\pi}\tau E_0)^3 \sum_{n=1}^{N} a_n \quad \sum_{k,v} |\langle g_n|\hat{\mu}|e_v\rangle|^2 |\langle g_k|\hat{\mu}|e_v\rangle|^2$$
$$\times \quad e^{-(\varepsilon_k-\varepsilon_v)^2\tau^2/2} e^{-(\varepsilon_n-\varepsilon_v)^2\tau^2}$$
$$\times \quad \left\{1 + e^{\imath(\varepsilon_k-\varepsilon_n)\tau_2}\right\} e^{\imath(\varepsilon_k-\varepsilon_v)t} e^{\imath(\varepsilon_v-\varepsilon_n)\tau_1}, \tag{6.17}$$

Using the same assumptions as in the derivation of $P_a^{(3)}(t)$ and replacing summations $\sum_{n=0}^{N}$ and $\sum_{k=0}^{\infty}$ with integrals $\int_0^N dn$ and $\int_0^\infty dk$, respectively, we get

$$P_b^{(3)}(t) = C' \frac{\sqrt{3\pi}}{\tau\Omega_0} e^{-\frac{2t^2+\tau_1^2}{4\tau^2}} \left(1 + e^{-\frac{\tau_2(4t+2\tau_1+3\tau_2)}{4\tau^2}}\right), \tag{6.18}$$

where $C' = \left(\frac{\imath}{\hbar}\right)^3 (\sqrt{2\pi}\tau E_0)^3 \mu_0^2 \langle S_{nv}^2 S_{kv}^2\rangle' \langle a_n\rangle \sqrt{\frac{\pi}{6}} \frac{2N\hbar}{\tau\langle\Delta E\rangle}$. Obviously the contribution of this term to the overall non-linear polarization is negligible when the conditions of pulse non-overlapping $t, \tau_1, \tau_2 > \tau$ are satisfied.

The last term to consider is $P_c^{(3)}(t)$,

$$P_c^{(3)}(t) = 2\left(\frac{\imath}{\hbar}\right)^3 (\sqrt{2\pi}\tau E_0)^3 \sum_{n=1}^{N} a_n \quad \sum_{v} |\langle g_n|\hat{\mu}|e_v\rangle|^4$$
$$\times \quad e^{-\frac{3}{2\tau^2}(\varepsilon_n-\varepsilon_v)^2} e^{\imath(\varepsilon_n-\varepsilon_v)(t-\tau_1)}, \tag{6.19}$$

which simplifies to

$$P_c^{(3)}(t) = 2C\frac{\langle S_{nv}^4\rangle}{\langle S_{nu}^2 S_{nv}^2\rangle'} e^{-\frac{(t-\tau_1)^2}{6\tau^2}}. \tag{6.20}$$

The overall third-order nonlinear polarization reads

$$\begin{aligned} P^{(3)}(t) &= P_a^{(3)}(t) + P_b^{(3)}(t) + P_c^{(3)}(t) \\ &= Ce^{-\frac{(t-\tau_1)^2}{6\tau^2}}\left(F(t) + 2\frac{\langle S_{nv}^4\rangle}{\langle S_{nu}^2 S_{nv}^2\rangle'}\right) + P_b^{(3)}(t). \end{aligned} \tag{6.21}$$

Here we did not substitute for small contribution of $P_b^{(3)}(t)$ in order not to overload formula. One can see that at $t = \tau_1$ we have an echo.

6.3 $F(t)$ for two types of statistics

Obviously, $F(t)$ carries the information about level statistics in the excited electronic state. We now consider the two cases of statistics separately.

6.3.1 Poisson statistics

Systems with regular dynamics possess energy level statistics which is similar to Poisson statistics. The expressions for the r-th nearest-neighbor distribution functions are given in Appendix 6.6. For Poisson statistics we have

$$\sum_{r=1,2,\ldots}^{\infty} \rho_r(\Delta) = \frac{1}{\langle \Delta E\rangle/\hbar}. \tag{6.22}$$

Thus, $F(t)$ for systems with regular dynamics reads

$$F(t) = \frac{\hbar\sqrt{3\pi}}{\tau\langle\Delta E\rangle}\left(e^{-\frac{(2t+\tau_1+3\tau_2)^2}{4\tau^2}} + e^{-\frac{(2t+\tau_1)^2}{4\tau^2}}\right) \tag{6.23}$$

Photon-echo signal measured in experiments is given by [1]

$$\chi(\tau_1,\tau_2) = \int_0^\infty |P(t)|^2 dt \tag{6.24}$$

Substituting (6.21) and (6.23) in the above integral results in monotonically decaying signals shown in Figs.6.3a-6.3b.

6.3.2 GOE statistics

For GOE statistics, the summation of distribution functions (6.30)-(6.31) is shown in Fig 6.4 and can be well-approximated by the error function

$$\sum_{r=1,2,\ldots}^{\infty} \rho_r(\Delta) = \frac{\hbar}{\langle \Delta E \rangle} \mathrm{erf}\left(\frac{\pi}{2}\frac{\hbar\Delta}{\langle \Delta E \rangle}\right). \tag{6.25}$$

The result of numerical integration of (6.15) gives

$$F(t) = 2\left\{ f_\alpha\left(\frac{\langle \Delta E \rangle}{\hbar}\left[\frac{2t+\tau_1}{3}+\tau_2\right]\right) + f_\alpha\left(\frac{\langle \Delta E \rangle}{\hbar}\frac{(2t+\tau_1)}{3}\right)\right\} \tag{6.26}$$

where $\alpha = \tau\langle \Delta E \rangle/\hbar$ and functions $f_\alpha(x)$ can be well-approximated by analytic functions

$$f_\alpha(x) = \frac{\sqrt{3\pi}}{2\alpha} e^{-\frac{3x^2}{4\alpha^2}} - \frac{8}{\pi}\frac{\mathrm{erf}^2\left(\frac{x}{3}\right)}{x^2} \tag{6.27}$$

One can see that $f_\alpha(x)$ has a minimum, which corresponds to $x_{min} \approx 2.4\alpha^{3/4}$. Calculation of signal (6.24) with (6.26) and (6.27) is shown in Figs.6.3c-6.3d. $\chi(\tau_1, \tau_2)$ has a minimum at $\tau_1 \sim 4\tau$ for any given value of τ_2 and its location along τ_1 axis is independent of τ_2. We call this minimum a suppression of photon-echo signal.

6.4 Poisson nearest neighbor statistics in the ground electronic state

So far we considered the vibrational spectrum in the ground state electronic surface to be harmonic and assumed that we can find $N \gg 1$ such levels. Yet, for real systems like polyatomic molecules this is not true. Instead, the low-energy vibrational spectrum of polyatomic molecule formed by many degrees of freedom looks like random spectrum with Poisson distribution of nearest neighbor energy levels [111]. Thus, the better approximation for the bottom N (with $N \gg 1$) vibrational energy levels is a random distribution (i.e. Poisson distribution of nearest neighbor). The latter does not introduce any complications to the above equations. In this case we just need to represent the summation over nuclear states $\sum_{n=1}^{N}$ in the ground electronic state surface in different way. For harmonic

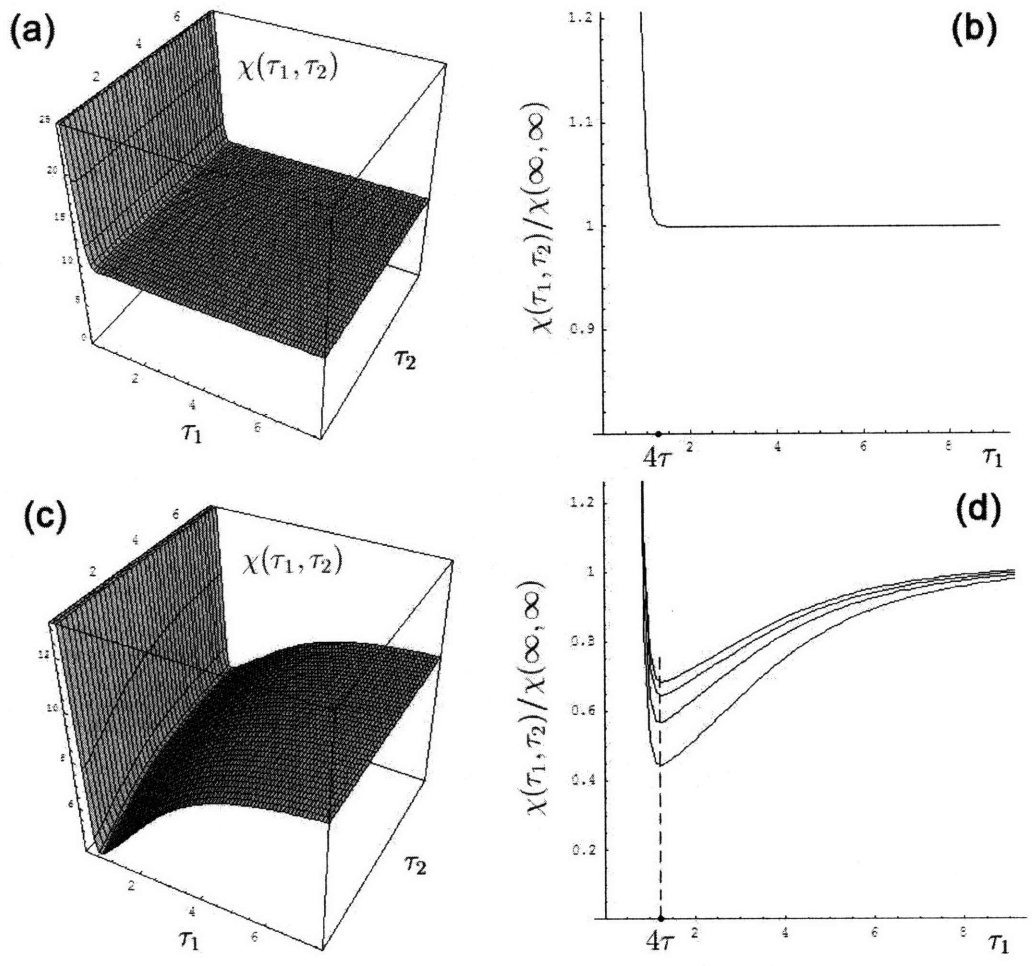

Figure 6.3: Photon-echo signals for regular systems (a)-(b) and irregular systems (c)-(d). Time scale is given in $\hbar/\langle \Delta E \rangle$ units. Inset (d) contains plots for different values of τ_2 going upwards: $\tau_2 = 2, 4, 6, \infty$.

spectrum we had $\sum_{n=1}^{N} \approx \int dn$, with $\varepsilon_n = n\Omega_0$. For random spectrum we can write $\sum_{n=1}^{N} \approx N \int \frac{1}{N\langle \Delta E \rangle_0} d\epsilon_n$, where ϵ_n is now a random variable uniformly distributed on the interval $(0, N\langle \Delta E \rangle_0)$, with $\langle \Delta E \rangle_0$ the mean vibrational energy level spacing in the ground electronic state. Thus, for the case of Poisson nearest neighbor statistics in the ground electronic state, all the previously derived equations remain valid except everywhere one needs to replace harmonic frequency Ω_0 with the mean level spacing $\langle \Delta E \rangle_0$.

6.5 Results and discussion

The main result of present analysis is that the photon-echo experiment carried out with the conditions discussed in the Introduction should always result in the suppression of echo-signal at $\tau_1 \sim 4\tau$ for chaotic systems, where τ is a pulse duration. The time interval between second and third laser pulse τ_2 does not influence the location of signal's minimum along τ_1 axis. This suppression can be considerable, the general formula for the ratio $\chi(\tau_1, \tau_2)/\chi(\infty, \infty)$ near the global minimum $\tau_1 = 4\tau, \tau_2 = 0$ is:

$$\frac{\chi(4\tau, 0)}{\chi(\infty, \infty)} \approx \left| 1 - \frac{8}{\pi} \frac{\langle S_{nu}^2 S_{nv}^2 \rangle'}{\langle S_{nv}^4 \rangle} \left[2 \frac{\mathrm{erf}^2\left(\frac{4\tau}{3}\right)}{(4\tau)^2} \right] \right|^2, \tag{6.28}$$

where τ has dimensionless units $\hbar/\langle \Delta E \rangle$. We can estimate the above ratio assuming $|S_{nu}|$ and $|S_{nv}|$ are uncorrelated uniformly distributed variables, then $\langle S_{nu}^2 S_{nv}^2 \rangle' / \langle S_{nv}^4 \rangle = \langle S^2 \rangle \langle S^2 \rangle / \langle S^4 \rangle = 5/9$, which results in $[\chi(4\tau, 0)/\chi(\infty, \infty)] \to 0.36, \tau \to 0$. Thus the suppression of photon-echo signal can be more than 50%.

On the other hand, the photon-echo signal of regular systems $\chi(\tau_1, \tau_2)$ do not have any minima (Figs 6.3a, 6.3b). Thus, the following conditions always hold: $\frac{\chi(4\tau, \tau_2)}{\chi(\infty, \infty)} \geq 1$ for regular systems and $\frac{\chi(4\tau, \tau_2)}{\chi(\infty, \infty)} < 1$ for irregular systems (in real experiments $\chi(\tau_1, \tau_2)$ decays to zero due to different broadening mechanisms, but on the time scale of ultra-fast experiment we can neglect broadening effects and thus to consider long time limit of $\chi(\tau_1, \tau_2)$ as a constant, which we plot in Fig.6.3 as $\chi(\infty, \infty)$). Since the the location of correlation minimum at $\tau_1 = 4\tau$ does not depend on τ_2 (Fig.6.3d), we can make above inequalities stronger by averaging over some interval of τ_2. The latter averaging can

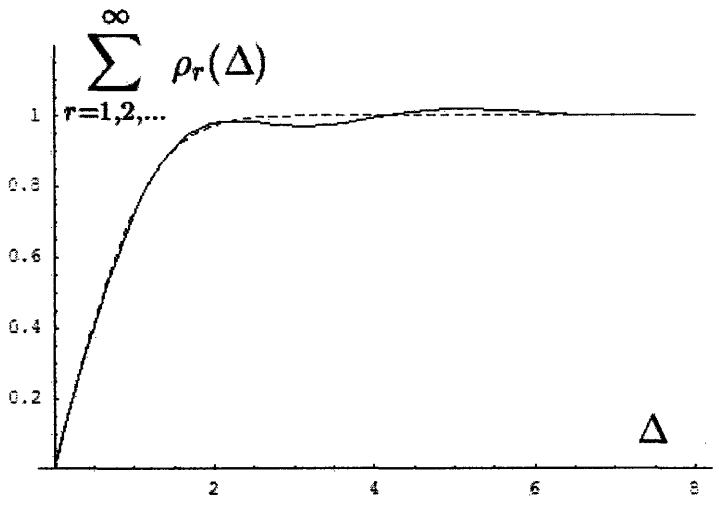

Figure 6.4: The sum of r-th nearest neighbor distributions for GOE statistics (6.30)-(6.31) (solid line). The approximation with error function (6.25) (dashed line).

remove experimental non-ideality and thus provide more conclusive measurements.

The physics of the observed suppression of the echo signal is the same as the physics for the suppression of the averaged survival probability $|\langle\psi(0)|\psi(t)\rangle|^2$ discussed in Refs. [105, 106]. The main idea is that since the energy levels obeying GOE statistics correlate on the energy scale $\langle\Delta E\rangle$, then the superposition state $|\psi(t)\rangle = \sum \exp(-\imath E_n t/\hbar)|n\rangle$ would remember its initial conditions on the time scale $\Delta t = \hbar/\langle\Delta E\rangle$. This time scale defines the interval of quantum coherence, which will "survive" after the averaging over initial conditions and energy level statistics. During this time $|\langle\psi(0)|\psi(t)\rangle|^2$ would behave as a typical quantum decoherence process with oscillatory behavior around its average value due to quantum coherence effects. As a result $|\langle\psi(0)|\psi(t)\rangle|^2$ can go *below* its long-time limit (it could have made several oscillations around its long-time limit, however the time of coherence Δt ends up earlier than the second oscillation). For the regular motion, however, the energy levels do not have any correlation, and thus no time interval Δt of quantum coherence exists after the averaging over ensemble of levels. Therefore $|\psi(t)\rangle$ is not correlated with its initial conditions, decaying to the limit of its statistical average.

6.6 Appendix

The distribution functions $\rho_k(\omega)$ for regular systems (Poisson Ensemble) are [106]

$$\rho_k(\omega) = \left(\frac{\omega\hbar}{\langle\Delta E\rangle}\right)^{k-1} \frac{\hbar \exp\left\{-\frac{\omega\hbar}{\langle\Delta E\rangle}\right\}}{\langle\Delta E\rangle(k-1)!}. \tag{6.29}$$

The distribution functions for chaotic systems can be described by spacing distributions of the Gaussian Orthogonal Ensemble [106]

$$\rho_1(\omega) = \frac{\pi}{2}\frac{\omega\hbar}{\langle\Delta E\rangle}\frac{\hbar \exp\left\{-(\pi/4)\langle[\frac{\omega\hbar}{\langle\Delta E\rangle}\rangle]^2\right\}}{\langle\Delta E\rangle} \tag{6.30}$$

$$\rho_k(\omega) = \frac{2\hbar}{\sqrt{2\pi\sigma_k^2}\mathrm{erfc}\left(-\frac{k\langle\Delta E\rangle}{\sqrt{2}\sigma_k}\right)} \exp\left\{-\frac{(\omega\hbar - k\langle\Delta E\rangle)^2}{2\sigma_k^2}\right\}, k = 2, 3, ... \tag{6.31}$$

with the variances $\sigma_k \approx \sqrt{k(4/\pi - 1)}\langle\Delta E\rangle$.

Bibliography

[1] S. Mukamel. *The Principles of Nonlinear Optical Spectroscopy.* Oxford, London, 1995.

[2] R. Kubo, N. Toda, and N. Hashitsume. *Statistical Physics II.* Springer, Berlin, 1985.

[3] S. Mukamel, V. Khidekel, and V. Chernyak. *Phys. Rev. E*, 53:R1, 1996.

[4] W. G. Noid, G. S. Ezra, and R. F. Loring. *J. Chem. Phys.*, 119:1003, 2003.

[5] W. G. Noid, G. S. Ezra, and R. F. Loring. *J. Phys. Chem. B*, 108:6536, 2004.

[6] J. Wu and J. Cao. *J. Chem. Phys.*, 115:5381, 2001.

[7] L. D. Landau and E. M. Lifschitz. *Quantum Mechanics (Non-Relativistic Theory).* Pergamon, Oxford, England, 1977.

[8] J. A. Leegwater and S. Mukamel. *J. Chem. Phys.*, 102:2365, 1994.

[9] A. J. Lichtenberg and M. A. Liberman. *Regular and Chaotic Dynamics.* Springer-Verlag, New York, 1992.

[10] N. Van Kampen. *Phys. Norv.*, 5:279, 1971.

[11] M. Kryvohuz and J. Cao. *Phys. Rev. Lett.*, 96:030403, 2006.

[12] M. P. Jacobson, R. J. Silbey, and R. W. Field. *J. Chem. Phys.*, 110:845, 1999.

[13] M. P. Jacobson, C. Jung, H. S. Taylor, and R. W. Field. *J. Chem. Phys.*, 111:600, 1999.

[14] E. J. Heller and S. Tomsovic. *Phys. Today*, 46:38, 1993.

[15] E. J. Heller. *J. Chem. Phys.*, 99:2625, 1995.

[16] S. A. Schofield and P. G. Wolynes. *Picturing Quantized Intramolecular Vibrational Energy Flow: Action Diffusion, Localization, and Scaling.* Dekker, New York, 1996.

[17] D. M. Leitner and P. G. Wolynes. *Chem. Phys. Lett.*, 280:411, 1997.

[18] H. Tang, S. Jang, M. Zhou, and S. A. Rice. *J. Chem. Phys.*, 101:8737, 1994.

[19] M. Zhou and S. A. Rice. *Int. J. Quantum Chem.*, 58:593, 1996.

[20] A. A. Stuchebrukhov and R. A. Marcus. *J. Chem. Phys.*, 98:8443, 1993.

[21] R. A. Marcus. *J. Chem. Phys.*, 105:5446, 1996.

[22] C. Jaffe and P. Brumer. *J. Chem. Phys.*, 73:5646, 1980.

[23] E. L. Sibert, W. P. Reinhardt, and J. T. Hynes. *J. Chem. Phys.*, 77:3583, 1982.

[24] J. Wilkie and P. Brumer. *Phys. Rev. A*, 55:27, 1997.

[25] J. C. Tully. *J. Chem. Phys.*, 93:1061, 1990.

[26] D. F. Coker and L. Xiao. *J. Chem. Phys.*, 102:496, 1995.

[27] S. Hammes-Schiffer and J. C. Tully. *J. Chem. Phys.*, 101:4657, 1994.

[28] R. Kapral and G. Ciccotti. *J. Chem. Phys.*, 110:8919, 1999.

[29] B. J. Schwartz, E. R. Bittner, O.V. Prezhdo, and P. J. Rossky. *J. Chem. Phys.*, 104:5942, 1996.

[30] D. J. Tannor and S. A. Rice. *J. Chem. Phys.*, 83:5013, 1985.

[31] N. F. Scherer, R. J. Carson, A. Matro, M. Du, A. J. Ruggiero, V. Romero-Rochin, J. A. Cina, G. R. Fleming, and S. A. Rice. *J. Chem. Phys.*, 95:1487, 1991.

[32] M. Shapiro and P. Brumer. *Acc. Chem. Res.*, 22:407, 1989.

[33] W. Zhu and H. Rabitz. *J. Chem. Phys.*, 118:6751, 2003.

[34] R. J. Gordon and S. A. Rice. *Annu. Rev. Phys. Chem.*, 48:595, 1997.

[35] J. Cao, C. J. Bardeen, and K. R. Wilson. *Phys. Rev. Lett.*, 80:1406, 1998.

[36] B. J. Berne, M. E. Tuckerman, J. E. Straub, and A. L. R. Bug. *J. Chem. Phys.*, 93:5084, 1990.

[37] J. S. Bader, B. J. Berne, E. Pollak, and Hanggi. *J. Chem. Phys.*, 104:1111, 1996.

[38] K. F. Everitt, E. Geva, and J. L. Skinner. *J. Chem. Phys.*, 114:1326, 2001.

[39] R. B. Williams and R. F. Loring. *J. Chem. Phys.*, 110:10899, 1999.

[40] B. Fain, S. H. Lin, and N. Hamer. *J. Chem. Phys.*, 91:4485, 1985.

[41] Y. J. Yan, L. Fried, and S. Mukamel. *J. Phys. Chem.*, 93:8149, 1989.

[42] S. Garashchuk and D. J. Tannor. *Annu. Rev. Phys. Chem.*, 51:553, 2000.

[43] C. Dellago and S. Mukamel. *Phys. Rev. E*, 67:035205, 2003.

[44] Ao Ma and Richard M. Stratt. *Phys. Rev. Lett.*, 85:1004, 2000.

[45] T. I. C. Jansen and J. G. Snijders. *J. Chem. Phys.*, 113:307, 2000.

[46] C. W. Eaker, G. C. Schatz, N. D. Leon, and E. J. Heller. *J. Phys. Chem*, 83:2990, 1985.

[47] W. H. Miller and A. W. Raczkowski. *Farad. Disc. Chem. Soc.*, 55:45, 1973.

[48] C. Jaffe, S. Kanfer, and P. Brumer. *Phys. Rev. Lett.*, 54:8, 1984.

[49] Y. Tanimura and S. Mukamel. *J. Chem. Phys.*, 99:9496, 1993.

[50] Shinji Saito and Iwao Ohmine. *Phys. Rev. Lett.*, 88:207401, 2002.

[51] M. S. Child. *Semiclassical Mechanics with Molecular Applications.* Oxford University Press, New York, 1992.

[52] W. Heisenberg. *The Physical Principles of the Quantum Theory.* New York, Dove, 1949.

[53] M. L. Koszykowski, D. W. Noid, and R. A. Marcus. *J. Phys. Chem.*, 86:2113, 1982.

[54] V. I. Arnold. *Mathematical Methods of Classical Mechanics.* Springer, New York, 1978.

[55] N. De Leon and E. J. Heller. *J. Chem. Phys.*, 78:4005, 1983.

[56] C. W. Eaker, G. C. Schatz, N. D. Leon, and E. J. Heller. *J. Chem. Phys.*, 81:5913, 1984.

[57] C. C. Martens and G. S. Ezra. *J. Chem. Phys.*, 83:2990, 1985.

[58] M. Cho, K. Okumura, and Y. Tanimura. *J. Chem. Phys.*, 108:1326, 1997.

[59] D. W. Noid, M. L. Koszykowsky, and R. A. Marcus. *J. Chem. Phys.*, 67:404, 1977.

[60] E. J. Heller. *J. Chem. Phys.*, 62:1544, 1975.

[61] J. Cao and G. A. Voth. *J. Chem. Phys.*, 100:5106, 1994.

[62] W. H. Miller. *Adv. Chem. Phys.*, 25:69, 1974.

[63] S. Chapman, B. C. Garrett, and W. H. Miller. *J. Chem. Phys.*, 63:2710, 1975.

[64] M. V. Karasev and V. P. Maslov. *Nonlinear Poisson Brackets. Geometry and Quantization.* American Mathematical Society, Providence, R.I., 1993.

[65] T. Voronov. *Quantization, Poisson brackets and beyond.* American Mathematical Society, Providence, R.I., 2002.

[66] S. R. de Groot and L. G. Suttorp. *Foundations of Electrodynamics.* Noord-Hollandsche U.M., Amsterdam, 1972.

[67] M. Hillery, R. F. O'Connel, M. O. Scully, and E. P. Wigner. *Phys. Rep.*, 106:121, 1984.

[68] E. J. Heller. *J. Chem. Phys.*, 67:3339, 1977.

[69] M. V. Berry. *Phil. Trans. R. Soc. London*, 287:237, 1977.

[70] C. Jaffe and P. Brumer. *J. Chem. Phys.*, 82:2330, 1985.

[71] A. K. Pattanayak and P. Brumer. *Phys. Rev. Lett.*, 77:59, 1996.

[72] M. L. Koszykowski, D. W. Noid, and R. A. Marcus. *J. Phys. Chem*, 86:2113, 1982.

[73] M. V. Berry. In M. J. Giannoni, A. Voros, and J. Zinn-Justin, editors, *Chaos and Quantum Physics.* North-Holland, Amsterdam, 1991.

[74] W. R. Greenberg, A. Klein, and Ching-Teh Li. *Phys. Rev. Lett.*, 75:1244, 1995.

[75] M. Kryvohuz and J. Cao. *J. Chem. Phys.*, 121, 2004.

[76] W. G. Noid and R. F. Loring. *J. Chem. Phys.*, 122:174507, 2005.

[77] Pooja Shah and Charusita Chakravartya. *J. Chem. Phys.*, 116:10825, 2002.

[78] J. M. Deutch, J. L. Kinsey, and R. Silbey. *J. Chem. Phys.*, 53:1047, 1970.

[79] M. Kryvohuz and J. Cao. *Phys. Rev. Lett.*, 95:180405, 2005.

[80] P. Pechukas. *J. Chem. Phys.*, 57:5577, 1972.

[81] W. H. Zurek. *Rev. Mod. Phys.*, 75:715, 2003.

[82] J. Gong and P. Brumer. *J. Mod. Opt.*, 50:2411, 2003.

[83] D. Giulini, E. Joos, C. Kiefer, J. Kupsch, I. O. Stamatescu, and H. D. Zen. *Decoherence and the Appearence of a Clessical World in Quantum Theory.* Springler, New York, 1996.

[84] S. Habib, K. Shizume, and W. H. Zurek. *Phys. Rev. Lett.*, 80:4361, 1998.

[85] H. Y. Han and P. Brumer. *J. Chem. Phys.*, 122:144316, 2005.

[86] F. Toscano, R. L. de Matos, and L. Davidovich. *Phys. Rev. A*, 71:010101, 2005.

[87] R. Zwanzig. *Nonequilibrium statistical mechanics.* Oxford University Press, US, 2001.

[88] F. Grossmann. *J. Chem. Phys.*, 103:3696, 1995.

[89] E. Pollak. *J. Chem. Phys.*, 127:074505, 2007.

[90] M. Kryvohuz and J. Cao. *Chem. Phys.*, 322:41, 2006.

[91] A. M. Levine, M. Shapiro, and E. Pollak. *J. Chem. Phys.*, 88:1959, 1988.

[92] Y. I. Georgievskii and A. A. Stuchebrukhov. *J. Chem. Phys.*, 93:6699, 1990.

[93] M. Tuckerman and B. J. Berne. *J. Chem. Phys.*, 98:7301, 1993.

[94] S. Yang, J. Shao, and J. Cao. *J. Chem. Phys.*, 121:11250, 2004.

[95] H. Wang, M. Thoss, K. L. Sorge, R. Gelabert, X. Gimenez, and W. H. Miller. *J. Chem. Phys.*, 114:2562, 2000.

[96] M. V. Berry and M. Tabor. *Proc. R. Soc. Lond. A*, 356:375, 1977.

[97] M. Lombardi, P. Labastie, M. C. Bordas, and M. Broyer. *Ber. Bunsenges. Phys. Chem.*, 92:387, 1988.

[98] M. Lombardi, P. Labastie, M. C. Bordas, and M. Broyer. *J. Chem. Phys.*, 89:3479, 1988.

[99] E. Haller, H. Koppel, and L. S. Cederbaum. *Phys. Rev. Lett.*, 52:1665, 1984.

[100] T. H. Seligman, J. J. M. Verbaarschot, and M. R. Zirnbauer. *Phys. Rev. Lett*, 53:215, 1984.

[101] R. L. Sunberg, E. Abramson, J. L. Kinsey, and R. W. Field. *J. Chem. Phys.*, 83:466, 1985.

[102] Y. Chen, S. Hallet, D. M. Jonas, J. L. Kinsey, and R. W. Field. *J. Opt. Soc. America B*, 7:1805, 1990.

[103] L. Michaille and J. P. Pique. *Phys. Rev. Lett.*, 82:2083, 1998.

[104] E. Abramson, R. W. Field, D. I. Innes, and J. L. Kinsey. *J. Chem. Phys.*, 80:2298, 1983.

[105] P. Pechukas. *J. Phys. Chem.*, 88:4823, 1984.

[106] J. Wilkie and P. Brumer. *J. Chem. Phys.*, 107:4893, 1997.

[107] J. Wilkie and P. Brumer. *Phys. Rev. Lett*, 67:1185, 1991.

[108] S. V. Malinin and V. Y. Chernyak. *Phys. Rev. E*, 2008.

[109] M. V. Berry. *J. Phys. A*, 10:2083, 1977.

[110] E. J. Austin and M. Wilkinson. *Europhys. Lett.*, 20:589, 1992.

[111] H. Nakamura and S. Kato. *Chem. Phys. Lett.*, 297:187, 1998.